



Climate Change and Extreme Surface Flooding in Northern Italy

For WWF Deutschland
and Allianz SE

11th November 2011

Authors:

Dr Erasmo Buonomo
Dr Carlo Buontempo
Dr Matt Huddleston
Cressida Ford

The Met Office aims to ensure that the content of this document is accurate and consistent with its best current scientific understanding. However, the science which underlies meteorological forecasts and climate projections is constantly evolving. Therefore, any element of the content of this document which involves a forecast or a prediction should be regarded as our best possible guidance, but should not be relied upon as if it were a statement of fact. To the fullest extent permitted by applicable law, the Met Office excludes all warranties or representations (express or implied) in respect of the content of this document.

Use of the content of this document is entirely at the reader's own risk. The Met Office makes no warranty, representation or guarantee that the content of this document is error free or fit for your intended use.

This document is published by the Met Office on behalf of the Secretary of State for Business, Innovation and Skills, HM Government, UK. Its content is covered by © Crown Copyright 2011 aside from Annex 3 which is © Copyright Jeremy Benn Associates Limited 2011.

Contents

Executive Summary	3
Study conclusions.....	3
Introduction and aims	5
Scientific approach	7
Data analyses	8
Observed surface water flood event in Northern Italy	9
Extreme rainfall events under climate change	10
Surface water flood modelling	11
Results	12
Future research and potential applications	13
Annex 1: Climatological analysis	14
Introduction.....	14
The Venezia Region September 2007 event: meteorological conditions	15
Extreme precipitation from a climatological perspective.....	16
Improving the climatological description: bias correction	20
Climate model projections for extreme rainfall	22
Choice of events for a case studies on surface water floods	25
Spatial downscaling of extreme rainfall	27
Summary	30
References	31
Annex 2: About the consortium	33
Allianz SE	33
WWF Deutschland.....	33
Intermap® Technologies	34
Met Office	34
JBA Consulting	35
Annex 3: Flood analysis	36

Executive Summary

Are the risks of loss-making atmospheric hazards changing because of climate change?

Are any changing risks quantifiable and should they be taken into account by the insurance industry when writing business?

This study aims to address these questions by comparing the characteristics of a recent major loss-making event with those identified in present and future projections.

Specifically, surface water (pluvial or flooding related directly to heavy rainfall) flooding is examined for Northern Italy. Surface water flooding occurs from the flow of water over land before entering the river systems and is triggered by intense localised downpours. The reference event chosen for the project was that of 26th September 2007; it caused rainfall around the city of Venice which is estimated to be exceeded on average only once in 160 years.

In this project climate models are used in addition to traditional analysis based on historical data. These numerical models appear able to reproduce the basic features of extreme precipitation and are validated for the Venice event. The study indicates an increase in the intensity of such events in the future is plausible (three possible realisations of future climate scenarios show a significant increase in these flooding events, and none of the scenarios show a decrease in the period 2070-2099).

This study is unique in several respects:

- The potential climate change impact on the business model of a large insurance company is being assessed.
- A previously under-researched peril is analysed by linking observed current rainfall extremes and flooding to future climate risk by the means of climate and hydrological modelling.
- The project developed new methods that can be applied globally where sufficient observations exist.
- The study combined public and private expertise in a unique consortium including JBA Consulting, Intermap, Allianz SE, WWF DE and the UK Met Office.

In these ways, the case study proves the viability of using currently available methods and data to manage future extreme risk.

Study conclusions

The September 2007 flood in the Venezia region, with intensity close to 300 mm/day measured at one station, has a return period of approximately 1 in 160 years. Events such as these are not seen in the present period (under current greenhouse gas level) in the climate models – which may be due to the length of the dataset or the nature of the natural climate variability during the current climate. However, analysis indicates that extreme events of this nature with up to 50% more intense rainfall are seen in 3 out of 11 future scenarios under higher greenhouse gas levels at the end of the 21st century.

Hydraulic modelling by flood experts JBA Consulting successfully mapped the areas at risk from flooding in nine extreme rainfall events from the climate model scenarios and compared these events to the extent of flooding of the 2007 event.

In the modelled future events examined, in line with the variable spatial patterns of rainfall events in the climate scenarios, certain areas were found to be potentially at greater risk of flooding than in 2007, while others were less heavily affected. The most extreme events in the future climate scenarios show a pronounced increase in flood risk due to considerably larger flood plains.

However, for the period 2021-2050 no significant changes are seen in the modelled precipitation and therefore no changes are detected in the risks from surface water flooding. Any signal present during this time period may likely be hidden in the large (natural) climate variability “noise“. Its identification will require a larger set of climate model integrations with respect to what is currently available, specifically designed to include a proper sampling of climate variability.

We conclude that there is potential for severe surface water flood events to occur in Northern Italy both given today’s climate and under potential future climate scenarios. It is possible that a future climate may cause more frequent and/or more severe flooding associated with heavy rainfall. However, the possibility of such events is not only present in a future scenario related to climate change, and so we would recommend that insurers and other bodies consider how best to quantify and deal with surface water flood risk today, rather than delay taking action until tomorrow.

With regard to the impact of climate change and how it is dealt with by insurers, since the insurance industry’s practice of writing insurance is focusing on relatively short-term considerations (i.e. on a yearly basis) it has proved very difficult to translate these results in today’s practice. In other words, although a change in weather patterns that could have massive repercussions on the insurability of the risk is deemed possible, there is no direct possibility for the insurance industry to react proactively. This result is not unexpected. Even if the specific project described above will not lead to measurable changes in the way an insurance company is dealing with the risks of extreme flooding, we hope that the exercise has served to convince decision-makers that a long-term view on the impact of climate change on their business is an important element to any strategy incorporating the practicalities of climate change.

It is also worth noting that no absolute monetary amounts were derived in this study since no attempt was made to link, for example, the calculated flood depths to losses using vulnerability assumptions of any affected exposure. This could be an area for further study.

Introduction and aims

Whilst there is growing awareness of climate change, the analysis of more robust regional predictions of extreme loss-making events is still challenging. In particular, it is uncertain whether changes in the numbers and the impacts of localised extreme events will adversely affect insurability of property and overall expected future losses.

Current methods for assessing loss-making events within the insurance industry use historical data to assess current risk. This study particularly aims to assess the question of whether climate projections could be used to estimate future hazard likelihood at regional level.

Surface water (or “pluvial”) flooding is a relatively under-researched peril particularly in the insurance and reinsurance industry and is often only a simple add-on to sophisticated river flood models. In this respect, Central Europe insurance markets are behind standard practice in (for example) the UK, where consideration of surface water alongside river flood by underwriters is relatively common practice.

Resulting from the flow of rainwater over land, prior to it entering the river system, pluvial flooding can be triggered by intense localised downpours rather than by widespread precipitation, and as such presents a considerable challenge to climate modellers because high resolution is needed to assess these small-scale features and this is not easily available.

Increases in the global mean air temperature allow an increase in the water vapour content of the atmosphere, which in turn may increase the precipitation intensity. This means that pluvial flooding is a peril that will plausibly increase under warming scenarios of climate change.

In 2010, WWF Deutschland approached a consortium of experts in relevant fields to construct a study into the effects of climate change in the Venezia region of northern Italy. Among its constituent parties, the consortium has all of the relevant expertise to develop and conduct a study of this nature (see annex 3).

Allianz SE and WWF Deutschland share the concern and ambition that dangerous climate change needs to be avoided. Based on climate science there is a guiding limit on global warming, which is also a politically well established one – the 2°C limit on the increase of global mean temperature compared to pre-industrial levels.

Allianz SE and WWF Deutschland defined a common work agenda in 2007 to address the role capital markets can and will have in averting dangerous climate change whilst understanding what the virtual certainty of exceeding 2°C of global warming in the 21st century under some scenarios means for the business.

In the Allianz SE and WWF Deutschland collaboration the focus of work basically rested on three work streams towards the business implications for Allianz SE in insurance and investment management, in conducting research to better understand the challenges ahead and also to find ways to advocate towards policy makers the need and relevance of low carbon regulation and policy frameworks. In the insurance part of the business one aspect that was focussed on were the options to integrate emissions mitigation into insurance products.

The other priority was to better understand the potential impact of climate change on the business model of Allianz SE in its insurance business. The specific project described here is visionary in that it genuinely incorporates the long-term climate risk and tries to evaluate whether the result should translate in actual business decisions related to the insurance sector today.

The consortium represented public (the Met Office), private (JBA Consulting, Allianz SE and Intermap) and NGO (WWF Deutschland) interests and as such was a unique consortium cutting across a range of expertise and interests.

This document introduces the methods and conclusions of the climate change study, which took the extreme rainfall event of 26th September 2007 as a calibration event.

Objectives

The objectives of this specific study across the consortium were fourfold:

1. Provide an estimate of the return period of the September 2007 Venezia event.
2. Generate high-resolution precipitation maps for the area of flooding.
3. Provide a quantitative assessment of the likelihood that these events will become more frequent or intense with climate change, along with a range of potential scenario events based on the output from an ensemble of climate model simulations for the comparison of future and present climate.
4. Carry out flood hazard mapping for precipitation scenarios associated with different climate scenarios so as to illustrate the possible impact of climate change on surface water flood risk.

Scientific approach

The project required a number of steps to isolate extreme rainfall events from rainfall observation data and modelled climate projections, ascertain the relative frequency of these events and then drive hydraulic water flow models for these events with high-resolution data. A summary of the steps is shown schematically in Figure 1.

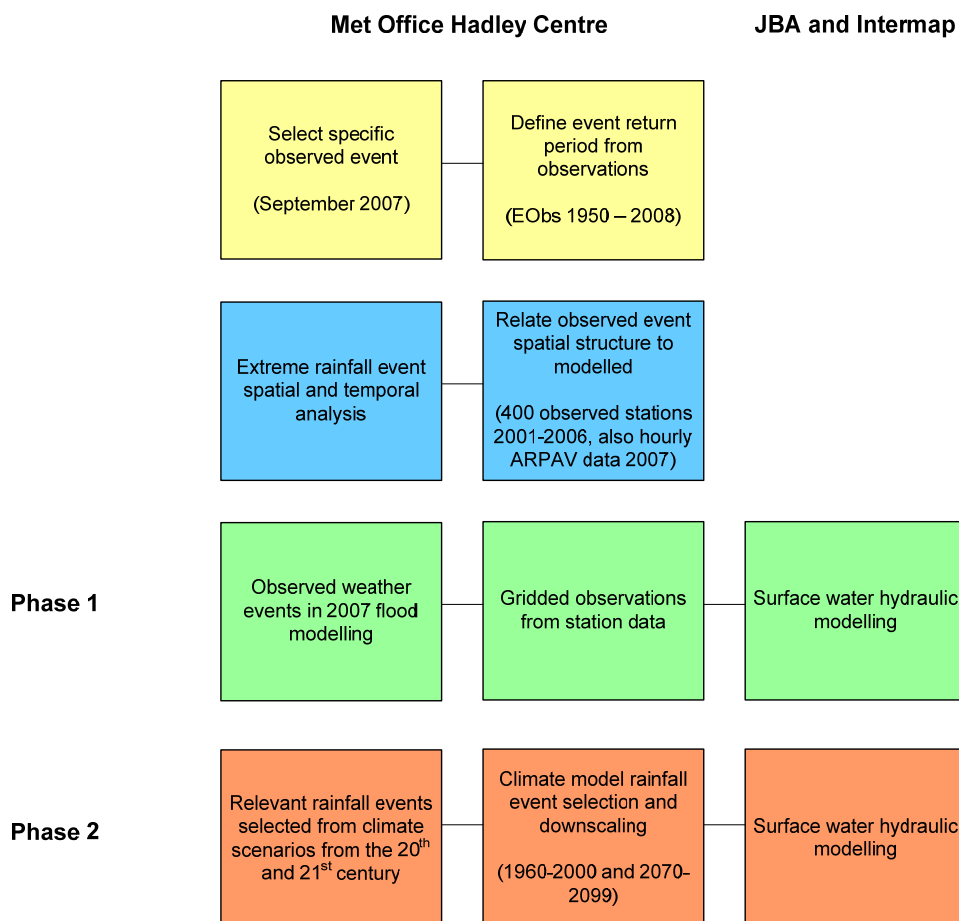


Figure 1: Schematic showing work flow for the project for illustration purposes. Phase 1 and 2 relates to the JBA Consulting documentation (see annex 3). For descriptions of EObs and ARPAV data see Rainfall observations data below.

A key innovation in the project was relating station-based observations of the rainfall events to low-resolution climate data (both modelled and observed). This enabled climate projection data at lower resolution (25km) to be *downscaled* to the high resolution (5km) needed for the hydraulic modelling. See Figure 2 for an example of the changes in intensity related to changes in the spatial scales of the data.

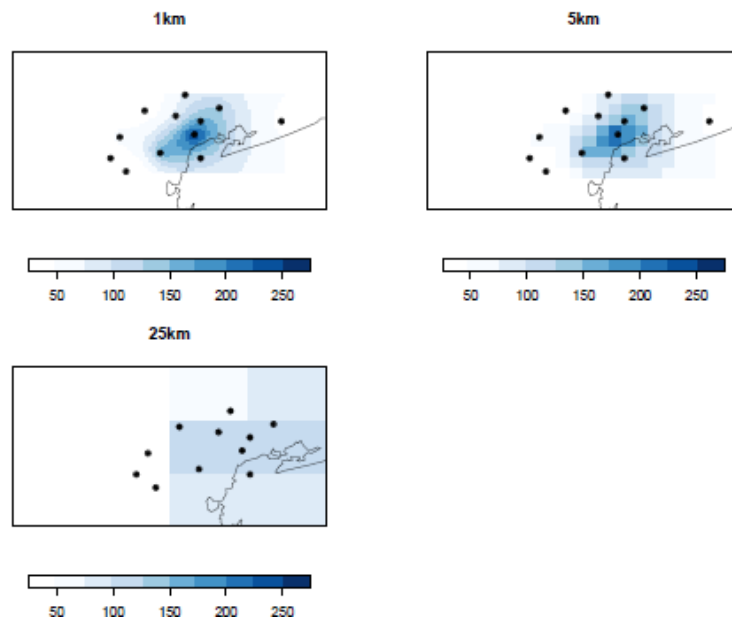


Figure 2: Daily precipitation (mm/day) interpolated from ARPAV stations around Venezia over a grid of 1km (top left panel), 5km (top right panel) and 25km. The 1km grid could be considered as representative of the stations value. The locations of the stations are represented by the black dots. At the three resolutions, the maximum intensity of the events is 260mm/day (1km), 220mm/day (5km) and 120mm/day (25km). For descriptions of EObs and ARPAV data see Rainfall observations data below.

Data analyses

Underlying datasets are key to be able to analyse the past likelihood of extreme events and future changes in hazard. The main three sources are:

Rainfall observation data: Three sources of observations were used. An historical gridded analysis (EObs 3.0 1950 to 2008 at 25km resolution) provided long-term perspective on the extreme events. Observations from a dense network of 400 sites available for 2001-2006 in Northern Italy were re-gridded to 5km and related to the 25km data to provide a “downscaling” relationship. Additionally, hourly data for 12 stations from the regional environmental agency ARPAV (Agenzia Regionale per la Prevenzione e protezione Ambientale del Veneto) provided fine spatial structure information to inform on event selection.

Climate model scenarios: The climate projections used in this study have been taken from an extensive set (ensemble) of current climate and climate change projections¹ for 1961-2000, 2021-2050 and 2070-2099. The Met Office Hadley Centre has developed a rigorous approach to providing probabilistic climate projections for current and future climate. This was designed to particularly sample the different realistic options in model parameters.

The method employed at the Met Office Hadley Centre has been to run the same model a number of times with a different (but equally valid) set of values for the parameters describing unresolved processes. For this project, 11 integrations were selected which

¹ See UK Climate Projections (<http://ukclimateprojections.defra.gov.uk>)

followed the A1B SRES² scenario for the period 1951-2009 at a resolution of 25km over an area that included the whole of Europe. Note under the A1B SRES scenario, there is a virtual certainty of exceeding 2°C of global warming in the 21st century (Joshi et al. 2011).

Digital Terrain Data: Digital terrain data provide a digital representation of the ground surface and are a critical input to flood hazard modelling. The Digital Terrain Model (DTM) map used was Intermap's NEXTMap Europe DTM with 5m posting (cell size) for the Venezia region. Because a DTM is taken from overhead imaging, structures such as bridges that pass over the top of a watercourse or drainage path are displayed as solid embankments that block the natural flow of the water. As part of their core product, Intermap edits "cuts" through embankments such as these to allow watercourses above a given size to pass through, as seen by comparing the two maps in Figure 3 (see areas highlighted by the red boxes in the map on the left). These can have an important effect on the results of the model.



Figure 3: Left: Quarto d'Altino with red boxes to show roads crossing watercourses and other roads (Bing Maps © 2011 Microsoft Corporation and its data suppliers); Right: Quarto d'Altino as represented by the Digital Terrain Model showing the overpasses digitally removed to permit through-flow with colour legend for elevation of the DTM (lilac/light purple shows high elevation, greens show low elevation).

Observed surface water flood event in Northern Italy

The Met Office Hadley Centre estimated the observed rarity of the September 2007 event by applying Extreme Value Analysis – a statistical approach to analyse probabilities of rare events. The analysis indicated that precipitation intensity observed in the September 2007 event is, on average, exceeded once every 160 years, with a 90% confidence interval ranging from 30 years to 1,800 years. In analysing the regional climate model projections the Met Office used this estimate to select events of a similar rarity.

² The A1 storyline and scenario family describes a future world of very rapid economic growth, global population that peaks in mid-century and declines thereafter, and the rapid introduction of new and more efficient technologies. A1B, a version of A1, particularly emphasises a balanced use in energy sources. See Special Report on Emissions Scenarios (SRES) at <http://www.ipcc.ch/pdf/special-reports/spm/sres-en.pdf>

Extreme rainfall events under climate change

Estimating the future frequency and intensity of an extreme event is scientifically challenging. This is even more so in areas such as the Mediterranean where the natural variability of the climate can be pronounced. Using the extreme value analysis on the regional climate model data it is possible to obtain an estimate of the way in which extreme events may be changing in the future.

Figure 4 below shows potential changes in extreme precipitation at the end of the 21st century for events whose intensity is expected to be exceeded once in 20 years on average.

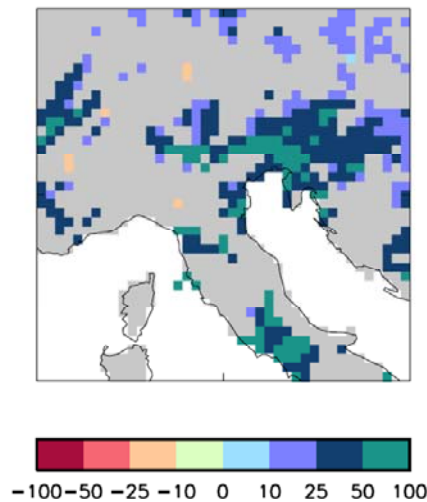


Figure 4: Changes in precipitation intensity (mm/day) for the 1-in-20-year frequency events for the period 2070-2099 with respect to the present climate (1961-2000) for one climate projection (11 were examined in the study – this is the projection from the perturbed model HadRM3Q4). The colours represent change toward wetter conditions (blue to green) or to drier ones (orange to red). Grey areas indicate regions where changes are not statistically significant at 5% level.

While the figure (and generally all the other 10 projections) shows a general increase in extreme precipitation over Northern Italy, the actual regional features are not robust between projections. This analysis provides a good example of the difficulty in obtaining robust estimates of extreme events from records of limited length.

Generally, longer observational records help to reduce the uncertainty associated with the extreme event frequency and intensity. The results in Figure 4 show an example which also indicates that projections with significant increased extreme precipitation intensities for the Venezia region are plausible: three models out of the eleven show an increase in the frequencies and/or intensities of extreme rainfall events. This means that climate change could lead to a change of the expected frequency and severity of extreme events.

Detailed analysis has been undertaken of the return level (intensity; mm/day of rainfall) and the return period (frequency of event) for the 11 climate scenarios at the end of the 20th and 21st century. Diagrams showing the extreme value analysis are presented in Appendix figure A8. For long return periods, uncertainty increases but 2 of the scenarios show a *significant* increase in extreme precipitation by the end of the 21st century (significant at the 5% level, that is values equal or higher would have occurred by chance only 5% of the time), while a third model is quite close to a significant change in

very rare extreme. See annex 1 for detailed description of the climatological components of the project.

Surface water flood modelling

In phase 2, the Met Office supplied JBA with rainfall data for each of nine selected events generated by the future climate models. This dataset provided the quantity of rainfall per hour over the course of the event selected. These data represented the hourly rainfall at any point across an area (or "tile") 6km x 6km. Each tile overlapped with its adjacent tiles by 500m (leaving an area of 5km² unique to that tile) to produce a continuous flood extent.

JBA carried out hydrological modelling based on soil type and land use information values to produce the volume of water that would become surface runoff (i.e. after soil infiltration). Recent rainfall conditions were also taken into account at each hourly interval, allowing for slower infiltration on saturated soil according to the volume of rainfall over the event prior to that hour. The regionalisation of soil type and land use means that, while the raw rainfall across the 6km tile is consistent, the modelled runoff values reflect the changes in terrain in that area.

These values were then supplied to JBA's advanced and scientifically-acclaimed hydraulic model, JFlow+. The JFlow+ technology has been recently developed by JBA and builds on the acclaimed JFlow-GPU system, which uses commercial computer graphics cards (graphics processing units, or GPUs) to facilitate the quick processing of flood depth calculations. Incorporating special advances such as shallow water equations and longer time steps, JFlow+ is a fully hydrodynamic model, providing more accurate simulations without simplifications or shortcuts, and is capable of modelling large areas in a single simulation. JFlow+ is run in-house at JBA on the world's largest dedicated flood modelling grid.

The output of the model is in the form of depth grids in GIS raster format, which are also converted to extent polygon shapefiles after post-processing. The grids are post-processed to remove shallow depths; because rainfall is applied on every DTM cell across the tile, there are no "dry" cells, and so a depth threshold must be set to remove depths that are less significant, and small isolated ponds of flooding. The depth threshold used was 30cm, considered appropriate for removal of "noise" in the DTM data. Following this process, isolated ponds smaller than 1800m² were also cleaned.

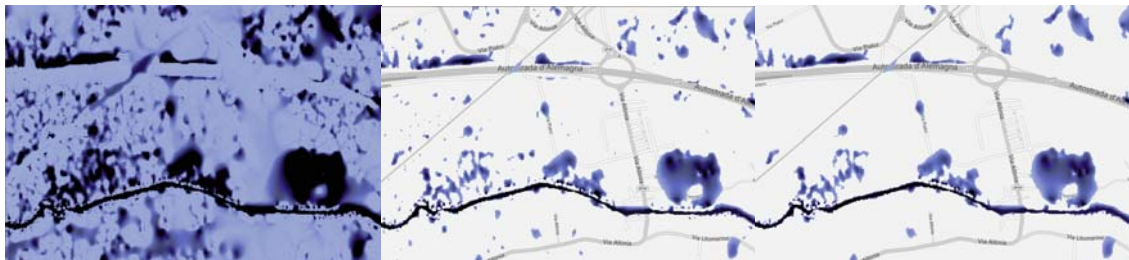


Figure 5: from right to left, the post-processing stages for the depth grids outputted by JFlow+. At first (left image), every cell of the DTM is shown as being wet to a greater or lesser depth (lighter = shallower, darker = deeper). Shallower depths are then removed below a threshold according to the assumed level of noise in the DTM (central image) and finally any resulting isolated ponds of a small size are cleaned from the dataset (right image).

Results

The event of 26th September 2007 around the city of Venice is unprecedented. Climate models when combined with observational downscaling methods are able to reproduce the basic features of that extreme precipitation event in Venezia. In particular, when the models are run for present day conditions, they rarely produce rainfall rates exceeding those observed in the September 2007 event, a result which is consistent with the observed rarity of this event.

The Met Office's analysis of future simulations suggests that there is a possibility (3 of the 11 available projections) that climate change may induce events that are much more intense (up to 50%) than the extremes in the present climate and well in excess of the event of 26th September 2007 around Venice. However, the findings of this study do not allow us to conclude how surface water flooding [in this region] will change with climate change.

One example of a flood scenario map generated by the climate modelling is given in Figure 6 and compared to the JFlow+ modelling of the September 2007 event. The event shown is chosen to be one that gives rise to more widespread severe flooding than in September 2007 in the specific area illustrated. The two events were modelled using the same data and assumptions apart from the event rainfall, which also varies in intensity within each individual footprint. This illustration shows the potential of future climate scenarios to generate significant surface water flood events, including events that are more extreme than the one experienced in 2007.

Since the number of events comparable to the September 2007 flood which could be selected from climate models scenarios is rather small no significant and consistent change to flood hazard can be discerned and, in general, the level of variability in the modelled flood depths is within the level of uncertainty associated with the DTM data. For clarity, this study does not provide a conclusive statement that says surface water flooding will increase with climate change, but does suggest an increased likelihood of extreme rainfall events and suggests these events may indeed become more common.

We conclude that there is potential for severe surface water flood events to occur in Northern Italy both given today's climate and under potential future climate scenarios. It is possible that a future climate may cause more frequent and/or more severe flooding associated with heavy rainfall. However, the possibility of such events is not only present in a future scenario related to climate change, and so we would recommend that insurers and other bodies consider how best to quantify and deal with surface water flood risk today, rather than delay taking action until tomorrow.

With regard to the impact of climate change and how it is dealt with by insurers, since the insurance industry's practice of writing insurance is focusing on relatively short-term considerations (i.e. on a yearly basis) it has proved very difficult to translate these results in today's practice. In other words, although a change in weather patterns that could have massive repercussions on the insurability of the risk is deemed possible, there is no direct possibility for the insurance industry to react proactively. This result is not unexpected. Even if the specific project described above will not lead to measurable changes in the way an insurance company is dealing with the risks of extreme flooding, we hope that the exercise has served to convince decision-makers that a long-term view on the impact of climate change on their business is an important element to any strategy incorporating the practicalities of climate change.

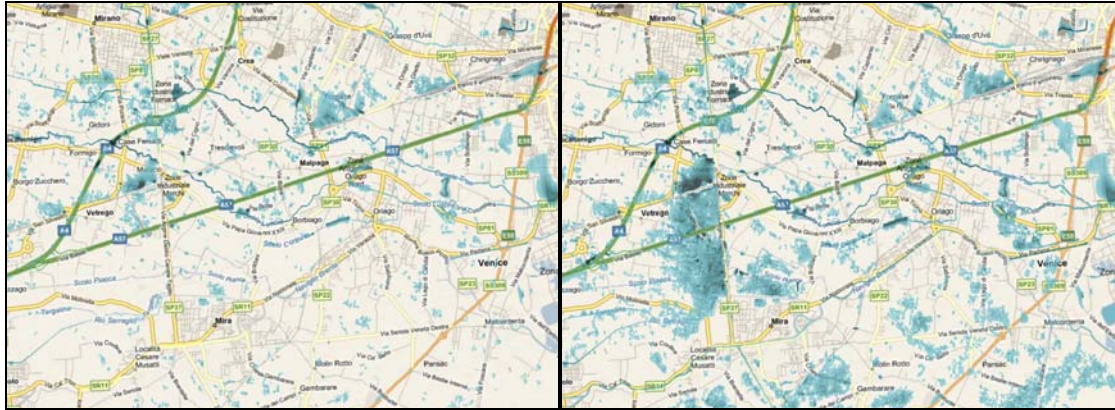


Figure 6: JFlow+ modelling of the September 2007 event in the Venezia region (left) and the simulated 2079 event from Table A1 in the annex (right). Comparison shows that certain areas could be affected more severely by a future event, while others could be less strongly affected. (Bing Maps © 2011 Microsoft Corporation and its data suppliers).

Future research and potential applications

The project has overcome a number of scientific hurdles and has stimulated new ways to relate station observations to numerical climate model projections.

The framework presented could be generalised and would be directly applicable to other geographic regions susceptible to surface water flooding. Given the downscaling methods that have now been developed, other regions would need less effort than required for the pioneering work in this study. Additionally, with suitable modifications the methods may be applicable to other perils such as hail.

Finally, the approach outlined will be of direct relevance to the wider discussions on the impact of extreme events from man-made climate change. Scientific papers are now in preparation that will allow the work to be peer-reviewed and included in, for example, the Intergovernmental Panel on Climate Change (IPCC) analysis.

Annex 1: Climatological analysis

Introduction

The intense, short-lived rainfall event of 26th September 2007 in the region around Venezia had a high impact, causing damages of tens of millions of euros in the urban areas of this region. The high impact of this event and its societal relevance are main reason for the choice of this event for this scientific investigation.

In this section, this extreme event is analysed from a climatic perspective, in particular to understand how similar events may be different in the future climate, changed by the increased concentrations of greenhouse gases in the atmosphere.

Since every meteorological event is unique, even when represented in the rather coarse spatial resolution of the current generation of climate models, a study of the climatological features of a specific weather phenomenon can only be done by isolating its main features and by identifying a set of physical parameters which allow the identification of its climatic analogues in the available record. Both observed data and model simulations are used for the present period, while the future climate can only be studied from available climate model projections. The analysis of future events from climate projections is complicated by the possibility of an unprecedented climatic change by the end of this century, caused by the increased greenhouse gases concentrations, which might alter the basic features of these climatic phenomena e.g. in the context of this study, we might have Mediterranean storms with some tropical features in the future. For this reason, events will be described in a simple way, from their spatial and temporal patterns of the rainfall. However, an understanding of the broader physical features of the phenomena is important in the context of a climatic change study, to support findings from a statistical analysis of precipitation. One way of addressing this issue is a multi-model study, by assessing the robustness of the changes with respect to their formulation. In addition to this criterion, a detailed analysis of the realism of the physical description of this class of intense rainfall events would also be useful in increasing our confidence in modelled climate scenarios. In particular, it could be possible to assess the dependence of the changes on the most robust features of the future, changed climate, such as the increased availability of moisture in the lower atmosphere.

The scale of the September 2007 event is toward the limit of what can be accurately described by the current generation of Regional Climate Models (RCMs), which have a resolution of 25km and use the hydrostatic approximation to eliminate explicit representation of the vertical motion of the atmosphere. In such models, convective processes are not explicitly resolved; in fact they are described as sub-grid scale physical processes in the parameterisation schemes of the climate models. Previous study have shown that, at the current resolution, RCMs are able to produce good estimates of extreme precipitation events using daily precipitation accumulations, but there are not many scientific studies on the quality of hourly rainfall extremes. Given the mismatch between the resolution of RCMs and the requirements of the JBA surface water flooding model, additional high resolution datasets are needed to reconstruct the rainfall at the required scale. The final outcome of this work is a set of events selected from the available high resolution climate projections, both from the present and future climate (2070-2099), described with a time frequency and spatial resolution sufficient to be used to drive the JBA surface water flooding model.

The Venezia Region September 2007 event: meteorological conditions

In the early morning of September 26th 2007, a very intense precipitation event took place inland from the Venezia Lagoon. Observed rainfall exceeded 300mm in less than 6 hours in rather small region (see figure A1), causing severe floods in the urban areas.

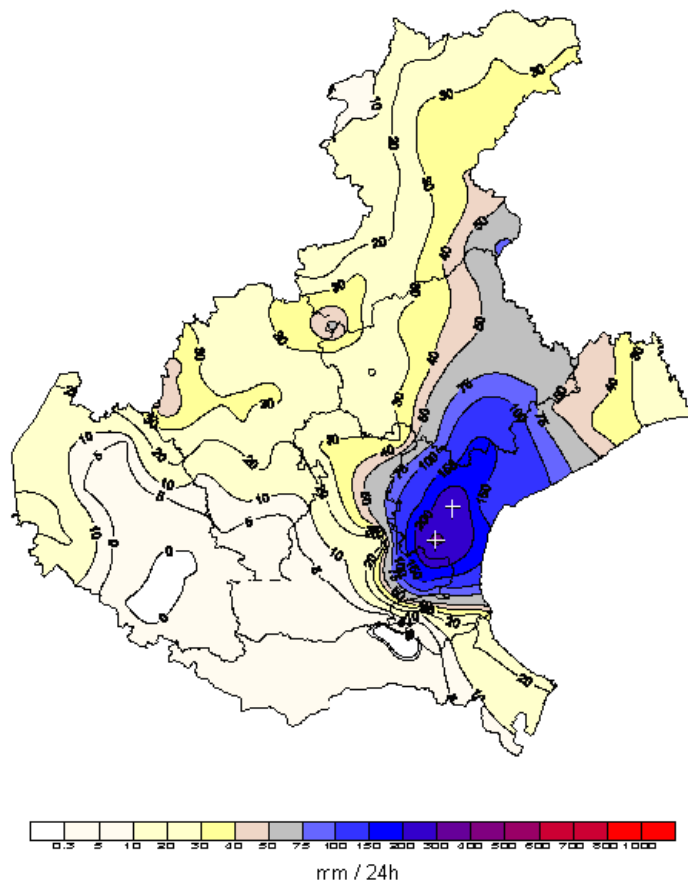


Figure A1: 24-hour accumulated rainfall isohyets (mm/day) from the ARPAV network of rain gauges (from Rossa et al, 2010).

The weather pattern of the event has been discussed by Davolio et al (2009) and Rossa et al (2010). According to these reconstructions, the event was caused by a Mesoscale Convective System (MCS), created by the interaction between an upper level trough and a mesoscale cyclone over the Gulf of Genoa (see figure A2). This synoptic situation created the conditions for the onset of the deep convection in the area and sustained it by allowing the convergence of moist air from the Adriatic Sea. The MCS was moving slowly and, at its peak intensity, included multiple convective cells which produced the extreme rainfall event.

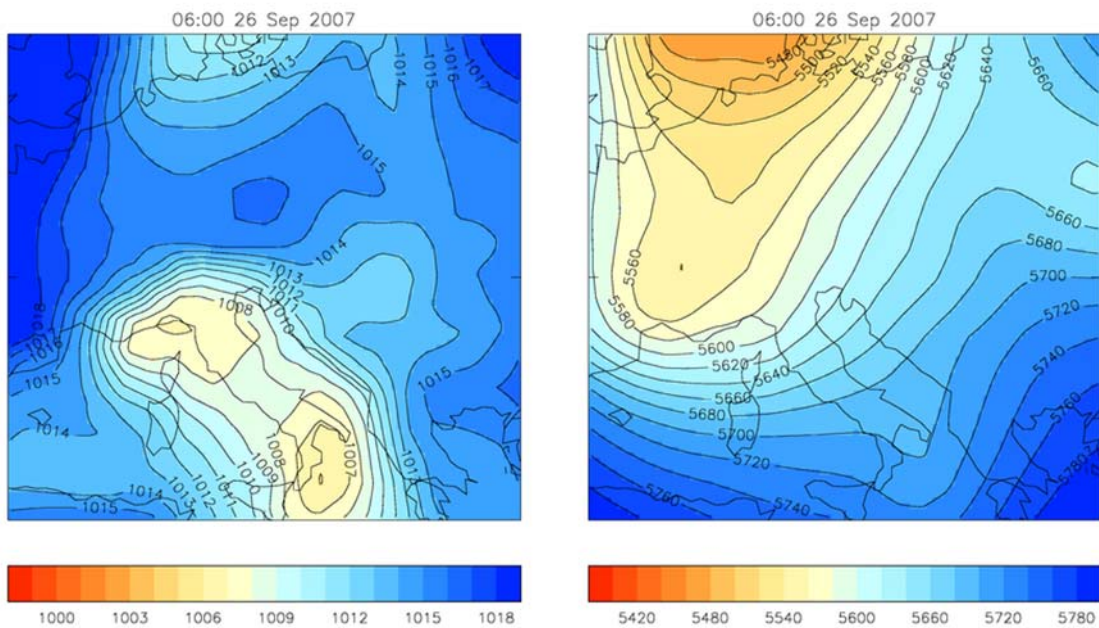


Figure A2: Mean sea level pressure (hPa) and geopotential height (dam) over Italy for September 26th 2007 at 06:00 UTC from the ERA-Interim reanalysis dataset (ECMWF).

Extreme precipitation from a climatological perspective

The climatological properties of the observed precipitation in the 2007 event, in particular its rarity, can only be assessed by studying a long, accurate, record of events and with a spatial resolution sufficient to capture the main features of the event. The gridded dataset of daily precipitation EObs version 3 (Haylock et al, 2008), covering the period from 1957 to 2008 with a spatial resolution of 25km, is the longest record available for the whole region. This record has been used as the main dataset to study the Venezia 2007 event from a climatic point of view.

As discussed above, the intense precipitation in the Venezia 2007 event has a rather small spatial extent and duration of few hours, as a result of a strong mesoscale system over the area. The quite coarse resolution of this dataset could limit our ability to estimate the rarity of such events, since peaks of intense rainfall might be averaged with areas of lower intensity in the same grid box. These events could therefore become comparable to extremes caused by frontal systems, usually more prolonged and widespread, which could give comparable rainfall intensities over a grid with a 25km resolution and for daily accumulation. If this is the case, these two phenomena could be mixed in a statistical analysis of extremes from EObs. Since frontal precipitation might have a different impact with respect to intense mesoscale systems similar to the Venezia 2007 event, the final result would be an incorrect estimate of the rarity of events causing flash floods. It is worth noting, that this problem exists for the RCM integrations as well, since EObs has the same resolution as the model integrations which will be used for the climate change study. Therefore, this work should also aim to understand how realistic a statistical analysis of events on a 25km grid might be, and to understand how its spatial features transform when upscaled to this spatial resolution. It is worth mentioning that the EObs dataset has been aggregated on the same grid used in the RCM simulations and can be directly compared, i.e. grid box by grid box, with the model

results. This choice is important for this study, since it will eliminate the smoothing of localised extreme events, unavoidable when interpolating a pattern from one grid to another with the same resolution but with grid boxes centred in different places. As mentioned above, the main feature of the EObs dataset is its length: since estimates of extreme events are strongly affected by the sampling uncertainty and by their possible dependence on large scale multi-decadal modes of variability (Scaife et al. 2008), the availability of a long record should be more important than the potential problems due to the spatial and temporal representations discussed above.

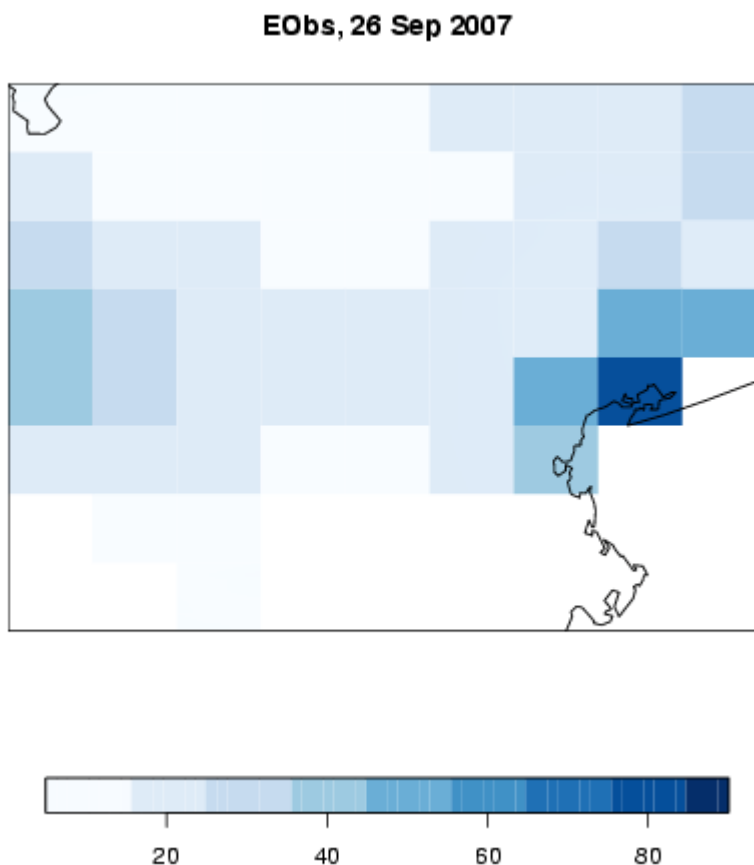


Figure A3: Daily accumulation (mm/day) on September 26th 2007 in Veneto from EObs.

The daily accumulation for the Venezia 2007 event represented in EObs is shown in figure A3. A direct comparison with Figure A1 is not possible because the precipitation in figure A3 is an areal average on a 25km grid while the field in Figure A1 represents rainfall as station values. However, it is clear the EObs is placing the peak of maximum intensity in a different position. A more accurate description of the event has been obtained from a set of 12 station records from the ARPAV rain gauge network, which has been interpolated on a very fine grid chosen to give a good description of the observed station rainfall. The interpolation has been done by applying the kriging method as implemented in the R package *spatial* (R Development Core Team 2008). In more detail, the algorithm has been applied to the logarithm of precipitation intensities, the covariance has been modelled by an exponential function decreasing with the distance, with a scale length of 30km and a nudging factor set to zero to avoid excessive smoothing. This setting has been chosen to optimise the interpolation of intense and

localised rainfall events. Daily precipitation obtained from this procedure for September 26th 2007 around the Venezia Lagoon is shown in figure A4.

ARPAV dataset, 25km res, 26 Sep 2007

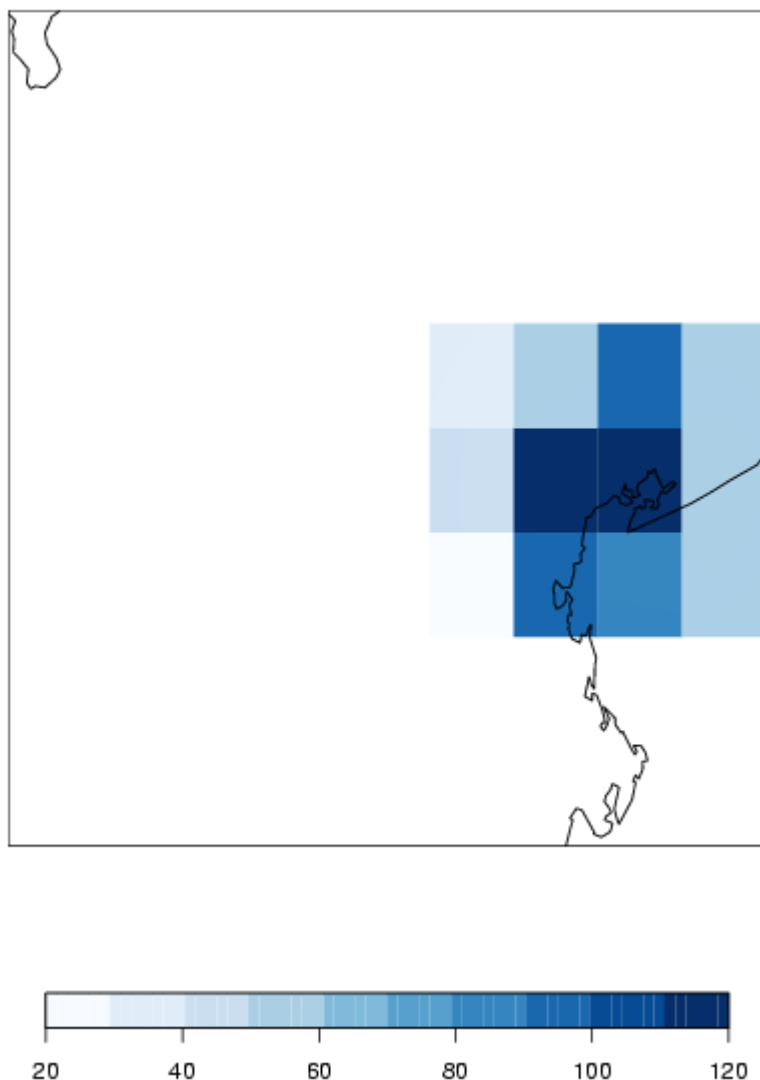


Figure A4: Daily accumulation (mm/day) from the 12 ARPAV stations, interpolated and averaged over the EObs 25km grid.

The spatial distribution from this dataset is slightly different from the EObs pattern. This distribution shows another grid box with rainfall intensity comparable to the maximum value located in the grid box at the northern edge of the Venezia Lagoon. The intensity is also much larger in the aggregated ARPAV network dataset, with a peak at 120mm/day, while EObs shows a maximum around 85mm/day. The underestimation of extreme precipitation in the EObs dataset has already reported (Hofstra et al, 2010) that two problems might be relevant in this context: i) the network density insufficient to completely describe small scale extreme processes (as seen from the comparison of figure A2 and A3) which could result in errors in the spatial representation of intense events and ii) a dependence of EObs bias from the intensity of rainfall, which leads to an underestimation of peak rainfall intensities. Both problems affect our estimates of the frequency of intense mesoscale events by increasing their rarity in a way which is very difficult to quantify. Nevertheless, as it has been discussed above, EObs is the only

available dataset available for a period sufficiently long to allow a meaningful assessment of the rarity of extreme precipitation events,

The statistical analysis to estimate the rarity of the Venezia 2007 event has been based on the Extreme Value Theory. In particular, for this problem, daily rainfall exceedances have been fitted to a Generalised Pareto Distribution (GPD) (Coles 2001). The analysis of the EObs dataset has been done from the precipitation distribution from summer-early autumn months (from June to October, JJASO) and for the whole year, in the period 1957-2007. In this period, in area surrounding Venezia (see figure 3), the September 2007 event gives the highest daily rainfall amount registered in single grid-box. The grid box with maximum intensity has been chosen as the reference point of our analysis. The estimate of the return period for events with intensities larger the September 2007 rainfall in summer to early autumn (JJASO) is 160 years, with a 0.9 confidence level ranging from 30 years to 1,800 years. The confidence interval has been estimated by the profile likelihood method (Coles, R package *ismev*).

When extremes are extracted from the whole year, the estimated return period for this event drops down to 110 years, with a 90% confidence interval ranging from 30 years to 600 years. This result indicates that winter weather systems can produce extreme events which are comparable to the strong convective events of late summer to early autumn. However, since the return period estimate is still much larger than the length of the dataset, this estimate also indicates that the intensity of the September 2007 Venezia event is still quite infrequent, even when assessed on the annual timescale.

The relevance of a study based on the rainfall statistics from a single grid box can be evaluated by estimating the X statistic (Coelho et al, 2008; Buishand 1984), a measure of the simultaneity of extremes at different locations. The pattern of these statistics has been calculated from EObs, using the grid box with maximum intensity in the September 2007 event as a reference and events above the 99th percentile (the same threshold used for the GPD fit). The result is shown in figure A5, for extremes from June to October in the period 1950-2007. The X statistics shows two interesting features: the small extent of its spatial pattern and its alignment with the coast, indicating a prevalence of high intensity rainfall events with spatial patterns which are not too different from the 26th September 2007 event as represented by EObs (figure A3). This statistic doesn't change markedly when evaluated over the whole year. This analysis can be used to refine the area for the impact study, since it will allow an accurate description of extreme rainfall patterns, based on the statistics from the reference grid box used to estimate the X statistics.

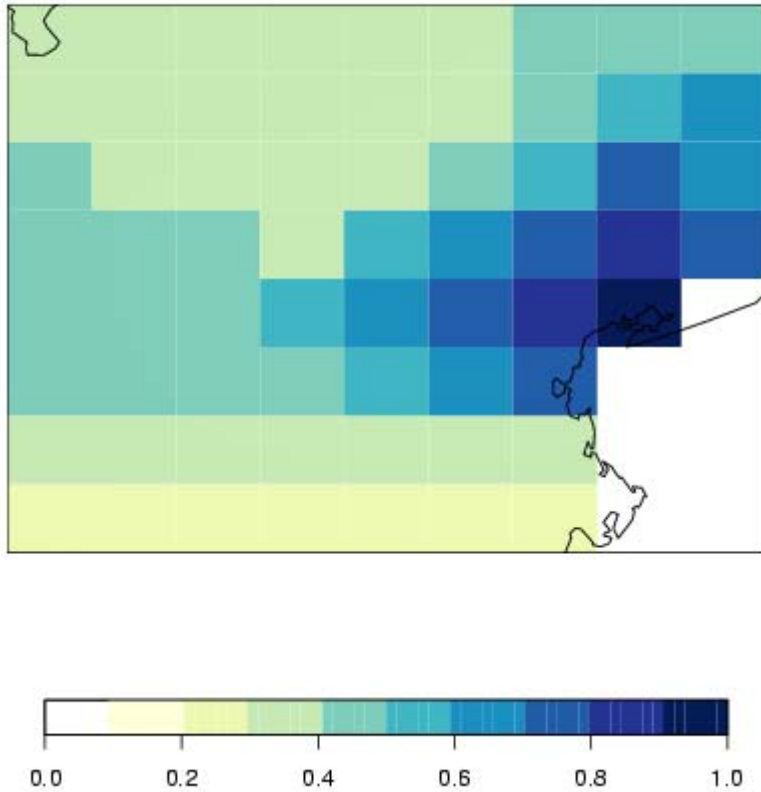


Figure A5: X statistic for the extreme events in EObs (JJASO, 1950-2007), with respect to the grid box at the north-eastern edge of the Venetian Lagoon.

Improving the climatological description: bias correction

In the previous section, the inaccurate representation of the peak intensity for the September 2007 event in EObs has been discussed. It has also been reported that the bias of this dataset is dependent on the intensity/frequency of precipitation, becoming larger for lower frequency/higher intensity events.

An attempt to correct the bias of this dataset needs two ingredients: i) a bias correction algorithm able to correct not only the mean but also the higher moments of rainfall distribution and ii) an observational dataset which is also able to reproduce the extremes quite accurately. A suitable approach to correct precipitation distributions has been described in Leander et al, 2007 and Terink et al. 2010. This is a two-parameter power transformation of the gridded precipitation:

$$P_c = a * P^b$$

The parameter b is determined by matching for the coefficient of variation (CV) of the corrected distribution with the CV from the observations while a is derived by the requirement of having the same mean for corrected and observed precipitation. The observational dataset available for this purpose is a set of 3-hourly precipitation from 400 stations located in the north and centre of Italy (NIObs, Coppola, pers. comm.)

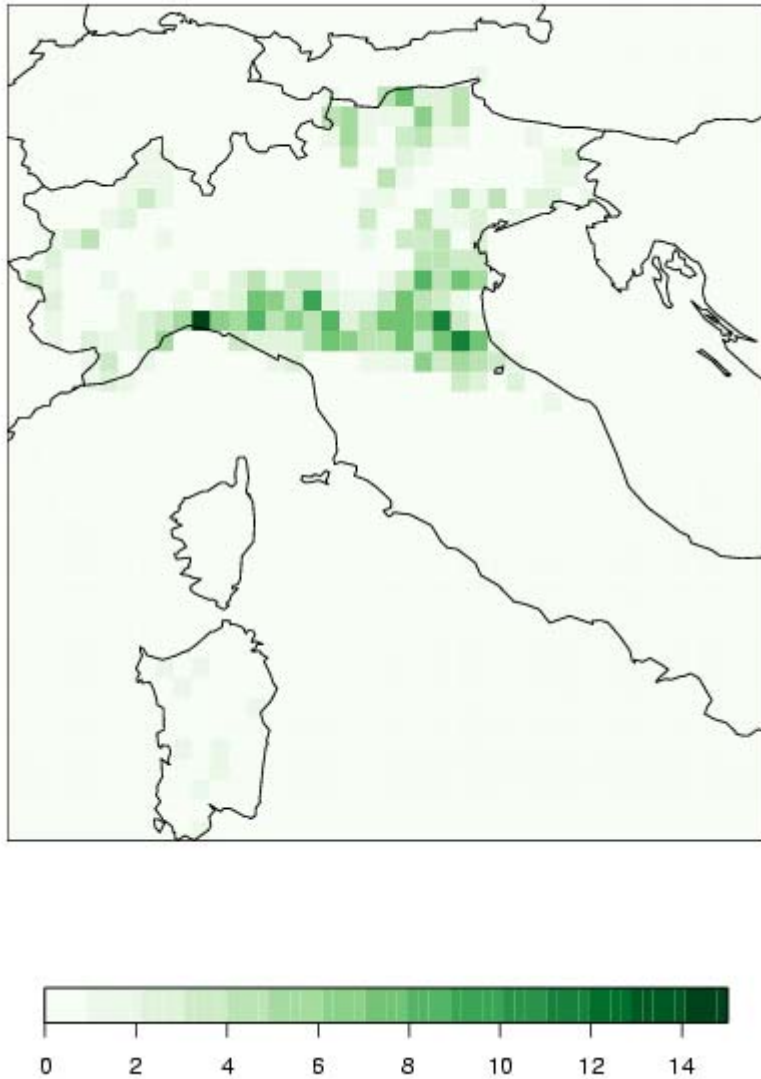


Figure A6: Density of stations for NIObs on the EObs grid.

From these station observations, daily rainfall has been obtained and gridded on the same high resolution grid used for ARPAV stations and by using the same parameters for the kriging algorithm. The result on the high resolution grid was then aggregated on the same rotated-pole grid used in EObs. With the two datasets on the same grid, it was possible to apply the bias correction for each grid-point.

Figure A7 shows the two parameters of the bias correction over the region of interest. These parameters have been estimated as average values for the whole year. The bias correction seems to work well for the northern and western part of the domain, where both parameters are close to 1, but appears to give an unreasonably large correction in the area around Venice. Possible reasons for this outcome could be both the limited length of the NIObs dataset and the lower station density in the EObs dataset in some of the areas of this region. The application of the bias correction to EObs does not produce a plausible representation of extreme precipitation events, as the spatial coherence of the rainfall pattern is heavily modified by the wide range of the bias correction

parameters. For this reason, bias correction has not been applied in the rest of this work.

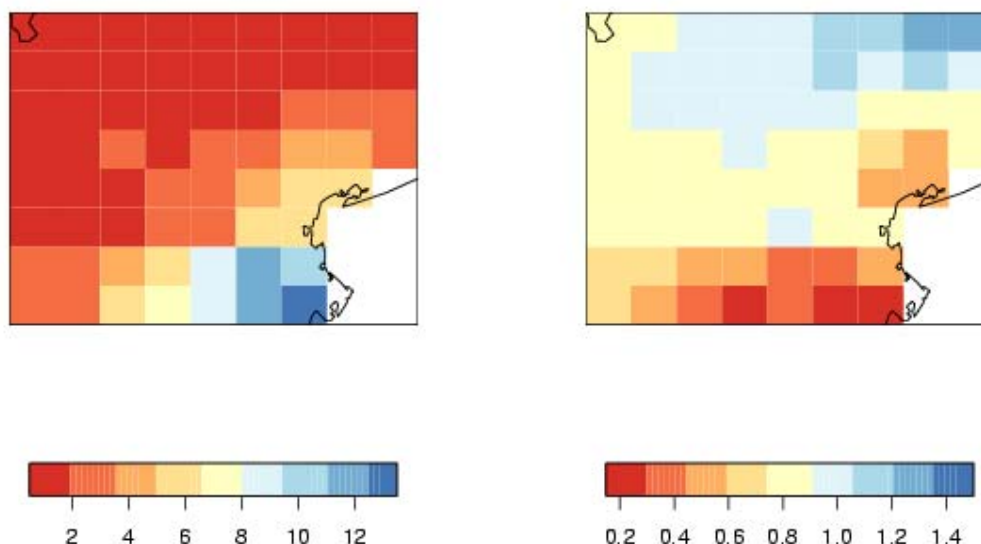


Figure A7: Multiplicative and exponential factors for the power transformation for the bias correction of EObs, based on NIObs re-gridded on the same grid for the period 2002-2006.

Climate model projections for extreme rainfall

When studying the future, greenhouse gas-forced climate, the uncertainty due to the possible different ways to construct climate models (model formulation) for precipitation is quite large. In some regions of the world, GCM projections do not even agree on the sign of the changes (IPCC, chap11). For extreme rainfall, the situation could be different since it is physically plausible (Allen et al. 2002) to expect positive changes on larger areas (e.g. Christensen and Christensen, 2003). However, robust patterns of change for extreme precipitation indices are also quite difficult to obtain (Kendon et al., 2008). An additional problem, in this case, comes from the limitation in the sample size: extreme events are just a small subset of the available data; therefore their sampling uncertainty is quite substantial.

The uncertainty on the description of events such as Venezia September 2007 due to the chaotic nature of climate is enhanced if these events are affected by major mode of variability such as El Niño Southern Oscillation (ENSO) or the North Atlantic Oscillation (NAO), since the effects of the different phases of these variability modes will need to be also represented in model data and the outcome of the climate change study will also depend on the model's ability to describe the effect of modes of variability.

Given the small scale of the events investigated in this study, the standard GCM resolution will not be sufficient for their explicit resolution: as it has been anticipated in the section above, regional climate models will be used to downscale the model integrations to a horizontal grid with a resolution of (25km). The downscaling process will also add another source of uncertainty to the process which could be quite

significant for small mesoscale events. The importance of this contribution can be assessed from the work by Davolio et al, 2009 on the Venezia September 2007 event, which included experiments with three different limited area forecast models driven by the same boundary conditions, showing convective systems with different centres and peak rainfall intensities. A large sensitivity to the initial conditions of the limited area forecast models has also been found, indicating a strong uncertainty component at smaller scales which is purely chaotic.

The quantification of model uncertainty on events such as Venezia September 2007 needs a set of integrations in which the components due to the model formulation, at all scales, have been sampled. Furthermore, any attempt to assess possible effects of climate change on these systems will depend on a proper assessment of the variability associated with these system at all scales, from the multi-annual, planetary scale modes to the small scales contributions driven by local forcing mechanisms. A suitable set of models for this task comes from the UK Climate Predictions 09 (UKCP09) ensemble of Regional Climate Model integrations. This ensemble has been built by a rigorous statistical approach aimed at sampling the model uncertainty due to the physical processes which are not explicitly resolved. These processes are usually represented in the models by schemes dependent on the model variables explicitly resolved and on a set of parameters, some of which are ill-constrained by available observations or by theoretical arguments. By varying this set of parameters, it is possible to sample the model uncertainty dependent on the sub-grid scale processes. Several modelling steps are needed to produce an ensemble of integrations which would allow the quantification of model uncertainty on events of the scale of the Venezia September 2007 event. Firstly, a mixed layer model based on atmospheric-ocean coupled model HadCM3 (Gordon et al, 2000), on which 400 different perturbations have been applied (Murphy et al, 2004) and used in two sets of simulations with concentration of CO₂ equal to pre-industrial levels and to two times this concentration. Secondly, a set of 17 perturbations have been applied to the flux-adjusted version of HadCM3, the resulting perturbed models have been used to perform 150-year transient integration under the SRES A1B emission scenario (Collins et al, 2006). The integrations have been done under the A1B SRES scenario for the period 1951-2099 at a resolution of 25km over an area which included the whole of Europe. Additional investigation has shown that this set gives the same range of model uncertainty as the multi-model set of integration used in IPCC 4th Assessment (AR4) (Collins et al, 2006). Thirdly, regional climate models based on the atmospheric component of HadCM3 have been built for 11 perturbed GCMs, using the same set of perturbations with exception of parameters which are explicitly dependent on the horizontal resolution, which have been scaled accordingly. These models have been used to downscale the corresponding GCMs in the A1B 150-year integration.

Daily precipitation extremes from the 11 RCMs have been analysed, for three different periods (1961-1990, 2021-2050 and 2070-2099). The extremes have been extracted from the whole year, over an area covering the north and part of central Italy. Annual maxima were fitted to Generalised Extreme Value (GEV) distributions, with uncertainty intervals estimate by profile likelihood method (following the approach fully described in Buonomo et al, 2007). Within the three selected periods, the assumption of a stationary climate has been made, i.e. the effects of climate change on extreme rainfall have been considered negligible within each 30-year period. This assumption is supported by the lack of significantly different results between estimates for the period 2021-2050 and 1961-1990, for all the models for the area near the Venetian Lagoon. However, the period 2070-2099 could be different since models give a faster warming with respect to the previous periods: this assumption could be tested by including a time-dependent covariate in the GEV model (Coles, 2001). Goodness-of-fit tests (as in Buonomo et al,

2007) show that the GEV estimated even for this period are good (<5% level), indirectly supporting the assumption of stationarity within the period 2070-2099.

Estimates for the grid box of maximum precipitation for the Venezia 2007 event (as identified in section 2) is shown in figure A8, for the annual extremes in the period 1961-1990 and 2070-2099. In this plot, 80% uncertainty bound curves, estimated by using the delta method (Coles, 2001) have been included. These uncertainty estimates are not as accurate as those derived by the profile likelihood method, in particular some of lower estimates decrease for the largest return periods, a result clearly wrong since return levels, by definition, are monotonically non-decreasing functions of return periods. Wherever the two sets of curves are not overlapping, the changes in return level are statistically significant, approximately, at the 5% level. From figure A8, one member, HadRM3Q10, shows significant changes between present and future extremes for the longer return period. Two other members show substantial differences, statistically different at the 5% level for a range of return periods, almost up to 50 years, for HadRM3Q4, very close to the statistical significant for another member, HadRM3Q16.

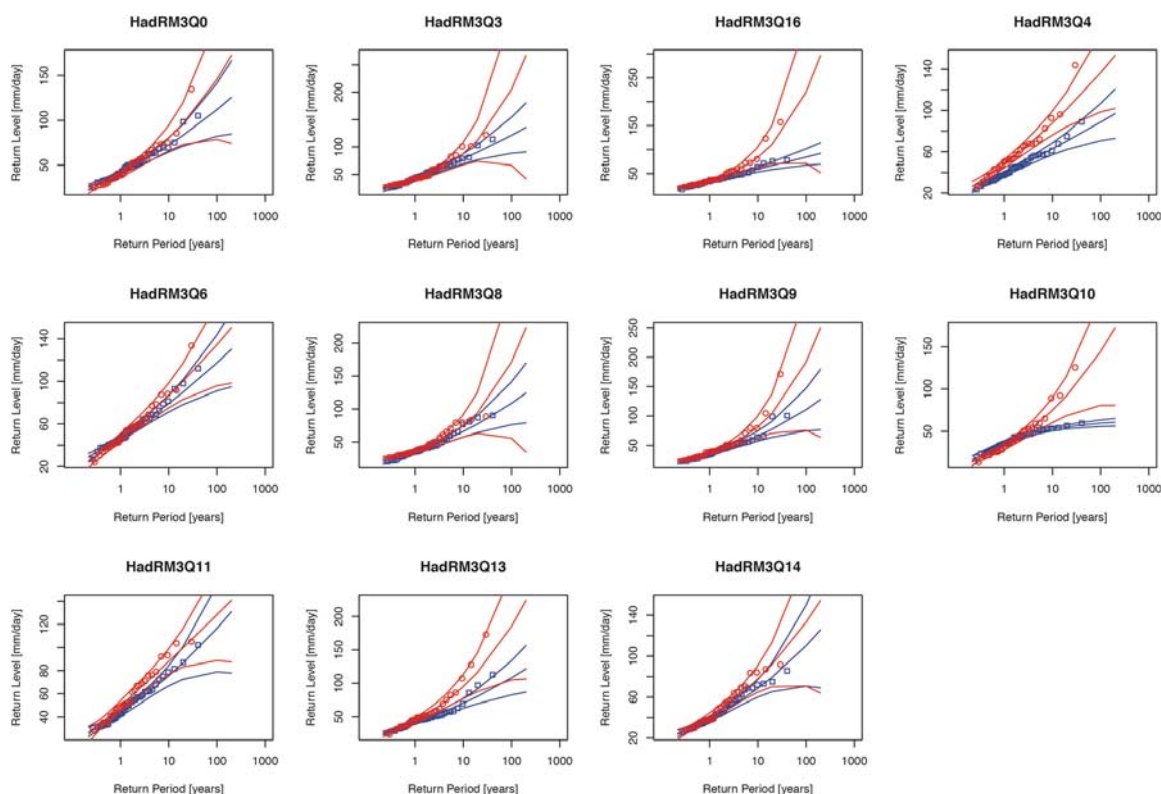


Figure A8: Return level as a function of the return period for total precipitation over the grid box of Venezia (blue curves present period, 1960-1990, red curves A1B future, 2070-2099) plus their 80% confidence levels (outer curves with the same colours).

For the most extreme events, rainfall from these three perturbed RCMs does not exceed 80mm/day in the present climate while it can be higher than 120mm/day in the future. The other perturbed models are not too far from this description. In particular, there are few events in the present climate exceeding 100mm/day, a rainfall amount which is compatible with the Venezia 2007 event while, in the future climate, simulated extreme rainfall larger than 120mm/day is reported for the majority of models, with some of the models producing events with intensity around 150mm/day. These results indicate a future climate in which extreme rainfall could increase well beyond the level reached in the Venezia 2007 event. In terms of rarity, present climate estimates give a return period exceeding 100 years for accumulation exceeding 100mm/day; the result is

in substantial agreement with analysis of the EObs dataset and support the idea of studying the most extreme rainfall events produced by the RCM ensemble, in a “worst case scenario” study, to understand the impact of events such as the Venezia 2007 flood. The analysis for the future shows that, for many climate runs, rainfall amounts exceeding 100mm/day can be expected once in periods ranging from 10 to 50 years, which is a substantial shortening of their rarity with respect to estimates from the present climate. Additional analyses (not shown) indicate a generalised reduction for extreme precipitation in summer and early autumn and a significant increase in winter, although very intense precipitation is still possible in early autumn even in the future.

Hyetographs of these events (not shown) indicate that the larger amount of rainfall from the larger events will be accumulated within few hours, suggesting a major role for convective processes even in the winter months in the future climate. Therefore, in the future’s changed climate, flash floods more severe than the Venezia 2007 event could occur, in the same region, more frequently than in the present climate. The UKCP09 ensemble of climate model integrations do not allow a quantitative estimate of the increased hazard, but suggest the non-negligible possibility of having a significant increase in precipitation (3 out of 11 members in the UKCP09 ensemble) and project a small set of events with very large intensity which are clearly unprecedented in the present climate.

Choice of events for a case studies on surface water floods

Starting from the main features of the Venezia 2007 flood, it is possible to introduce a simple set of criteria which allows the identification of events sufficiently close in their main features to the event under investigation.

The region has been defined based on the X statistic (see figure A5), which is sufficiently large to describe completely the daily precipitation pattern of the September 2007 event (see figures A1 and A4).

Events from the subset of three UKCIP09 ensemble members with significant changes in extreme rainfall has been chosen, both from the present climate (1961-2000), to compare their impact with the results obtained by driving the surface water model with the reconstructed precipitation of the September 2007 event, and from the future climate (2070-2099), to estimate differences in impacts in the changed climate. For the future climate, the most interesting events are those with daily rainfall amounts much larger than both the present climate events of the whole UKCP09 ensemble and the reconstruction of the Venezia 2007 event.

Two criteria have been used to select extreme events: i) highest correlation with the spatial pattern of daily precipitation for the September 2007 event, as described on the 25km grid (see figure A4); and ii) highest daily rainfall for the Venezia grid box.

The first criterion selects events with the rainfall distribution spatially similar to the September 2007 pattern, as an attempt to reproduce the main impact of the event in the region affected by the Venezia 2007 event, thereby avoiding any accumulation of rainfall at the edges of the domain, which might cause problems to the surface water model. The second criterion is the selection of events with the highest rainfall on the Venezia grid box. This is because, as it has been discussed previously, the September 2007 event has, for this grid-box, the highest rainfall reported in the longest available record at our disposal.

These criteria have been applied to select three events from each RCM integration in the subset of UKCP09 integrations with significant changes in extreme over the area around Venezia. Table A1 lists the main features of the events chosen from the three UKCP09 RCMs.

Model	Date of event	Spatial correlation	Daily amount
HadRM3Q4	16/10/1974	0.54	61
	09/12/2083	0.69	72
	02/12/2084	0.60	63
HadRM3Q10	14/09/1976	0.51	52
	04/01/1985	0.46	53
	25/09/2096	0.60	125
HadRM3Q16	03/11/1974	0.40	75
	02/02/2079	0.30	157
	02/11/2086	0.30	60

Table A1 List of events selected for the impact study. Daily rainfall amount are shown for the Venezia grid box in units of mm/day.

The table lists events taking place in autumn and winter; this is a feature of model integrations, in which late summer events are less frequent than in the observed record. A preliminary analysis of the weather conditions associated with these events has shown a range of synoptic conditions with lows centred either in the Ligurian Sea or more to the southeast, sometimes reaching the Adriatic Sea. For the lows centred on the Ligurian Sea, the weather charts are similar to the synoptic conditions of September 26th 2007 – see in figures A2 and A9.

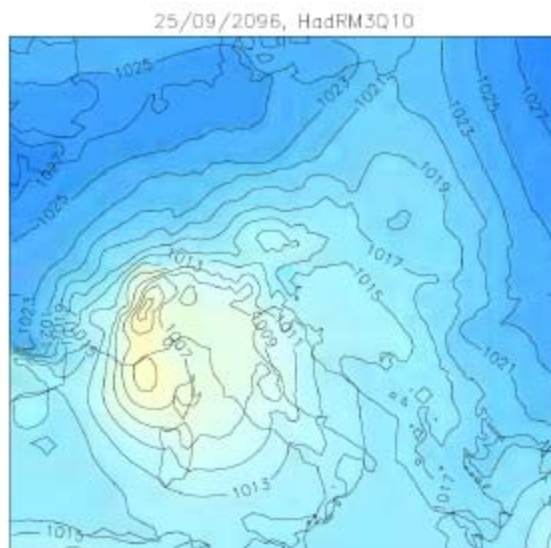


Figure A9 Mean sea level pressure (hPa) at 18:00 UTC for the HadRM3Q10 event of September 25th 2096.

The similarity in weather patterns indicates that RCMs are able to produce intense mesoscale systems from the synoptic conditions similar to those of September 26th

2007. However, this study does not allow one to understand scientifically whether the increase in extreme precipitation is due to thermodynamic effects associated with climate change, such as increase moisture content of the atmosphere, or to a change in the dynamics, e.g. by increasing the number of days with large-scale conditions suitable to generate intense mesoscale systems, given the very small number of relevant extreme events available from these integrations.

Spatial downscaling of extreme rainfall

Regional climate models are currently run at a resolution which is not suitable for many impact studies. This is the case of hydraulic models, which are driven by hourly data at a spatial resolution of few km, clearly beyond the range of current regional climate models. The solution to this problem requires a method which is able to reconstruct the effects of the improved description of the physiography and its interaction with the larger scale fields at the required resolution. The case of intense, localised precipitation is probably the most difficult as it can be seen from the reconstruction of the Venezia 2007 flood at three different resolution, based on the ARPAV dataset.

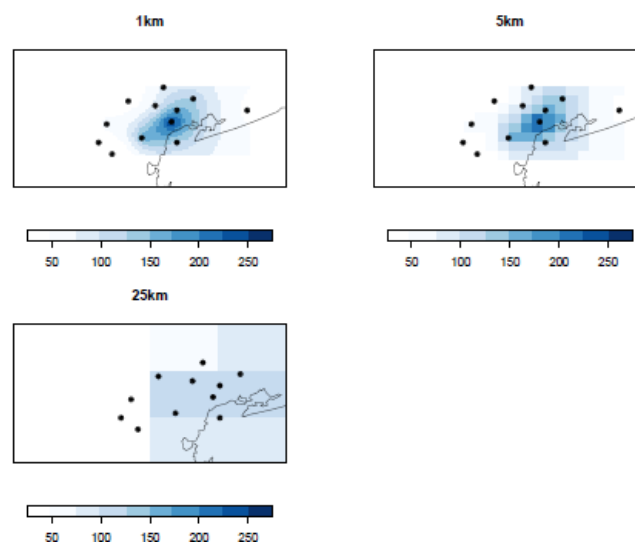


Figure A10: Daily precipitation (mm/day) interpolated from the ARPAV stations around Venezia over a grid of 1km (top left panel), 5km (top right panel) and 25km. The 1km grid could be considered as representative of the stations value. The locations of the stations are represented by the black dots.

Data in figure A10 have been produced by kriging the ARPAV stations on a 1km grid, using the procedure described previously. Two other grids have been defined, with approximately 5km and 25km resolutions. The 25km grid corresponds to the grid used in the RCM integrations. The three grids have been defined as perfectly overlapping, i.e. grid boxes from higher resolution grids are included in just one grid box of the lower resolution grid.

The pattern reproduced at 5km resolution is quite similar to the reconstruction at 1km resolution considered as representative of station values, while the 25km grid shows a substantial smoothing of the rainfall pattern. The intensity of the precipitation maximum change from 260mm/day in the 1km resolution to 220mm/day in the 5km but it goes down to 120mm/day in the 25km resolution. The downscaling method needs to

reconstruct both the spatial pattern and the peak intensity in order to produce a reliable reconstruction of an intense, localised precipitation event.

The method used in this work is based on the Reduced Space Optimal Interpolation (RSOI, Kaplan et al, 1997). The method is used to transfer information from a dense network of stations, usually available on a limited period, to a coarser network, available on a longer period. The algorithm is based on a principal component analysis of the denser network for the calibration period, on the definition of a relationship between denser and coarser station network, which includes an error term, and on the minimisation of a cost function to estimate the principal component scores, derived from the expansion of the denser field in principal components and from the relationship between the coarser and denser network. The cost function also includes an additional, arbitrary, term which favours the lower order, and smoother, principal components. This interpolation method has been successfully applied by Schiemann et al (2010) to generate a high resolution dataset of daily precipitation for the Alps, using a calibration period of few years.

RSOI can be reformulated as a downscaling method by taking into account that the fields at higher and lower resolutions represent precipitation as areal averages at their respective resolution. In particular, the association rule between finer and coarser resolution grid boxes can be redefined to take into account the areal averaging process. The minimisation of the new cost function will then allow identification of the principal component scores for the coarser grid which allows the reconstruction at the higher resolution.

For this study, the first step was to use the set of 400 stations in the NIObs dataset introduced previously, to generate 5km grid, by aggregating precipitation from a 1km grid obtained by kriging the station dataset. In addition, a 25km dataset has also been defined. These three grids are the same as in figure A11; in particular, they are perfectly overlapping and the aggregation process is simply done by summing the contributions of the grid boxes on finer grids included in each grid box of the coarser grid. In applying the downscaling procedure, 40 principal components have been included (additional components did not produce any changes) for daily precipitation events above the 75th percentile (including dry days) in order to calibrate the downscaling relationship on rainfall days with at least a moderate precipitation intensity.

The NIObs dataset is available for the period 2002-2006: the whole set of data has been used in the calibration. An example of the reconstruction is in figure A11.

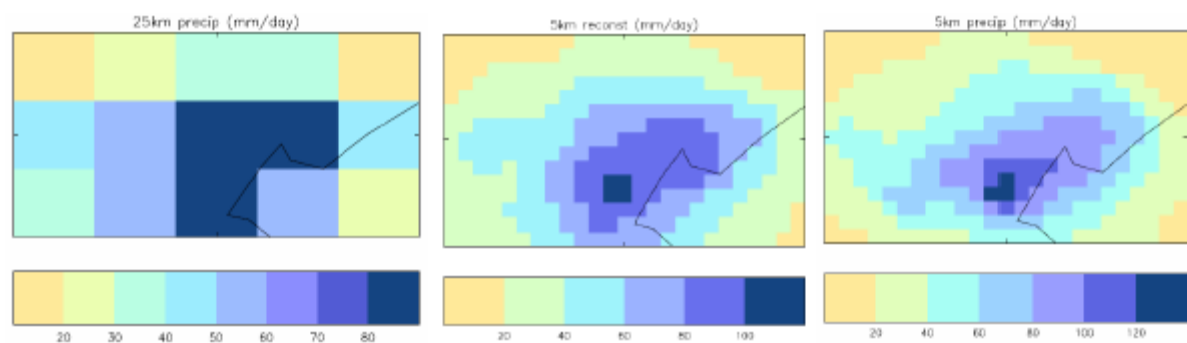


Figure A11: Daily rainfall (mm/day) pattern for the same event at 25km resolution (left panel), 5km resolution (right panel) and its RSOI reconstruction from the 25km grid.

While the precipitation patterns are quite close, there is a small but systematic underestimation of peak intensity usually of the order of few mm/day, but reaching 10mm/day in few cases. This feature could be a result of the smoothing imposed on the algorithm by weighting favourably the smoother principal components. However, there is a substantial increase of peak precipitation from its representation on the 25km grid, an indication of the effects of the downscaling relationship between points on the finer and coarser grid on the coefficients of the principal component expansion. Furthermore, this downscaling method is not altering the areal averages at the coarser resolution, i.e. it is just redistributing precipitation within a 25km box, and any small underestimation in a particular area within the box will be compensated by a slightly increase amount in the neighbouring areas and it is expected to have minor effect on modelling of surface water flooding.

The downscaling procedure has been applied to RCM data at 25km resolution, in particular to test whether smooth, physical meaningful patterns could be created from model data. This test is not as obvious as it may seem, precipitation is the result of sub-grid scale processes and it is parameterised in the RCMs used in this study. Therefore, as a result of any other noisy process at sub-grid scale level, the spatial consistency of a modelled precipitation pattern could be lost.

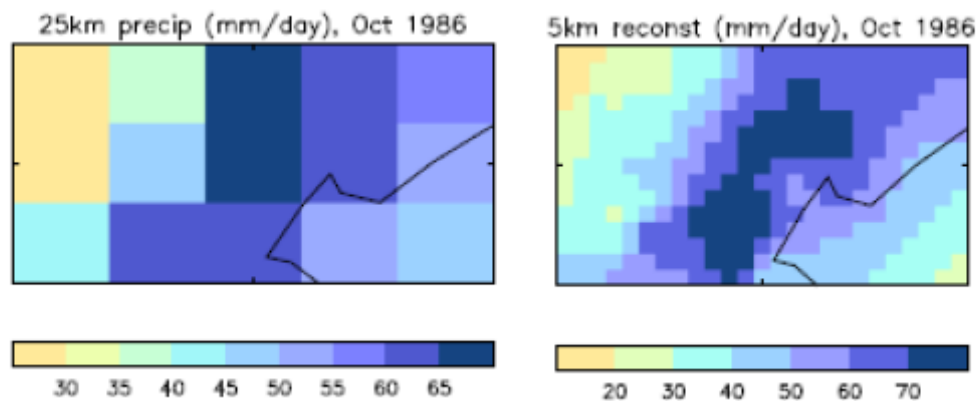


Figure A12: Daily rainfall patterns for an extreme event from HadRM3Q4.

Figure A12 shows a typical example from these tests; the reconstructed precipitation pattern on 5km grid seems to be physically plausible, showing a precipitation pattern with a much clearer coastal effect than is apparent on the coarser grid.

The second step in this process is to produce data suitable to drive hydrological models. For this purpose, the downscaling algorithm has been recalibrated using the 3-hourly precipitation from the NIObs dataset, on precipitation events exceeding the 99th percentile. The same period, 2002-2006, has been used in the calibration. Given the smaller spatial extent of hourly precipitation patterns and the absence of calibration data for the sea points, it was necessary to mask out sea points from model data and reconstruct the full field by kriging: this procedure produces precipitation over sea points in the same way for both model data and observation and produces smoother patterns of downscaled precipitation. Hourly precipitation from the nine events listed in table A1 has been downscaled using this procedure and used as input for the JBA surface water model.

Summary

The event of September 26th 2007 around Venezia is unprecedented and, when compared with the available observational record, it is expected to be exceeded no more than once in a hundred years. Models are able to reproduce the basic features of extreme precipitation in Venezia in particular they are rarely exceeding the rainfall observed in the September 2007 event. When the future climate is analysed, as described by the UCKP09 ensemble of RCM integration, there is the possibility (3 of the 11 available integrations) of having future scenarios with events much more intense (up to 50%) than the daily precipitation of September 26th 2007.

For the JBA study, a set of 9 events was selected from the three models runs with significant changes in extreme precipitations, with five from the present period part of the integrations and the remaining five from the period 2070-2099. All the events were chosen among those with a spatial distribution of precipitation similar to the event of September 26th 2007. Hourly precipitation from these events has been downscaled to a resolution of 5km, to generate a precipitation dataset which could be used to drive the JBA hydrological model.

References

- Allen, M.R., Ingram, W.J., 2002, *Nature*, **419**, 224-226.
- Buishand, T.A., *J. Hydrol.*, 1984, *Journal of Hydrology*, **69**, 77–95.
- Buonomo, E., Jones R., Huntingford C., & Hannaford, J. 2007. *Quart. J. Royal Met Soc*, **133**, 65-81.
- Christensen, J.H., and Christensen O.B., “Climate modelling: Severe summertime flooding in Europe”, 2003, *Nature*, **421**, 805-806.
- Coelho, C.A.S., Ferro, C.A.T., Stephenson, D.B., Steinksog, D.J., 2008, *J. Climate*, **21**, 2072-2092.
- Coles, S., “An Introduction to Statistical Modeling of Extreme Values”, 2001, Springer.
- Collins, M., Booth, B.B.B., Harris, G.R., Murphy, J.M., Sexton, D.M.H., and Webb, M.J., 2005: “Towards Quantifying Uncertainty in Transient Climate Change”. *Climate Dynamics*, **27**, nos 2-3, 127-147.
- Coppola, E., 2010, personal communication.
- Davolio, S., Mastrangelo, D., Miglietta, M.M., Drofa, O., Buzzi, A., Malguzzi, P., “High resolution simulations of a flash flood near Venice”, 2009, *Nat. Haz*, **9**, 1671-1678.
- Haylock, M.R., Hofstra, N., Klein Tank, A.M.G., Klok, E.J., Jones, P.D., and New, M., 2008, “A European daily high-resolution gridded dataset of surface temperature and precipitation”, *J. Geophys. Res (Atmospheres)*, **113**, D20119, doi:10.1029/2008JD10201.
- Gordon, C.; Cooper, C.; Senior, C.A.; Banks, H.; Gregory, J.M.; Johns, T.C.; Mitchell, JFB; Wood, R.A., 2000. *Clim. Dyn*, **16**, 147-168.
- Hofstra, N., New M., McSweeney, C, 2010, *Clim. Dyn*, **35**, 841-858.
- Joshi, M., E. Hawkins, R. Sutton, J. Lowe and D.Frame. Projections of when temperature change will exceed 2 °C above pre-industrial levels. *Nature Climate Change*. DOI: 10.1038/NCLIMATE1261. 2011.
- Kaplan, A., Kushnir, Y., Cane, M. A., and Blumenthal, M. B., *J. Geophys. Res.*, 1997, **102(D13)**, 27,835–27,860.
- Kendon, E. J., D. P. Rowell, R. G. Jones, and E. Buonomo, 2008: Robustness of future changes in local precipitation extremes. *J. Climate*, **21**: 4280-4297, doi: 10.1175/2008JCLI2082.1.
- Leander, R.; Buishand, T.A., *J. Hydrology*, 2007, **332**, 487-496.
- Murphy, J.M., Sexton, D.M.H., Barnett, D.N., Jones, G.S., Webb, M.J., Collins, M., *Nature*, 2004, **430**, 768-772.

Rossa, A.M., Del Guerra, F.L., Borga, M., Zanon, F., Settin, T., Leuenberger, D., J. Hydrology, 2010, **394**, 230-244.

Scaife, A.A., Folland, C.K., Alexander, L.V., Moberg, A., Knight, J.R., J. Climate, 2008, **21**, 72-83.

Schiemann, R., Liniger, M.A., Frei, C., J. Geophys. Res, 2010, **115**, D14109, doi:10.1029/2009JD013047.

R Development Core Team (2008). R: A language and environment for statistical computing. R Foundation for Statistical Computing, Vienna, Austria. ISBN 3-900051-07-0, URL <http://www.R-project.org>.

Terink, W., Hurkmans, R.T.W.L., Torfs, P.J.J.F., Uijlenhoet, R., Hydrol, Earth Syst. Sci. 2010, **14**, 687-703.

Venables, W.N., Ripley, B.D., Modern Applied Statistics with S, Springer, 2002.

Warren, R., Mastrandrea, M. D., Hope, C., and Hof, A.F., 2010. "Variations in the climatic response to SRES emissions scenarios in integrated assessment models".

Annex 2: About the consortium

Allianz SE

The Allianz Group is one of the leading integrated financial services providers worldwide. With approximately 151,000 employees worldwide, the Allianz Group serves more than 76 million customers in about 70 countries. On the insurance side, Allianz is the market leader in the German market and has a strong international presence.

In fiscal 2010 the Allianz Group achieved total revenues of over 106.5 billion euros. Allianz is also one of the world's largest asset managers, with third-party assets of 1,164 billion euros under management at year end 2010. Beyond the quality of our financial performance, a number of other activities and factors are important for the sustainable growth of our competitive strength and company value. These include, but are not limited to, our global diversification, the reduction of complexity, our value-based management approach, and our crucially important employees.

Natural catastrophes and climate change pose potential threats to reinsurance companies like Allianz, therefore a solid knowledge base and evaluation of risks are essential parts of our daily business. With respect to natural catastrophes one can state that thanks to ever better risk models insurers are able to manage their portfolios more precisely and make sure that their financial protection is adequate. Such models also help to determine in more detail where and at what cost insurance can be offered and ultimately this means that a better cover can be offered. Our re-insurance unit AllianzRe is responsible for the development and maintenance of such models.

Responding to climate change, Allianz created a dedicated Group-wide centre of competence on climate change: Allianz Climate Solutions (ACS) serves other Allianz entities as well as external customers with its risk analysis, investment and insurance expertise – with a clear focus on renewable energies, clean technologies and the carbon market. ACS bundles the expertise and experience of various Allianz business entities in order to offer the optimum service to our clients.

WWF Deutschland

WWF is one of the world's largest and most experienced independent conservation organisations, with over 5 million supporters and a global network active in more than 100 countries.

WWF's mission is to stop the degradation of the planet's natural environment and to build a future in which humans live in harmony with nature, by conserving the world's biological diversity, ensuring that the use of renewable natural resources is sustainable, and promoting the reduction of pollution and wasteful consumption.

Intermap® Technologies

Intermap® (www.intermap.com) is a leading provider of Location-Based Information (LBI), setting the industry standard for creating high-resolution 3D digital models of the earth's surface. The Company has remapped entire countries, to build NEXTMap® national databases consisting of affordably priced elevation data and geometric images of unparalleled accuracy. Turnkey solutions can be accessed through the Company's NEXTMap Online Store, a hosted web services platform offering a variety of subscription levels by geography, data-layer, individual or enterprise wide license. Intermap's cloud-based hosted model offers customers the most convenient and affordable method to satisfy a customer's needs with both a Platform as a service (PaaS) and Software as a service (SaaS) options.

Intermap®'s rich history in digital mapping and geospatial services began in 1974 by a team of radar engineers and scientists, many of whom continue to contribute to the development of the technology and award-winning production system. Intermap® was founded in 1997 with employees and operations worldwide that serve a diverse geospatial marketplace. Intermap® has headquarters in Denver, Colorado, with several other office locations around the world. Intermap® is publicly traded company on the Toronto Stock Exchange.

Met Office

The Met Office is the National Meteorological Service (NMS) for the United Kingdom and one of the world's leading weather and climate service providers. We support a large number of customers across civil aviation, defence, commerce, financial markets and industry. We supply data, products and services to many countries throughout the world. The Met Office provides essential services 24/7, 365 days a year, including weather, climate and environmental forecasts and severe weather warnings for the protection of life and property.

The Met Office is a UK-government trading fund formed in 1854 and now owned by the UK Department of Business, Innovation and Skills (as of July 2011). We have a staff of approximately 1,800 of which more than 500 are meteorologists, hydrologists and climate scientists.

The **Met Office Hadley Centre** is one of the world's leading climate change research centres. We produce world-class guidance on the science of climate variability and change, and provide a focus in the UK for the scientific issues associated with climate change. Largely co-funded by Department of Energy and Climate Change (DECC) and Defra (the Department for Environment, Food and Rural Affairs), we provide in-depth information to, and advise, the Government on climate change issues.

Our scientists make significant contributions to peer-reviewed literature and to a variety of climate change reports, including the Assessment Report of the IPCC. Our climate projections were the basis for the Stern Review (2006) on the Economics of Climate Change.

The Times Higher Educational Supplement named the Met Office as the world's "top geosciences research centre" in 2009 in comparison to the impact (citations) of its scientific papers.

JBA Consulting

JBA Consulting was founded in 1995 and now has 220 staff in 13 offices across the UK and Ireland. JBA is one of Europe's leading specialists in risk and environmental management and our expertise in hydrology and hydraulic modelling is respected worldwide. We also have key strengths in software development and programming, GIS, engineering, spatial modelling and extreme value statistics. JBA has a history of quality consulting to government organisations and private companies alike. In the insurance and reinsurance sector, we provide probabilistic analysis and loss calculation services to a range of clients and are the leading provider of flood hazard mapping solutions aimed at underwriting in the UK, Ireland and France. In 2010, JBA was named Medium Consultant of the Year at the New Civil Engineer Awards.

For more information please visit www.jbaconsulting.co.uk.

Annex 3: Flood analysis

See following report supplied by JBA Consulting -

2010s4094 - Italy Pluvial Flood Modelling

Final Report

May 2011

**Prepared for:
Intermap Technologies GmbH**

In collaboration with:

Allianz SE, WWF and the Met Office

Contract and report

This report describes work commissioned by Intermap Technologies on behalf of Allianz SE and WWF Deutschland under the contract dated 6th October 2010 for the provision of pluvial modelling for a defined territory in Italy.

Prepared by Cressida Ford BA Cert NatSci (Open)
Assistant Analyst

Leanne Farrell BSc
Technical Assistant

Reviewed by Jane Toothill BSc PhD FGS
Technical Director

Purpose

This document has been prepared as a technical report for Intermap Technologies. JBA Consulting accepts no responsibility or liability for any use that is made of this document other than by the Client for the purposes for which it was originally commissioned and prepared. JBA Consulting has no liability regarding the use of this report except to Intermap Technologies.

Copyright

© Jeremy Benn Associates Limited 2011

Carbon Footprint



A printed copy of the main text in this document will result in a carbon footprint of 239g if 100% post-consumer recycled paper is used and 304g if primary-source paper is used. These figures assume the report is printed in black and white on A4 paper and in duplex.

JBA is a carbon neutral company and the carbon emissions from our activities are offset.

Front page: High river levels in Treviso following heavy local and regional rainfall, October 2010. © J Toothill

Executive Summary

In October 2010, JBA was approached by Intermap Technologies to participate in a project involving the assessment of climate change on surface water (or "pluvial") flooding in northern Italy in a project in collaboration with WWF Deutschland, Allianz Re and the Met Office. JBA's role in the project is to conduct surface water modelling on Intermap's 5m-resolution NEXTMap Europe DTM, using data supplied by Intermap and the Met Office.

Two phases of work involve

- The simulation of flooding caused by a selection of historical events for testing
- Use of similar techniques to model flooding caused by a series of scenarios for current and future climate

This report follows the completion of the project, the first phase of which concerned the modelling of historic events in a test area surrounding Venice, affected by flooding in September 2007. This phase was used to determine the parameters under which Phase 2 should be carried out.

Phase 2 is concerned with the modelling of nine climate scenarios (five future, four present) derived from three separate climate models for an extended area surrounding and including the Phase 1 test area. As part of Phase 2, the flood map for Event 3 has been re-issued inclusive of a refined implementation of soil infiltration data and using improved post-processing techniques.

The depth grids and extents for the Phase 2 scenarios have been processed using the procedure determined in Phase 1 and various methods sought by which the results may be ranked. These include ranking by

- area of total extent
- area of extent intersecting suburban and urban areas (derived from soil data)
- volume of water in the final results
- combined ranking of all the above

From these ranking orders, the conclusion is generally drawn that two events can be said to be the most and least severe. These are the 2096 and 1985 scenarios respectively, both from the HADRM3Q10 climate model; although the 2079 scenario from HADRM3Q16 ranks equally high in the combined ranking, it is thought that emphasis should perhaps in this case lie more heavily on the event whose extent bears the greatest intersection with urban and suburban areas.

Contents

Executive Summary	ii
1. Data for Phase 1	1
1.1 Rainfall data.....	1
1.2 Soil data.....	6
1.3 DTM.....	7
2. Phase 1 - Hydrology	10
2.1 Calculation of runoff values.....	10
2.2 Manning's <i>n</i>	11
2.3 Antecedent conditions (combining soil data and rainfall).....	12
3. JFlow+	16
3.1 What is JFlow+?.....	16
3.2 Inputs.....	16
3.3 Outputs.....	17
3.4 Post-processing flood data.....	17
3.5 Impact of the DTM on results.....	17
3.6 Post-processing: An overview.....	19
4. Results and recommendations from Phase 1	28
4.1 Phase 1 deliverables.....	28
4.2 Recommendations for Phase 2.....	28
5. Phase 2: Running Climate Scenarios	29
5.1 Data.....	29
5.2 Hydrology.....	29
5.3 Modelling.....	29
6. Phase 2 Results	30
6.1 Nine modelled events.....	30
6.2 Rank by extent.....	38
6.3 Hydrological variations.....	39
6.4 Rank by area.....	42
6.5 Rank by volume.....	46
6.6 Rank by score.....	46
7. Conclusion	47
References	I
A. Appendix A: CORINE land use classes	II

List of Figures

Figure 1-1 Tiles overlapping by 500m: 6km tiles but a 5km grid	2
Figure 1-2 All data points with tiles (2,905 records)	2
Figure 1-3 Thinned dataset (114 records)	3
Figure 1-4 Peak data sample points	3
Figure 1-5 Identifying events from graph data	4
Figure 1-6 Event 01 average rainfall	4
Figure 1-7 Event 02 average rainfall	5
Figure 1-8 Event 03 average rainfall	5
Figure 1-9 Event 01 maximum rainfall	5
Figure 1-10 Event 02 maximum rainfall	6
Figure 1-11 Event 03 maximum rainfall	6
Figure 1-12 DTM tiles supplied for Venice test area	7
Figure 1-13 Obstructed drainage channel holds back water	8
Figure 1-14 Depths upstream of structure are alleviated; water flows through	9
Figure 2-1 Final merged and attributed CN polygons	10
Figure 2-2 Effects of altering Manning's <i>n</i>	12
Figure 2-3 Relationships between CN depending on antecedent soil moisture	14
Figure 2-4 Impact of antecedent moisture conditions on tile with CN 74 for Event 03	15
Figure 2-5 Depths of 0.3m or greater for steady AMCII (CN 74) and Rolling AMC	15
Figure 3-1 JFlow+ principles: direction of flow on DTM	16
Figure 3-2 Effect of DTM on water depths	18
Figure 3-3 Actual terrain, looking along surface path shown by red line in Figure 3-4	18
Figure 3-4 DTM elevation variation in rural area (Graph left to right = furthest from camera to nearest camera in Figure 3-3)	19
Figure 3-8 Flooding in Treviso	20
Figure 3-9 Location of Treviso (Bing Maps)	21
Figure 3-10 Before any post processing	22
Figure 3-11 0.05m depth removed	22
Figure 3-12 0.3m depth removed	23
Figure 3-13 0.4m depth removed	23
Figure 3-14 Red: 0.3m depths removed vs. Purple: 0.4m depths removed	24
Figure 3-15 Removed 0.3m depth / 75m ² area	25
Figure 3-16 Removed 0.3m depth / 250m ² area	25
Figure 3-17 Removed 0.3m depth / 900m ² area	26
Figure 3-18 Removed 0.3m depth / 1800m ² area	26

Figure 3-19 Comparing extents (Red: removed depths shallower than 0.3m, no ponds removed; Purple: removed depths shallower than 0.3m and areas smaller than 1800m ²)	27
Figure 6-1 FIXK_P85	30
Figure 6-2 FIXC_F84	31
Figure 6-3 FIXQ_F86	32
Figure 6-4 FIXK_P76	33
Figure 6-5 FIXC_P74	34
Figure 6-6 FIXC_F83	35
Figure 6-7 FIXQ_P74	36
Figure 6-8 FIXK_F96	37
Figure 6-9 FIXQ_F79	38
Figure 6-10 FIXK_P85 vs. FIXQ_F79, Treviso	39
Figure 6-11 Comparing average hourly rainfall between events	40
Figure 6-12 Comparing maximum hourly rainfall between events.....	41
Figure 6-13 Comparing total event rainfall between events.....	42
Figure 6-14 FIXQ_F79 overlay Event 3	43
Figure 6-15 Event 3 overlay FIXQ_F79	44
Figure 6-16 Showing discrepancy between Phase 1 (red) and Phase 2 (blue) modelling areas and data point locations.....	45

List of Tables

Table 1-1 Rainfall data input format.....	1
Table 1-2 Rainfall location data format.....	1
Table 1-3 Rainfall events identified.....	4
Table 1-4 Attributes of soil data polygons supplied	7
Table 2-1 Relating supplied CN (AMC II) to AMC I and AMC III.....	13
Table 2-2 Relating derived CN (AMC II) to AMC I and AMC III.....	14
Table 5-1 Scenarios identified.....	29
Table 6-1 Ranking events by total area and by sub/urban intersection area	42
Table 6-2 Ranking events by extent area within coincident model region	45
Table 6-3 Ranking events by floodwater volume	46
Table 6-4 Ranking events by total ranking scores	46

Abbreviations

AMC - antecedent moisture condition (AMC II being the standard assumption)
ARPAV - l'Agenzia Regionale per la Prevenzione e Protezione Ambientale del Veneto (Regional Agency of Environmental Prevention and Protection of Venice)
CN - curve number
DTM - digital terrain model
ECMWF - European Centre for Medium-Range Weather Forecasts
ETRS - European Terrestrial Reference System
LAEA - Lambert Azimuthal Equal Area
NRCS - Natural Resources Conservation Service
RCM - regional climate model
SCS - Soil Conservation Service (now NRCS)
SGDBE - Soil Geographical Database of Europe
USDA - United States Department of Agriculture
WGS - World Geodetic System
WWF - World Wide Fund for Nature

Definitions

ERA-40 - An ECMWF re-analysis of global atmosphere and surface conditions for the period from September 1957 to August 2002
ISIS - a suite of hydrological and hydraulic tools by Halcrow
Manning's n - a coefficient denoting the coarseness of terrain
TR-55 - USDA Soil Conservation Service's Technical Release 55: *Urban Hydrology for Small Watersheds*. This is a widely-used approach to hydrology dating back to 1975. A TR-55 computer program can now carry out the calculations automatically

Acknowledgements

Background maps, where displayed, Bing Maps © 2011 Microsoft Corporation and its data suppliers

Street view images © Google - these images are not licensed for distribution beyond the project group.

1. Data for Phase 1

The following datasets were our starting point for the work carried out. Following discussions between the project partners, the projection used for this project is ETRS 1989 Lambert Azimuthal Equal Area ("ETRS"). Allianz AG has requested that deliverables also be supplied in the geographic co-ordinate system WGS 84.

1.1 Rainfall data

1.1.1 Specification

Rainfall data were supplied by the Met Office. The format required was one that would allow import into JBA's database for surface water modelling. The specification for the data was as follows:

ID	TimeIntervalHours	NumberOfValues	1 (mm)	2 (mm)	...n
Identifier of rainfall point (point forms centroid of 5km x 5km tile) (unique)	Length of time between each value of the hyetograph	How many values form the hyetograph	Rainfall in first time interval	Rainfall in second time interval	Rainfall in n th time interval

A second table allows the information associated with each record in the first table to be linked to its location (to be spaced 5km apart in each direction):

ID	X (m)	Y (m)	X_min (m)	Y_min (m)	X_max (m)	Y_max (m)
Identifier of rainfall point (forms centroid of 5km x 5km tile) (unique)	Easting of point according to DTM projection	Northing of point according to DTM projection	Easting for SW vertex of tile	Northing for SW vertex of tile	Easting for NE vertex of tile	Northing for NE vertex of tile

It is important for modelling that points are spaced at 5000m; JFlow+ operates by drawing a "tile" around the data point, extracting the area of DTM that falls within that tile's boundaries, and placing the rainfall values defined by the hyetograph onto it over the course of the simulation, whilst modelling where and how it will flow over the ground.

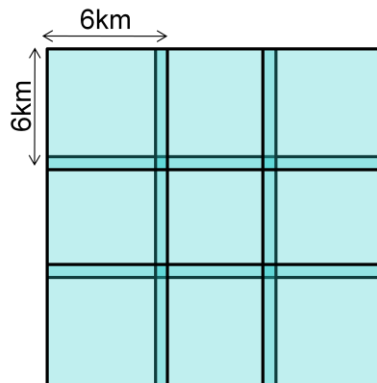
The "tile" is defined using four fields, "X min", "Y min", "X max" and "Y max". These are derived as follows:

$X_{min} = X_p - 3000$
$Y_{min} = Y_p - 3000$
$X_{max} = X_p + 3000$
$Y_{max} = Y_p + 3000$

where the X co-ordinate of the data point = " X_p " and the Y co-ordinate of the data point = " Y_p "

Tile widths of 6km are used so that the model results from each individual JFlow+ analysis (carried out for a single tile) overlap slightly to provide a continuous extent.

Figure 1-1 Tiles overlapping by 500m: 6km tiles but a 5km grid



1.1.2 Data received

The data supplied were evenly spaced in decimal degrees at approximately 1km spacing. In order to obtain data in the required data format (evenly spaced, projected data at 5km resolution), it was agreed that JBA would select from the initial dataset a projected dataset spaced at approximately 5km for the purposes of Phase 1. Tiles were generated for each of the points and a set of tiles was then selected manually to cover the same extent. Tiles which represented rainfall in the sea were excluded, as were those which did not intersect the extent of the DTM (shown in grey in the figures below).

Figure 1-2 All data points with tiles (2,905 records)

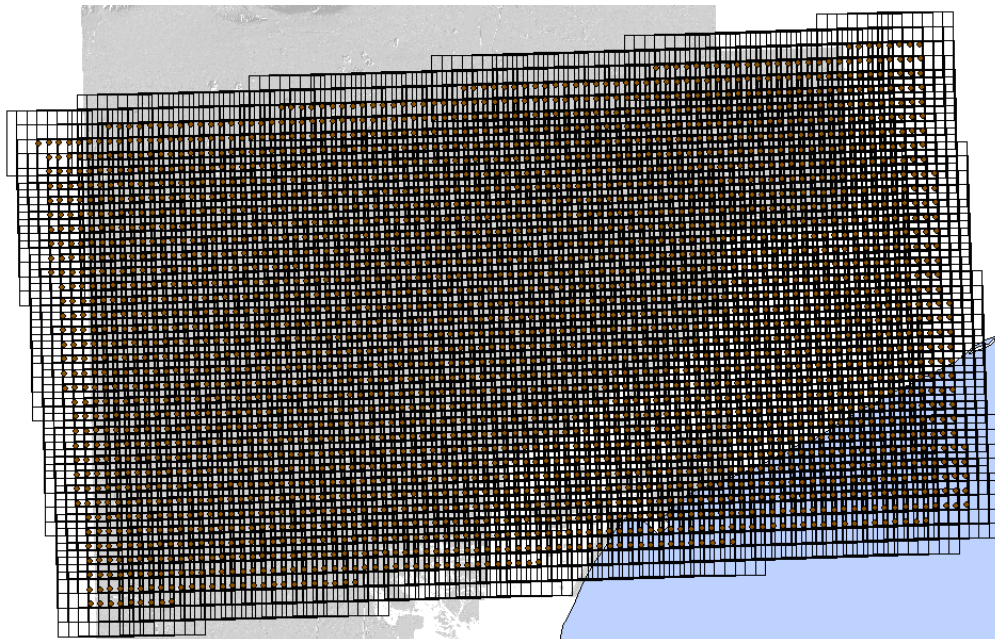
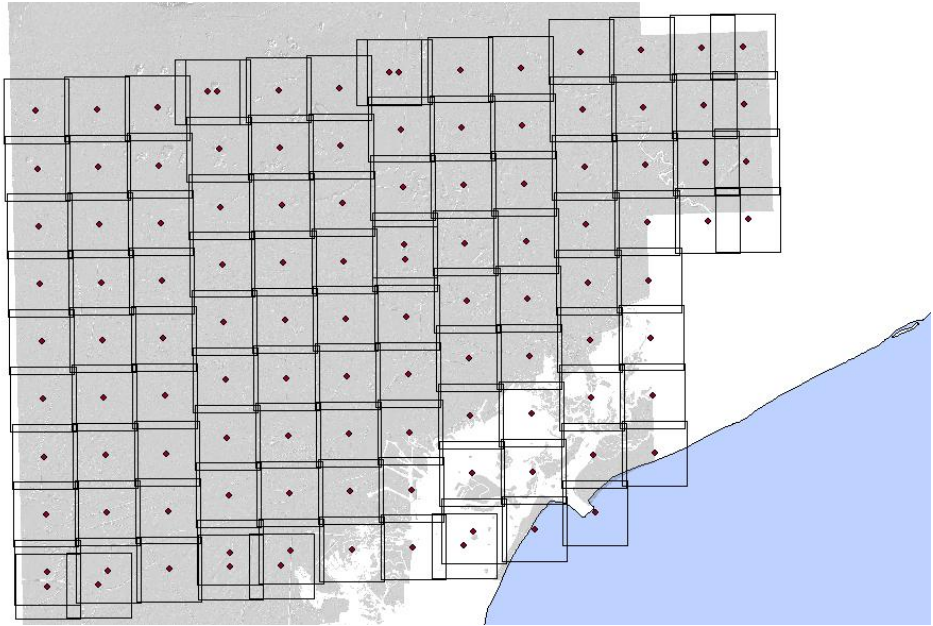


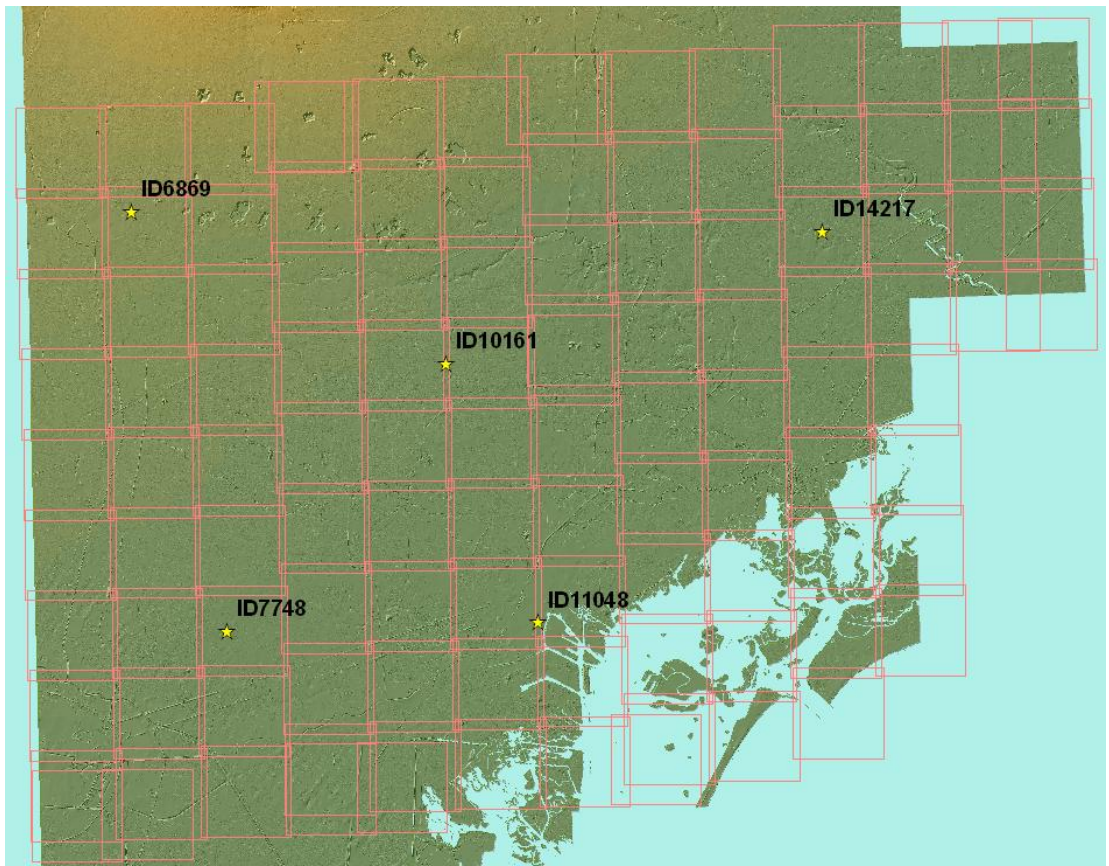
Figure 1-3 Thinned dataset (114 records)



1.1.3 Events

The three historic events for which modelling was required were contained in a month's worth of rainfall data supplied by the Met Office. In order to identify these events within the large dataset, five points were selected based on the visual criterion that they covered different areas of the test region.

Figure 1-4 Peak data sample points



The month-long records for these five points enabled the start and finish dates of the events to be identified, as illustrated in Figure 1-5.

Figure 1-5 Identifying events from graph data

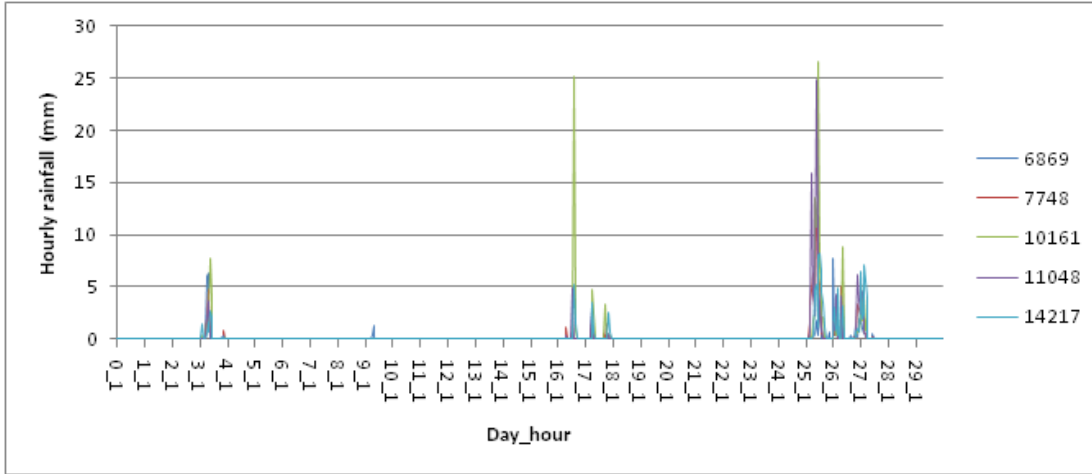


Table 1-3 gives the start and end times used for each of the three events.

Table 1-3 Rainfall events identified					
Event	Start day	Start hour	End day	End hour	Event duration (hours)
Event 01	Day 3	2	Day 3	13	12
Event 02	Day 16	8	Day 17	23	40
Event 03	Day 25	2	Day 27	15	62

1.1.4 The events

It is not possible, as it is with design events, to compare the events in terms of "biggest" or "smallest". The rainfall intensity, as is to be expected of historic data, varies by location and event. In brief, Event 01 is a short, intense event with a single peak, with heavy rainfall across the north-western and south-western parts of the study area, while Event 03 represents protracted spells of steady rainfall, with the most intense rainfall occurring in one spot around the urban area of Mogliano Veneto. Event 02 is, appropriately, in between these two extremes.

Figure 1-6 Event 01 average rainfall

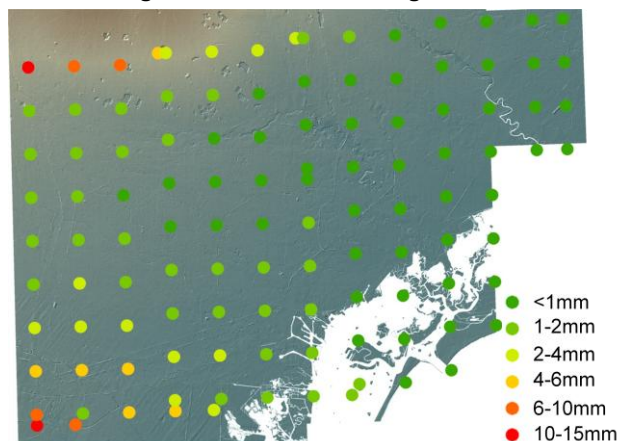


Figure 1-7 Event 02 average rainfall

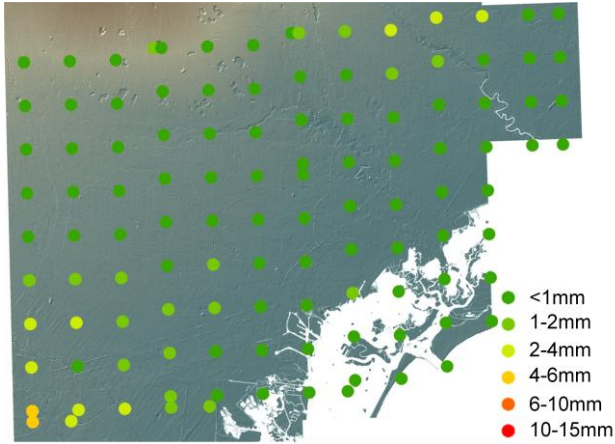


Figure 1-8 Event 03 average rainfall

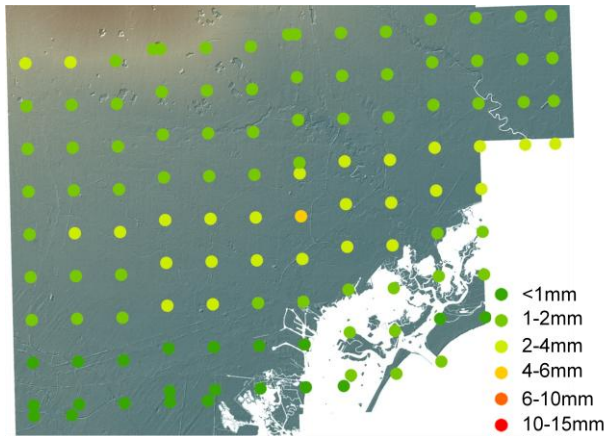


Figure 1-9 Event 01 maximum rainfall

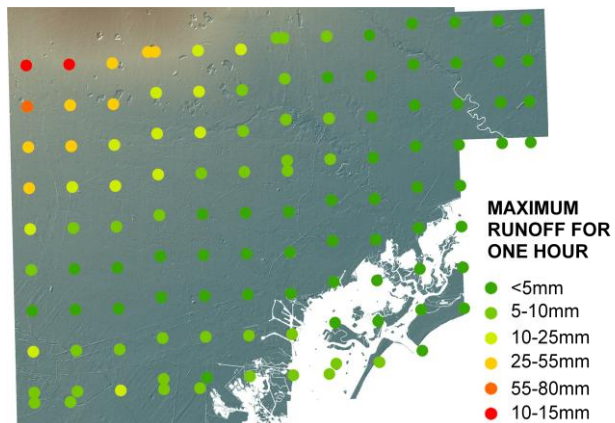


Figure 1-10 Event 02 maximum rainfall

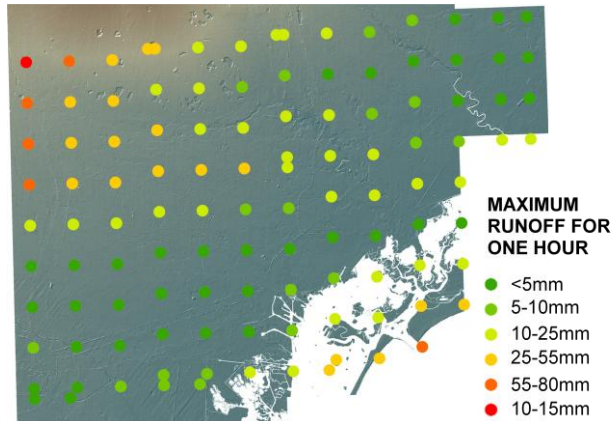
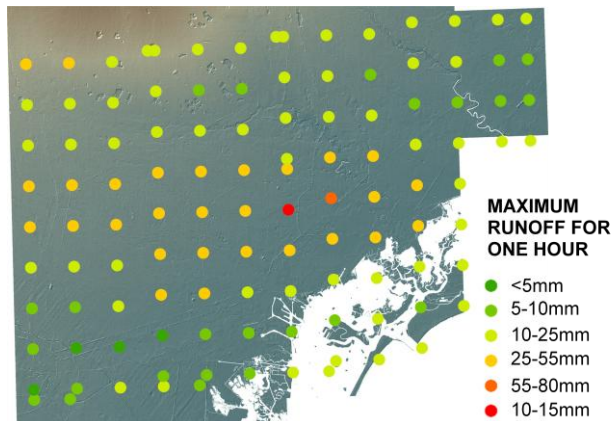


Figure 1-11 Event 03 maximum rainfall



1.2 Soil data

Soil data were sourced from the European Soil Database¹ and processed and prepared by Intermap Technologies for the purposes of deriving infiltration coefficients for the pluvial modelling. The hydraulic soil parameters were derived using pedotransfer functions from the following soil attributes:

- Dominant parent material
- Dominant annual average soil water regime class of the soil profile
- Hydrogeological class
- Presence of an impermeable layer within the soil profile
- Depth to a gleyed horizon
- Dominant surface textural class of the soil profile
- TEXT-SRF-SEC (Secondary surface textural class of the soil profile)

This information was supplied in the form of ArcGIS shapefile polygons, with the following attributes:

¹ The European Soil Database distribution Version 2.0, European Commission and the European Soil Bureau Network, CD-Rom, EUR 19945 EN, 2004

Table 1-4 Attributes of soil data polygons supplied				
HG_GROUP	HG	CODE_00	CODE	CN
Infiltration rate class (string)	Infiltration rate class (number)	CORINE land use	HG concatenated to CORINE code	Curve number (TR-55)

Values for CN and HG_GROUP were derived using the TR-55 methodology.

HG_GROUP (HG) denotes average infiltration rate estimates (typical values used in TR-55) classed as follows:

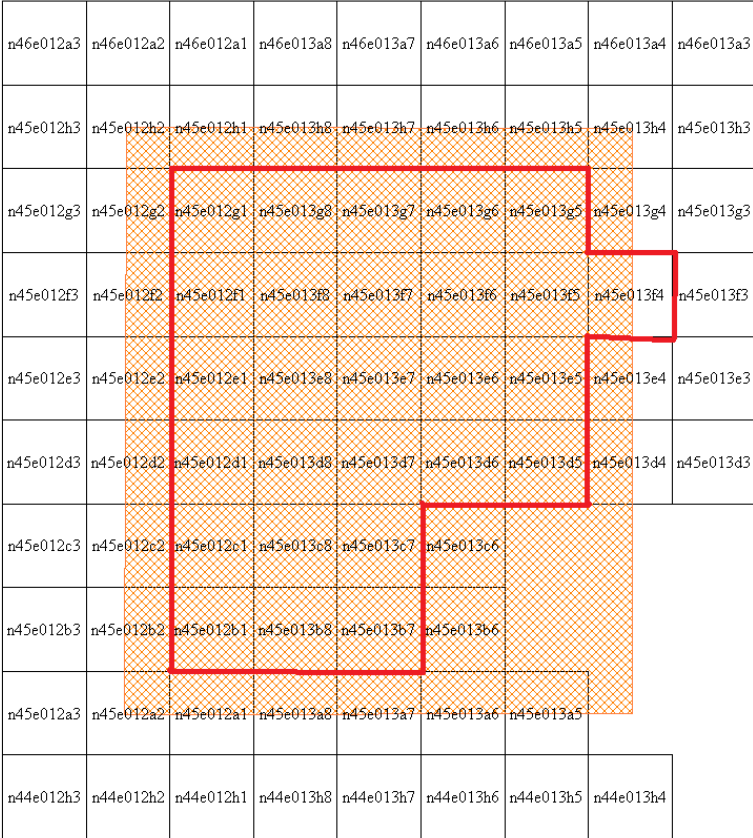
- A (1) = more than 0.12 mm/minute
- B (2) = 0.06 – 0.12 mm/minute
- C = 0.02 – 0.06 mm/minute
- BC (5) = in between B and C
- D (4) = less than 0.02 mm/minute

The CORINE² attribution was used to classify areas of urban, suburban and rural land use. This allowed the creation of a Manning's *n* grid for use in JFlow.

1.3 DTM

The DTM used was Intermap's NEXTMap Europe DTM with 5m posting (cell size) for the Venice area.

Figure 1-12 DTM tiles supplied for Venice test area



² CORINE Land Cover CLC2000

1.3.1 Edits and cuts

Because a DTM is taken from overhead imaging, structures such as bridges that pass over the top of a watercourse or drainage path are displayed as solid embankments that block the natural flow of the water. As part of their core product, Intermap edits "cuts" through embankments such as these to allow watercourses above a given size to pass through. These can have an important effect on the results of the model.

Very small watercourses, on the other hand, and drainage channels which might affect surface water modelling, are not automatically treated. They are identified by manual checking after an initial model run and the affected model tiles can be remodelled once the edits are made. These checks must be made against a background map (for example, Bing Maps aerial imagery, which is included for internal use with the licence for ArcMap 9.3). Without a background map, it would be impossible to determine whether there is a passage through for the water or if it represents a genuine obstructed drainage path. Once cuts have been made, affected tiles must be re-simulated. JBA was therefore prepared to carry out a stage of editing for small drainage paths where necessary; however, it was found that no additional edits to those carried out by Intermap prior to provision of the DTM were necessary.

Figure 1-13 Obstructed drainage channel holds back water

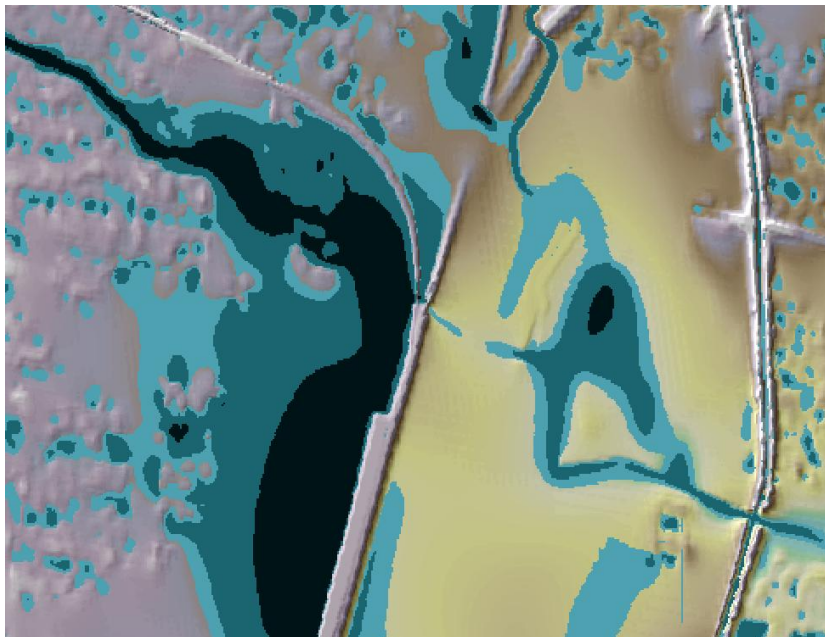
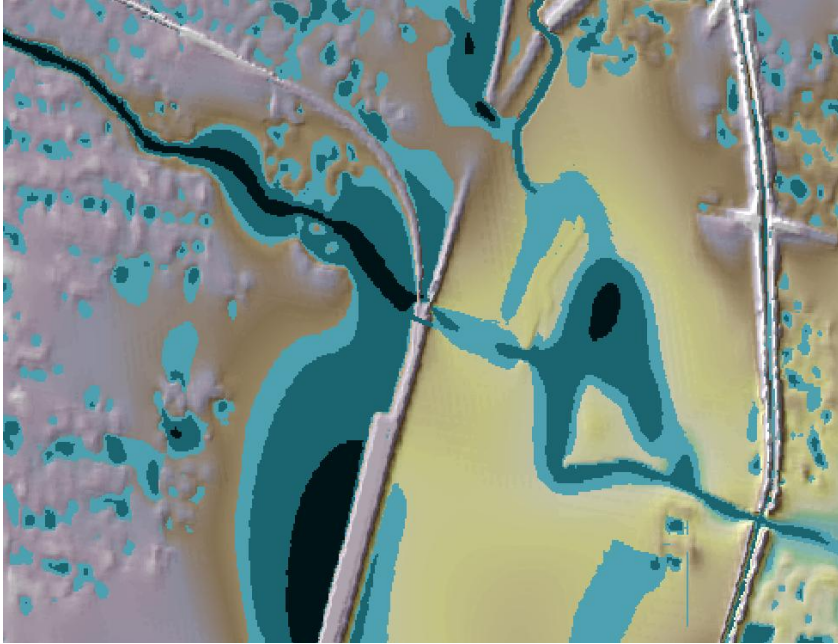


Figure 1-14 Depths upstream of structure are alleviated; water flows through



2. Phase 1 - Hydrology

2.1 Calculation of runoff values

2.1.1 Approach

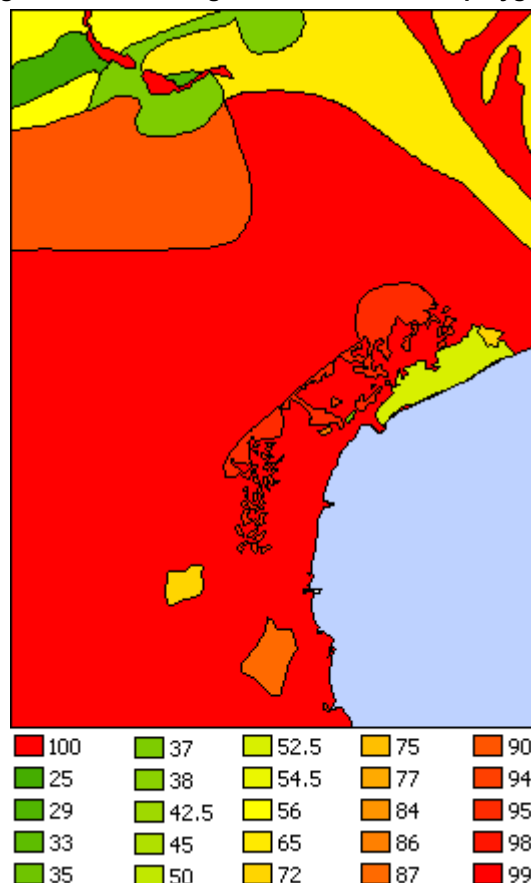
Prior to modelling work being carried out, rainfall data from the hyetograph must be converted to runoff values, accounting for infiltration of water by the soil. The chosen hydrological modelling approach was that of Cronshey et al. (1986). This method provides an equation that enables rainfall values to be converted to runoff values via adjustment of the hyetograph prior to modelling. Different soil types are associated with a curve number ("CN") which, when inserted into the equation below, enables recalculation of the amount of soil runoff. It was necessary to derive a CN for each modelled pixel of rainfall data and adjust the hydrograph for each of the three events accordingly, taking into account changes in infiltration rate that occur with time during (as well as prior to) the event. Event 3 has also been modelled using a CN number derived per pixel of the DTM (the recommended way forwards and approach later used in Phase 2).

2.1.2 Derivation of CN

Each hyetograph was derived for each tile based on the CNs that intersect it, with some tiles potentially having up to six different hyetographs. A 'rainfall mask' was produced by merging the CN shapefile. A curve number was assigned to each pixel of the DTM and the rainfall mask was used to assign the appropriate hyetograph to each cell of the DTM.

The resulting volume of water simulated over the DTM by the model is therefore not uniform but rather reflects the permeability and expected infiltration rate of water into the soil within the area of the tile.

Figure 2-1 Final merged and attributed CN polygons



This shapefile was intersected with the tiles.

2.1.3 Calculation of runoff

The equation linking rainfall to runoff given in TR-55 was then applied to the rainfall for each tile. The equation is as follows:

$$Q = \frac{(P - I_a)^2}{S} \quad \text{if } P > I_a$$

Where

- Q = runoff
- P = rainfall depth
- I_a = initial abstraction, i.e. losses prior to runoff; for example due to infiltration. The method of Cronshey et al. (1986), requires that this value is set to $0.2S$
- S = potential maximum retention after runoff begins.

This equation can be expressed in terms of CN and P , hence enabling calculation of the runoff.

$$Q = \frac{P^2}{1000 - CN} \quad \text{if } P > I_a$$

In some calculations with very small values of P , $(P - I_a)$ gave a negative value, resulting in $Q > P$ and implying that the rainfall was fully absorbed by the ground. In these cases Q was set to 0 for the purposes of modelling.

2.2 Manning's n

Manning's n is an important parameter in the hydraulic modelling process. It relates to the roughness of the ground surface and hence to the frictional effect of that surface in slowing water flow. The value of Manning's n used in modelling should vary with according to the land use type. In general, a higher value of Manning's n will generate slower flow. Information relating to land use was supplied alongside the soil data in the form of CORINE land use codes.

Based on its experience of hydraulic modelling, JBA recommends that the following Manning's n values are used:

- Urban - 0.03
- Suburban - 0.05
- Rural - 0.1

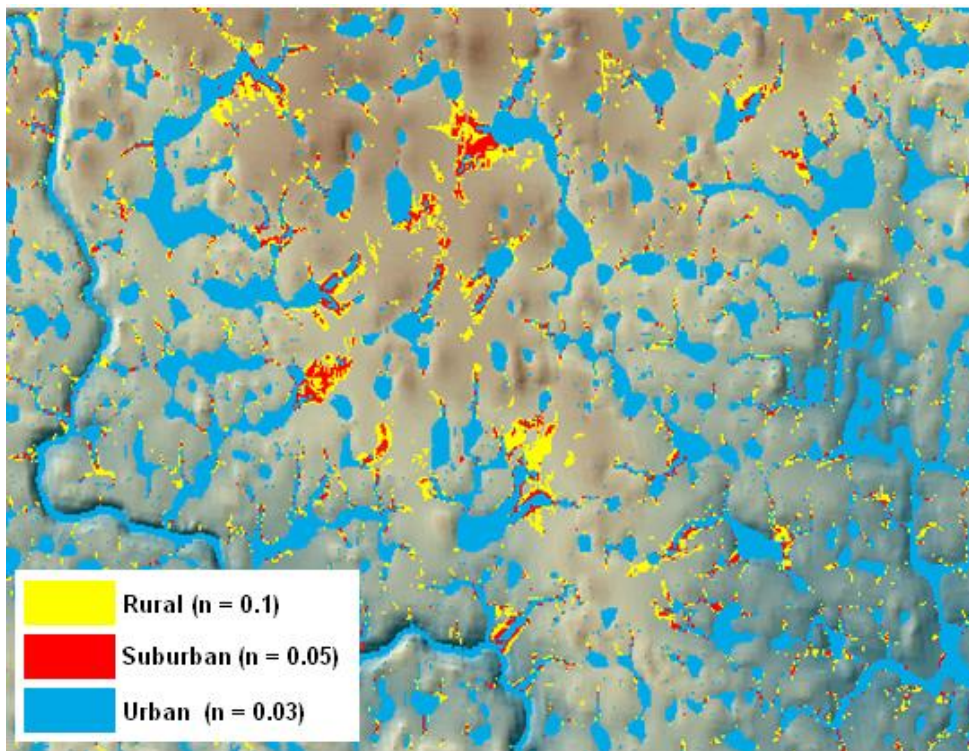
Higher values of Manning's n are used in rural areas, which are characterised by rougher ground surfaces, as opposed to in urban areas, where smooth areas of tarmac such as road provide flow paths along which flood water may spread relatively quickly. These are the values that have been used in the derivation of the Phase 1 flood area (and subsequently in Phase 2). The CORINE data classes were re-categorised to match these three classes and the procedure described above for preparation of the CN number was repeated to obtain a value of Manning's n per tile modelled.

The soil data was attributed with land use data in a shape file. The Land Use field was classified manually based on CORINE land use classes as described in Appendix A.

These were then merged into three categories to assign Manning's n whereby urban is 0.03, sub-urban is 0.05, and rural areas is 0.1. This mask thus informs the model as to the appropriate Manning's n for any given cell.

Relative to other factors in the modelling process, the impact of Manning's n on the eventual flood extents is relatively limited in modelling of this nature. The impact of varying the Manning's n value is demonstrated in the image below. For a test area, we have modelled the flood extent obtained for a single event using one of the three recommended values of Manning's n in each case. A higher value of n means that water does not flow as smoothly, nor therefore as quickly, across the ground. In the map below, the analysis carried out using the (highest) rural Manning's n is overlaid by the run using the suburban value and finally by the analysis carried out using the (lowest) urban Manning's n . The flood extent obtained using the rural value has the greatest flood extent because in a given analysis time, the water does not flow as far, hence has not had time to reach the areas in which rainwater is expected to pool.

Figure 2-2 Effects of altering Manning's n



2.3 Antecedent conditions (combining soil data and rainfall)

The ISIS hydrological tool suite recommends that antecedent conditions be taken into account from rainfall over the five days preceding the event of interest and, based on the quantity of preceding rainfall, groups Antecedent Moisture Conditions ("AMC") into three classes: AMC I, AMC II and AMC III. There are two versions of this grouping, depending on whether the study is for the "growing" (spring/summer) or "dormant" season (autumn/winter). It is assumed that the (September) events provided for modelling are "dormant season" events.

Intermap confirmed that the CNs in the soil data they supplied assumed the standard AMC II. ISIS gives the alternative CN values for the other two condition classes as shown in the table below.

Dormant season conditions

Where total rainfall over the preceding five days is less than 13mm: AMC I.

Total rainfalls from 13mm up to and including 28mm: AMC II (standard assumption, i.e. the figures supplied in the soil data)

Total rainfalls over 28mm: AMC III

The rainfall data supplied by the Met Office was therefore placed into a spreadsheet and the rainfall prior to each event calculated (for Event 01, which begins less than five days into the data period, rainfall prior to the data period was assumed to be 0mm).

Table 2-1 Relating supplied CN (AMC II) to AMC I and AMC III

AMC II	AMC I	AMC III
0	0	0
5	2	13
10	4	22
50	31	70
55	35	75
60	40	78
65	45	82
70	51	85
75	57	88
80	63	91
85	70	94
90	78	96
95	87	98
100	100	100

However, due to the figures supplied, values were required for certain CNs not in the table above. To deal with this problem, the values above were plotted on a graph and the nearest appropriate integer CN read from the trend curve.

Figure 2-3 Relationships between CN depending on antecedent soil moisture

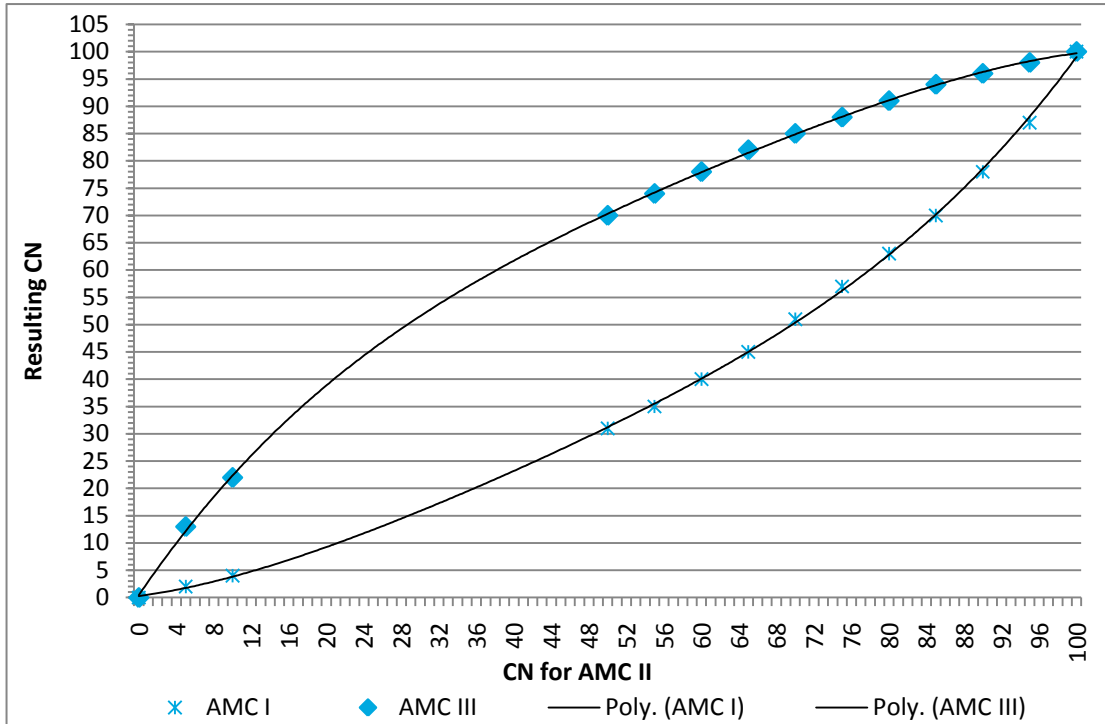


Table 2-2 Relating derived CN (AMC II) to AMC I and AMC III

AMC II	AMC I	AMC III
29	16	48
33	19	53
38	21.5	53.5
42.5	25	63
54.5	34	73
65	45	82
72	51	86
75	57	88
87	74	90
90	78	96
94	85	97
95	87	98
98	94	99
99	96	99.5
100	100	100

Due to the length of the events modelled (12 hours for Event 1, 40 hours for Event 2 and 60 hours for Event 3), CN values were applied to the data on a rolling basis; that is to say, each rainfall value throughout the event took the total for the five days' data preceding it. This was particularly important for the sixty-two-hour-long Event 03, which had little rain in the five days

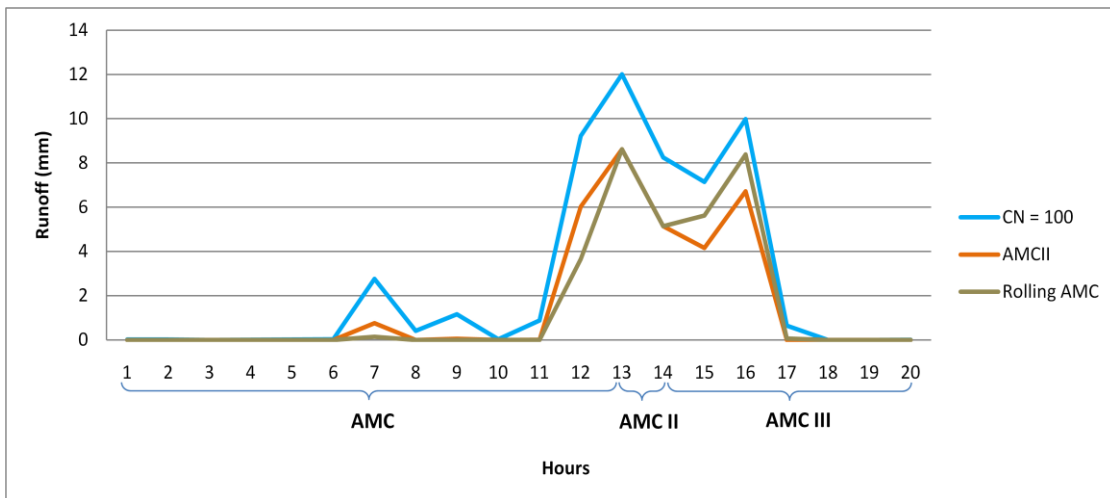
preceding the start of the event but through the course of which the rainfall total well exceeded the upper threshold for AMC II.

In this way, the hydrology for each event takes into account not only antecedent soil conditions but also the change in soil conditions through the course of the event.

The graph below shows the difference between estimating runoff using just the given CN and estimating runoff using a rolling value for antecedent conditions. For comparison, the rainfall values are also given. The graph represents the first 20 hours of a tile in Event 03.

The CN of the tile represented by this graph is 74 as supplied, i.e. for AMC II. For AMC I this is 55 and for AMC III this is 87.

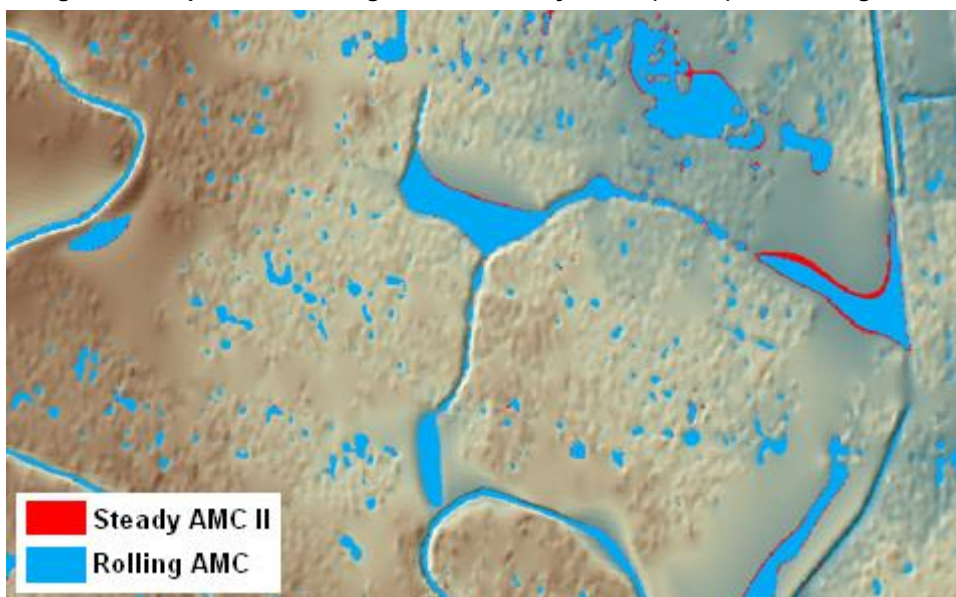
Figure 2-4 Impact of antecedent moisture conditions on tile with CN 74 for Event 03



Note that only at 13 and 14 hours does AMC II apply; after this, AMC III applies and the runoff is much greater than would be calculated using AMC II. Prior to this, runoff is considerably lower than would be calculated using AMC II.

The tile demonstrated above was modelled for Event 03 using both steady AMC II (that is, the runoff calculations directly used the CN derived from the soil data in Section 2.1) and using the rolling AMC value shown in the graph above. The difference in results is relatively minor and shown in Figure 2-5:

Figure 2-5 Depths of 0.3m or greater for steady AMCII (CN 74) and Rolling AMC



3. JFlow+

3.1 What is JFlow+?

JFlow is JBA's proprietary 2D hydraulic model. It can be used to model flooding caused either by overtopping of river defences or surface water flooding. The model solves the full shallow water equations (as opposed to a diffusion wave model) and includes calculations of velocity and momentum to produce depth, velocity and hazard index grids.

JFlow has been coded to run on GPU machines. The resulting "JFlow-GPU" allows the fast and precise modelling of large areas on reasonable timescales. It capitalises on the power of graphical processing units (GPUs) to run flood modelling methodologies up to 1000 times faster. These processors, originally designed for the computer gaming market, are ideal for the grid-based mathematics on which JFlow is based.

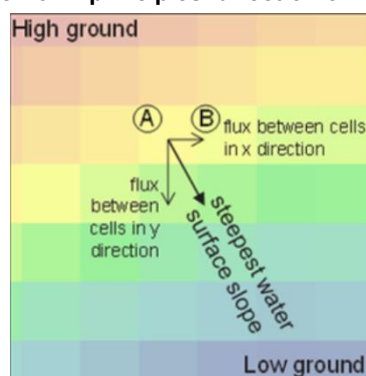
Most recently, the latest upgrade to JFlow, JFlow+, includes improvements to the way in which water momentum and velocity are modelled. JFlow+ represents the latest technology of its kind, its validation having been accepted at the BHS International Symposium in June 2010.

For the Italy project we have used the GPU version of JFlow+.

The mathematic and scientific technology behind JFlow-GPU has been widely published in peer-reviewed scientific literature including the papers Bradbrook (2006), Bradbrook et al. (2004) and Lamb et al. (2009) published by JBA authors. Specific references are provided at the end of this report and can be provided on request. Publicised validation of JFlow model has taken place, comparing outputs against publicly available flood mapping and other models owned by JBA. External benchmarking studies comparing JFlow-GPU with other industry standard software such as ISIS, TUFLOW and MIKE are available on request.

JFlow+ is informed by a hydrological model. In surface water modelling, the quantity of water specified by the hyetograph (Table 1-1) is placed on every cell of the DTM across a tile of a given size (defined by the co-ordinates given in Table 1-2). For this project, a grid of 6km x 6km tiles was used for modelling purposes. This water is then allowed to flow over the DTM, driven by gravity, from high ground to lower ground.

Figure 3-1 JFlow+ principles: direction of flow on DTM



3.2 Inputs

The inputs required by JFlow+ for surface water modelling are as follows:

- Rainfall hyetograph (inclusive of the effects of infiltration)
- Co-ordinates of south-western and north-eastern vertices of each rainfall tile
- Specification of Manning's *n*
- DTM

3.3 Outputs

The outputs of the modelling process are a floodplain extent for each tile of data, for the specific combination of input data analysed. The information available includes water depth, velocity and "hazard" (a combination of depth and velocity data). The output data must be post-processed to form a single continuous floodplain. The sections that follow illustrate some of the post-processing work carried out.

3.4 Post-processing flood data

Prior to progressing towards Phase 2 modelling, it was necessary to determine the criteria that would be used to post-process the flood extent data without impairing them. This is necessary for the following reasons:

- Local inaccuracies and noise in the DTM cause water to pond artificially in apparently "low lying" areas that are in fact an artefact of the DTM data. Such areas can be identified as scattered patches of (normally shallow-depth) flooding.
- The hydraulic modelling process places water on all areas of the ground, generating at least a very shallow water depth on every cell of the DTM; this may flow away from this cell during the course of the modelling but the results show the maximum depth for each cell at any point during the model run and so shallow depths are visible universally prior to processing.

3.5 Impact of the DTM on results

Flood modelling is highly dependent upon the accuracy of the DTM used. 2D hydraulic modelling used the elevation of each DTM cell to calculate flow between cells at each timestep in simulation.

Intermap's NEXTMap DTM is one of the leading products in the market and its high resolution, combined with its widespread availability, make it a good option for flood modelling studies.

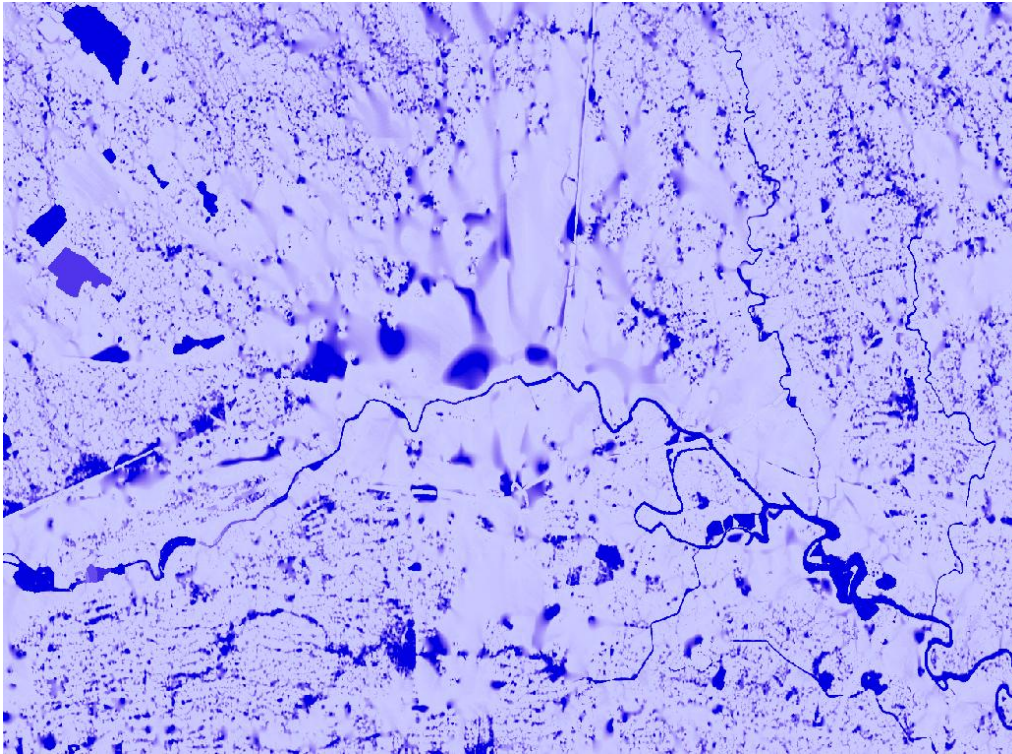
However, while the quality of the input DTM is a direct driver - and the most important - to the quality of the model outputs, no DTM is perfect. A key part of JBA's work is to assess the quality of the DTM and its effects on the model output.

Buildings and other structures are removed in order to create the DTM; this process can result in smoothing effects such as those demonstrated in the image below. Meanwhile, rural areas contain many features and artefacts that require post-processing, such as tall crops, trees, or metal fences, which can cause "noise" and artificial undulations in the terrain.

The figure below shows the unprocessed flood depths for the area surrounding Treviso. As explained in the second point above, water is placed on every cell of the DTM as part of the modelling process, so the unprocessed depth grid shows universal coverage; greater depths are shown by darker shades of blue.

It clearly shows that the water flows very smoothly in the urban area (the smoothed area in the centre of the image) but the "speckled" areas around the edges and in the corners show that the rural terrain is uneven and causes considerable ponding.

Figure 3-2 Effect of DTM on water depths



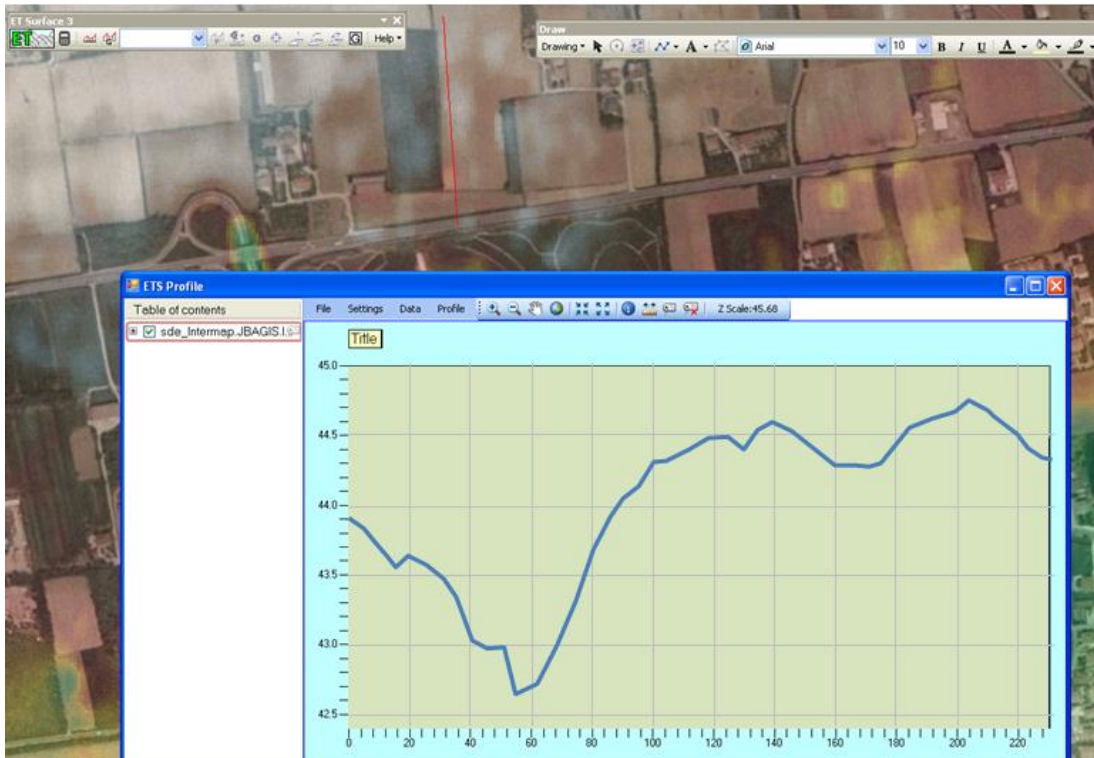
The model region for this project provides a significant challenge in these matters as it is largely very flat, meaning that artificial undulations are more apparent and have a great effect on the flow of water.

Several studies of the DTM revealed that these undulations may be caused by the removal of crops and are not present in the actual terrain. The "ET Surface" tool in Arc GIS was used to show the profile of a straight path (shown by a red line) over a patch of the DTM, as shown below:

Figure 3-3 Actual terrain, looking along surface path shown by red line in Figure 3-4



Figure 3-4 DTM elevation variation in rural area
(Graph left to right = furthest from camera to nearest camera in Figure 3-3)



3.6 Post-processing: An overview

The post-processing stage used follows two key steps:

1. Cut out depths less than a specified measurement
2. Exclude isolated ponds smaller than a defined area

This section of the report sets out the measures taken to establish the values that will be used for post processing; these measures have been determined based on Event 3 from Phase 1 and then applied in the exact same way to every scenario in Phase 2 so as to generate a comparable set of flood outlines based on the same set of assumptions

Samples of the extent at Treviso, taken from Phase 1 Event 3, will be used through this section to show variations in extents that result from different assumptions.

Figure 3-5 Flooding in Treviso



Treviso has been used as a suitable area for detailed investigation of the assumptions required for a number of reasons:

- It represents an area with a concentration of insured exposure
- The area in and around Treviso offer contrasting examples of rural and urban areas, in each of which the DTM is expected to differ in nature
- Treviso is a city with a high exposure to flooding, being built between and around some significant rivers (the centre of the city is surrounded by a river-fed defensive moat) and protected from heavy rainfall events by a series of open storm sewers

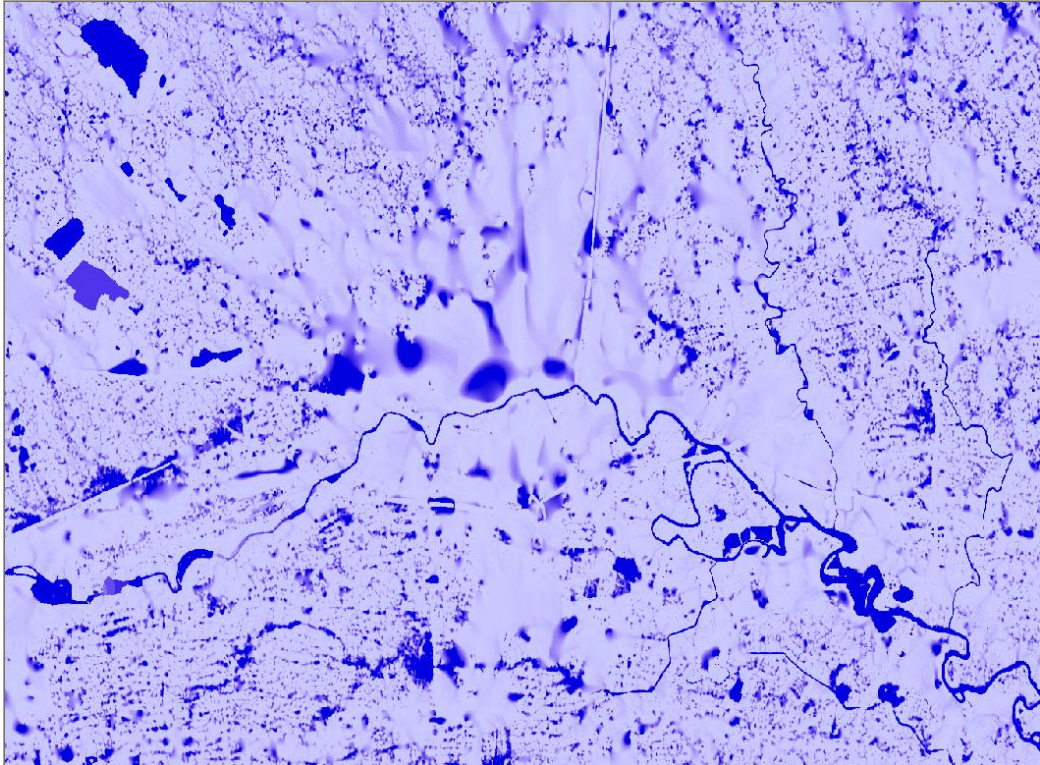
Figure 3-6 Location of Treviso (Bing Maps)



3.6.1 Cut out depths

The first screenshot shows how the extent would look without any depths or areas removed. As stated previously, the model "rains" on every cell of the DTM, meaning that, prior to processing, all cells show up as blue (i.e. wet). Darker shades represent deeper water. In most cases these shallow flood depths are only millimetres deep, and frequently shallower.

Figure 3-7 Before any post processing



Successive depths between 5cm and 40cm were then removed from the results to investigate the impact on the results and optimum level at which depth processing should be applied. Three cases are shown below: 0.05m, 0.3m and 0.4m. No polygons are cut out at this initial stage.

Figure 3-8 0.05m depth removed

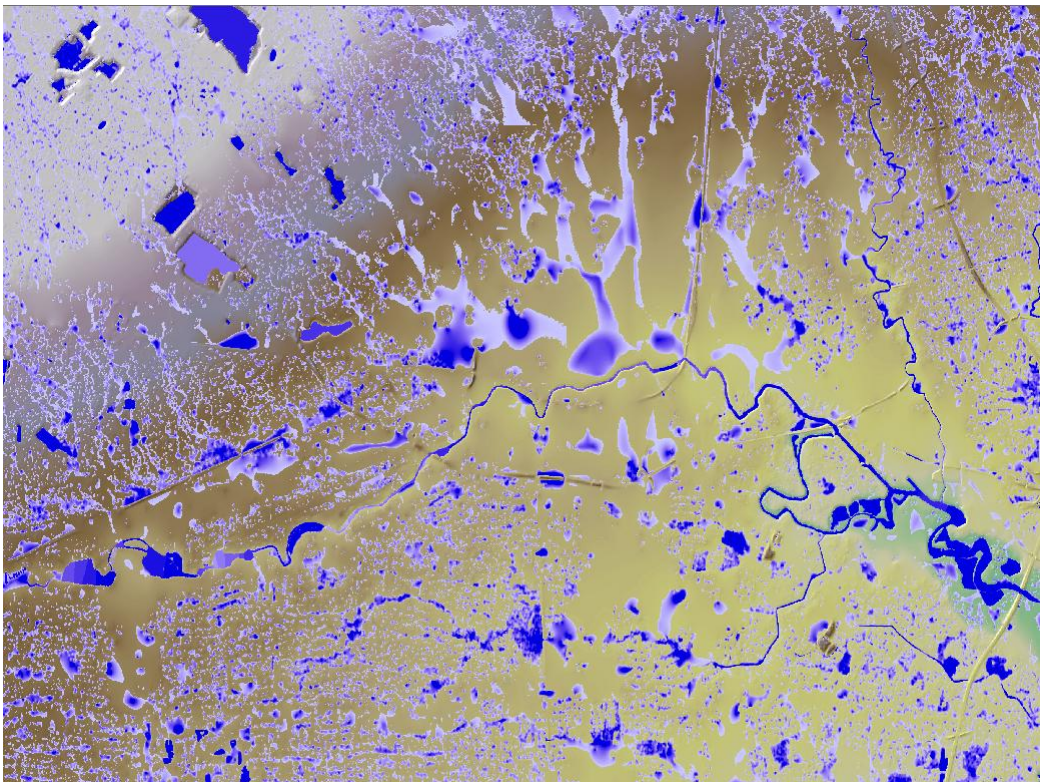


Figure 3-9 0.3m depth removed

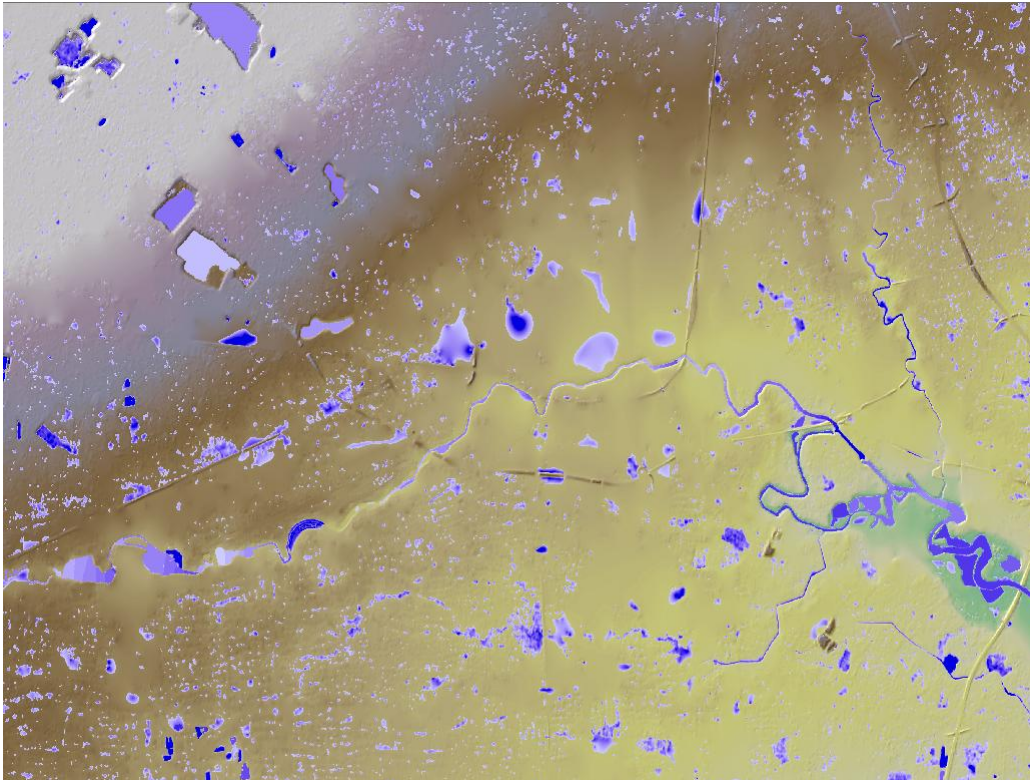
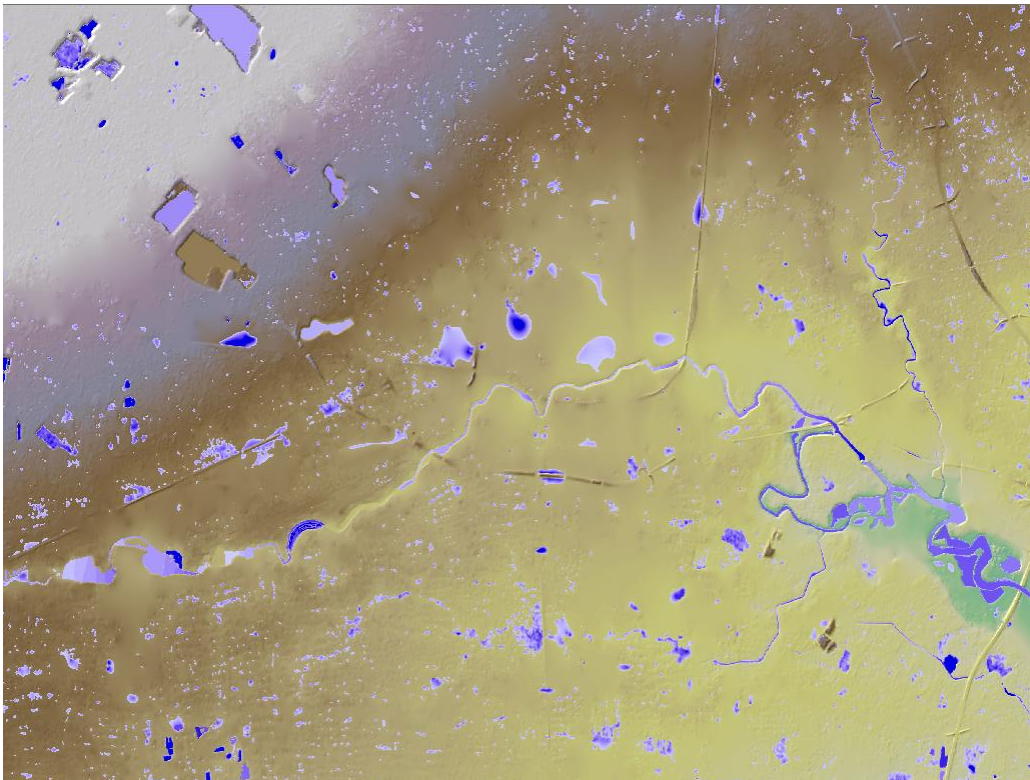
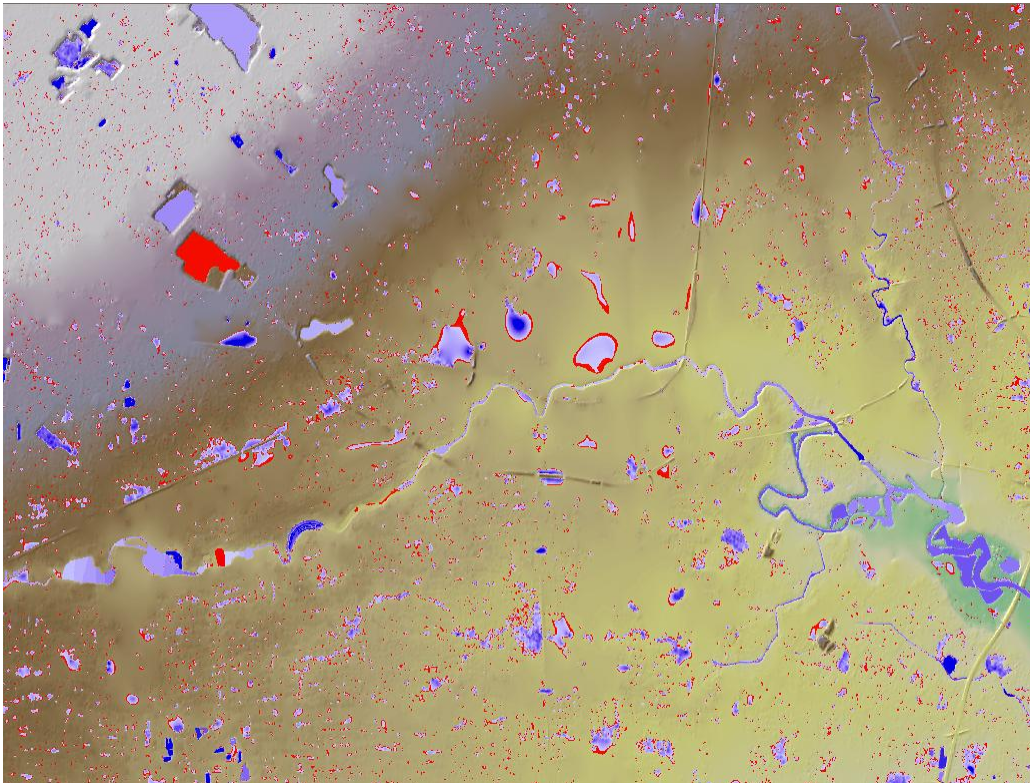


Figure 3-10 0.4m depth removed



The following diagram compares the results in a single map:

Figure 3-11 Red: 0.3m depths removed vs. Purple: 0.4m depths removed



The comparison of the 0.3m and 0.4m above shows that the 0.4m removal potentially strips out significant areas of flood that are “real features”. This is seen where the red “blobs” (the 0.3m depths) show through. This is notably visible in the top left of the screenshot where one red feature stands out. Following discussion with Intermap, who indicated that noise in the DTM may be on the order of 0.3m, it was concluded that 0.3m depth should be used as a cut-off point.

3.6.2 Exclude Isolated Ponds

The next variable that was scrutinized was the minimum polygon size to be included. From the extent with the 0.3m depths cut out, a range of areas were removed: 50m², 75m², 125m², 175m², 250m², 300m², 600m², 900m², 1200m², 1500m² and 1800m². Some examples are displayed below:

Figure 3-12 Removed 0.3m depth / 75m² area

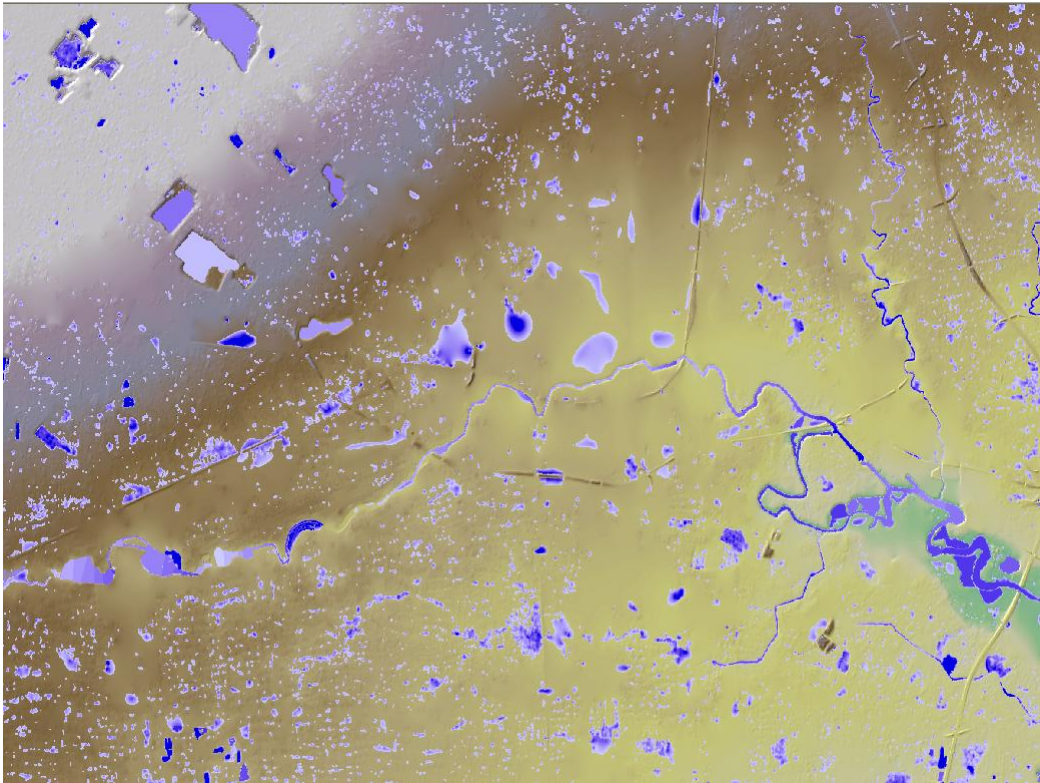


Figure 3-13 Removed 0.3m depth / 250m² area

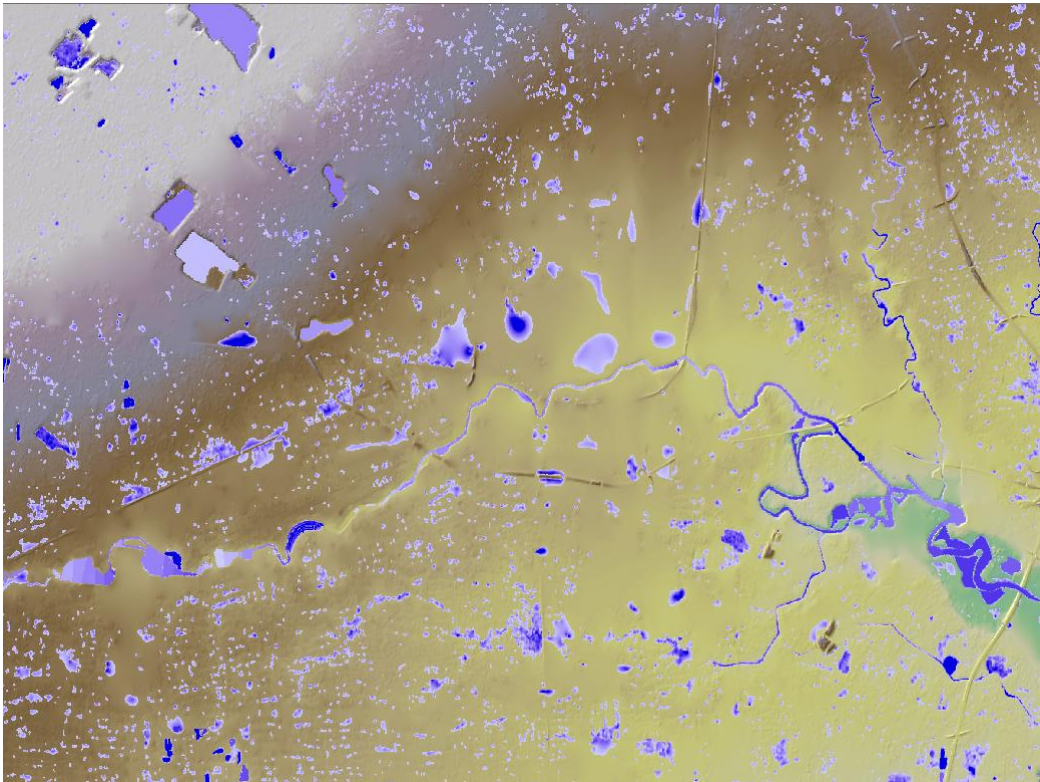


Figure 3-14 Removed 0.3m depth / 900m² area

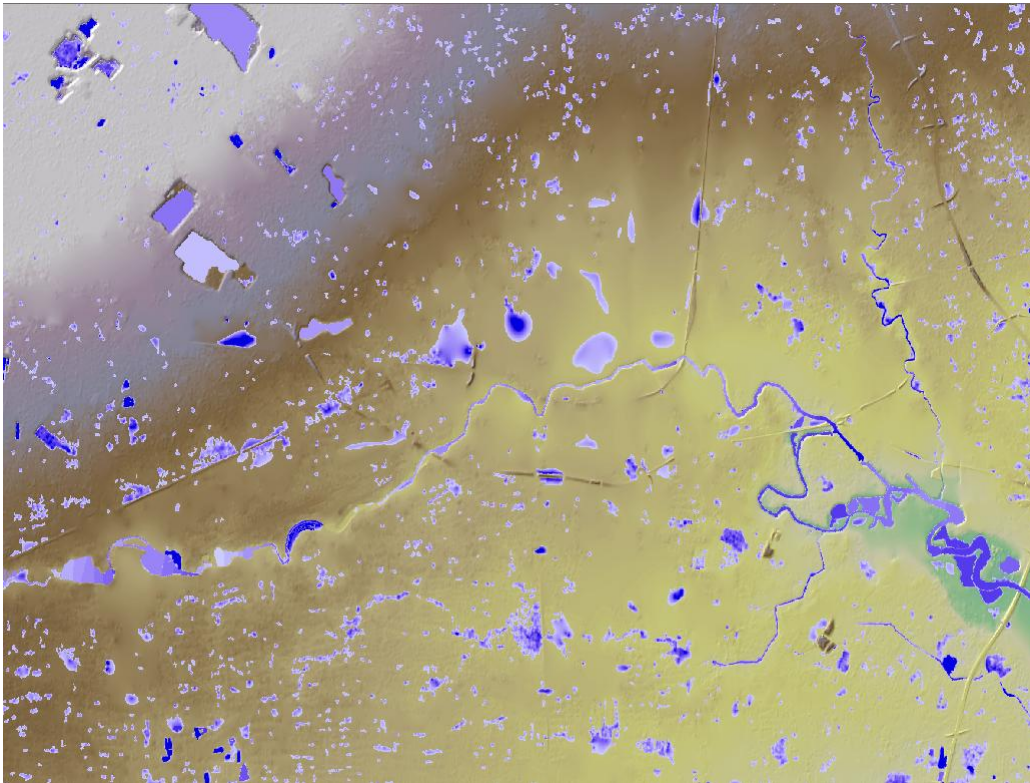
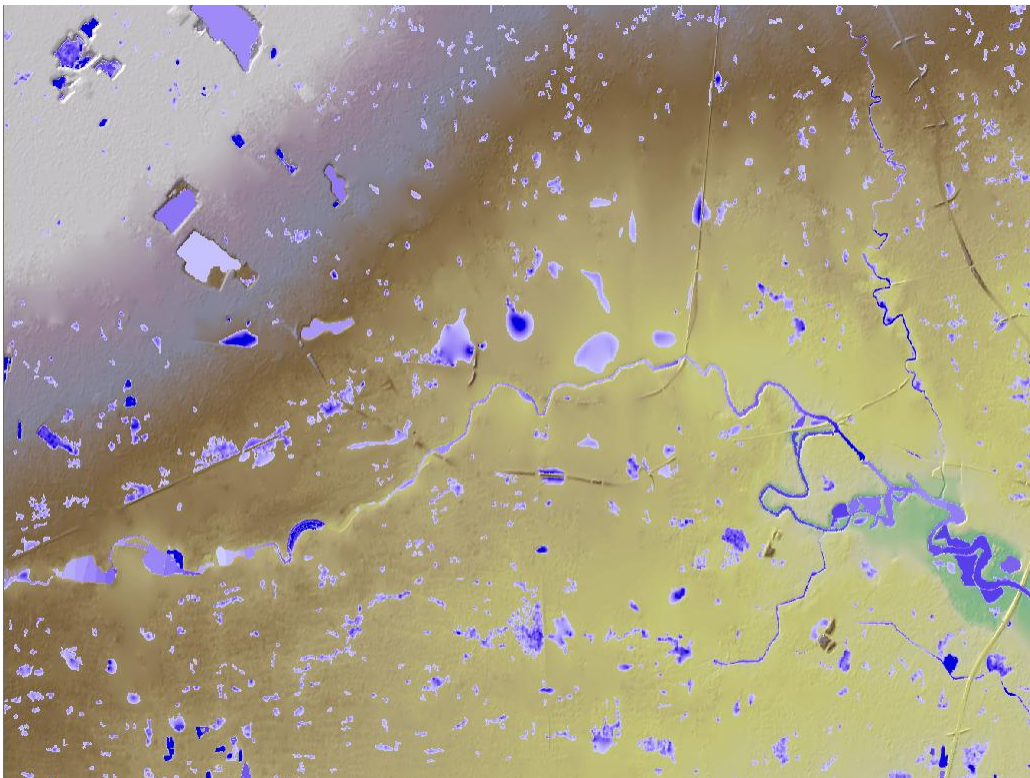


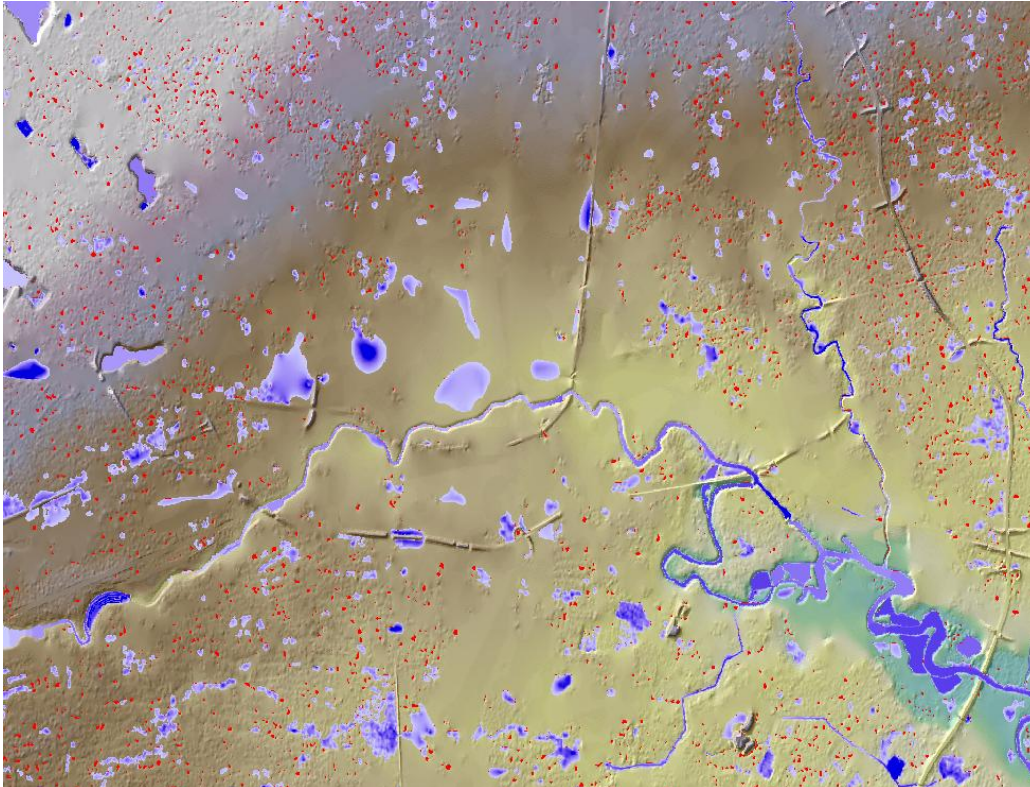
Figure 3-15 Removed 0.3m depth / 1800m² area



A careful review of the maps generated from each of the areal cuts led to the conclusion that the minimum polygon size should be set to 1800m². A comparison of the original data with

the final output having removed ponds smaller than 1800m² from the output is shown below alongside other considerations to illustrate examples of the amount of extent that will be cut out.

Figure 3-16 Comparing extents
(Red: removed depths shallower than 0.3m, no ponds removed;
Purple: removed depths shallower than 0.3m and areas smaller than 1800m²)



3.6.3 Conclusion

The parameters that were selected to be applied through the post processing stage were removal of water depths <0.3m and subsequent removal of polygons <1800m² in extent.

4. Results and recommendations from Phase 1

4.1 Phase 1 deliverables

The deliverables from Phase 1 were given to Intermap on CDs on Tuesday, 30th November 2010:

- A GIS raster grid of maximum water depths for pluvial flooding from the test event, set to the projection defined for the project (ETRS 1989 LAEA)
- A GIS raster grid of maximum water depths for pluvial flooding from the test event, unprojected (WGS 84), consistent with Allianz AG's requirements
- A GIS raster grid for maximum water velocity, set to the projection defined for the project (ETRS 1989 LAEA)
- A GIS raster grid for maximum water velocity, unprojected (WGS 84), consistent with Allianz AG's requirements
- Shapefiles for the clipped water grids

We have subsequently re-modelled Event 3 using a more detailed definition of Manning's *n* and soil infiltration coefficients and the post-processing techniques described in Section 3 and on the exact 5m cell-size projection of the DTM used by the climate scenarios; the re-modelled version is supplied alongside the deliverables for Phase 2.

4.2 Recommendations for Phase 2

At the end of Phase 1, our recommendations for Phase 2 were as follows:

- Since the results from Phase 1 are robust and consistent, Phase 2 modelling work should be carried out in the same way as has been described here for Phase 1. Checks should be carried out for problems relating to tile overlaps (as described in Section 3.3.2) after analysis and re-analysis carried out where necessary
- JBA should create a set of projected points at 5km spacing and supply these to the Met Office with co-ordinates expressed in both metres and decimal degrees. This will overcome problems related to the irregular format of data provided on an unprojected grid
- The DTM used should be that issued by Intermap and the soils information compiled during Phase 1 is used for Phase 2
- The following parameters should be used: Manning's *n* in urban area - 0.03; suburban - 0.05; rural - 0.1
- The parameters used for post-processing should remove depths below 0.3m and areas less than 1800m²

5. Phase 2: Running Climate Scenarios

5.1 Data

Rainfall data were supplied by the Met Office for nine climate scenarios. Three scenarios were derived from three different climate models, HADRM3Q4, HADRM3Q10 and HADRM3Q16, bearing the abbreviation codes FIXC, FIXK and FIXQ respectively. Four of the scenarios represented the present climate and five were derived for future climate scenarios. The climate models supplied were

- HADRM3Q4 (FIXC): 1974, 2083 and 2084
- HADRM3Q10 (FIXK): 1976, 1985 and 2096
- HADRM3Q16 (FIXQ): 1974, 2079 and 2086

For the purpose of simplicity, the years were reduced to two figures and prefixed with a "P" or "F" to denote present or future scenario (e.g. "FIXC_P74" refers to a "present climate" scenario from 1974 run in HADRM3Q4).

These scenarios are individual events, rather than comparable floodplain outlines for any one return period, as illustrated by Table 5-1. The effect that this has on extent comparison is discussed in Section 6.2 and 6.3.

All other data sources were as described for Phase 1.

5.2 Hydrology

The start and end date and time of each event was determined in the same way as in Phase 1; the first record where the sum rainfall rose from 0 toward the peak was taken as the start time, and the first record where the sum rainfall returned to 0 was taken as the end time.

The details for each scenario are therefore as follows:

Table 5-1 Scenarios identified			
MODEL	START (Month.Day.Hour)	END (Month.Day.Hour)	DURATION (Hours)
FIXC_P74	10.16.7	10.17.24	42
FIXC_F83	12.08.12	12.10.18	54
FIXC_F84	12.01.12	12.03.13	50
FIXK_P76	09.13.14	09.17.01	85
FIXK_P85	01.04.06	01.04.22	17
FIXK_F96	09.24.20	09.27.04	57
FIXQ_P74	11.03.02	11.03.24	23
FIXQ_F79	02.01.09	02.03.13	53
FIXQ_F86	11.01.16	11.03.11	44

5.3 Modelling

Using the same rainfall-to-runoff calculations as in Phase 1 and again applying the relevant curve number and Manning's n to represent soil type and land use, the rainfall values for each of these events were converted to the hydrological model for input to JFlow+. All nine scenarios were then modelled with JFlow+ and the output processed following the parameters determined from the modelling of Phase 1 Event 3.

6. Phase 2 Results

6.1 Nine modelled events

These maps present each post-processed event at the full extent of the area modelled. The maps have been delivered to Intermap via JBarn on 29th March 2011.

Figure 6-1 FIXK_P85

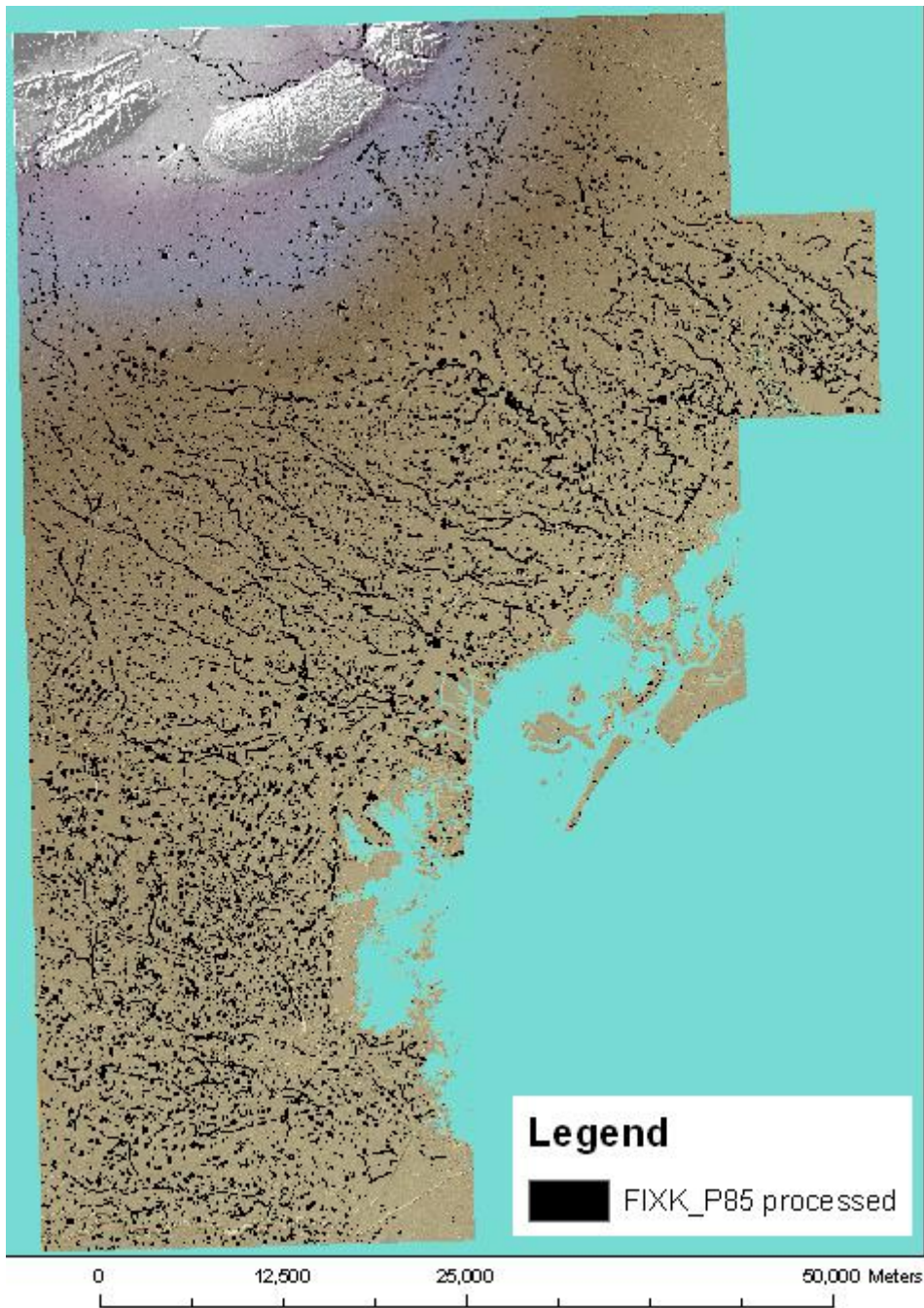


Figure 6-2 FIXC_F84

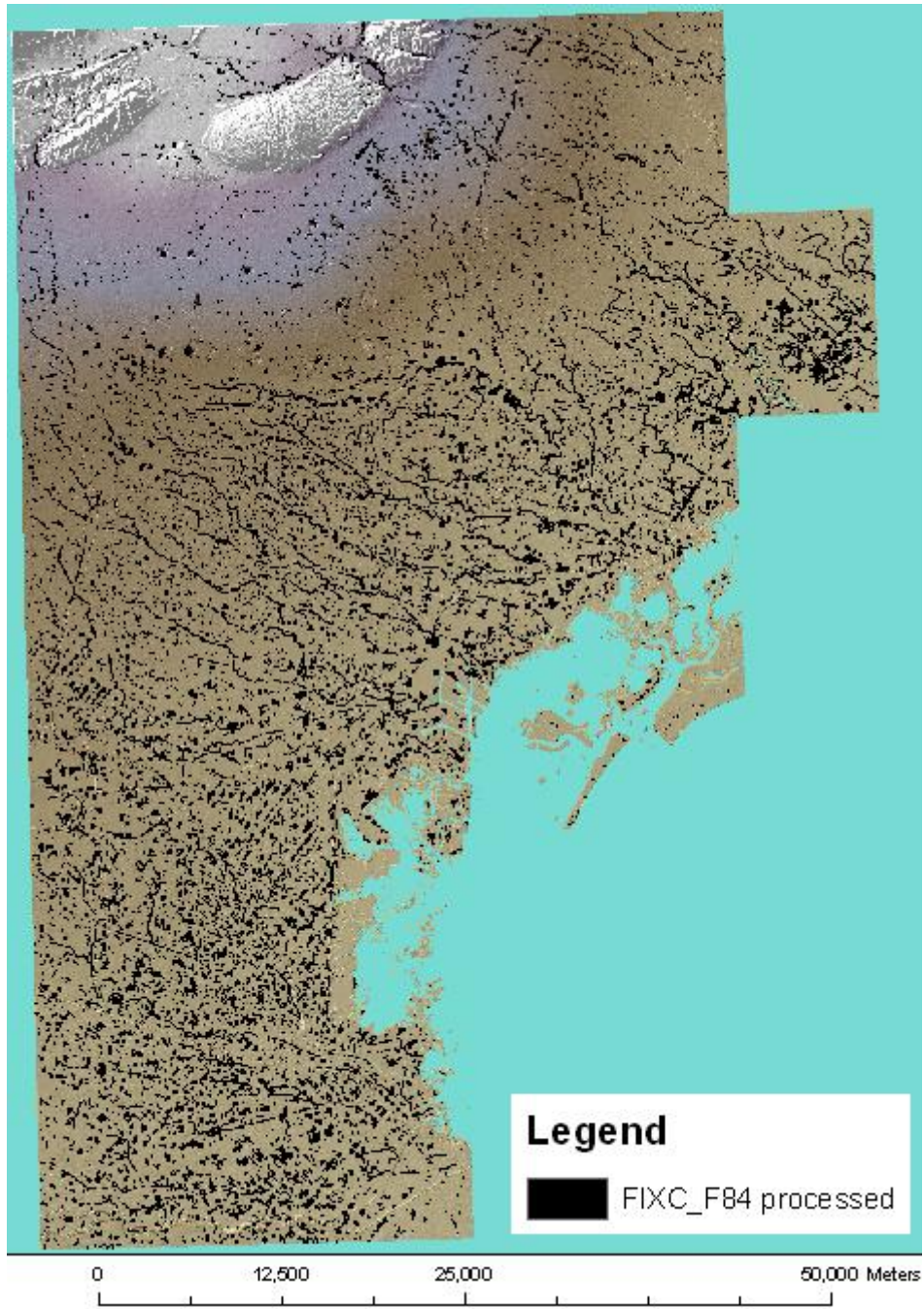


Figure 6-3 FIXQ_F86

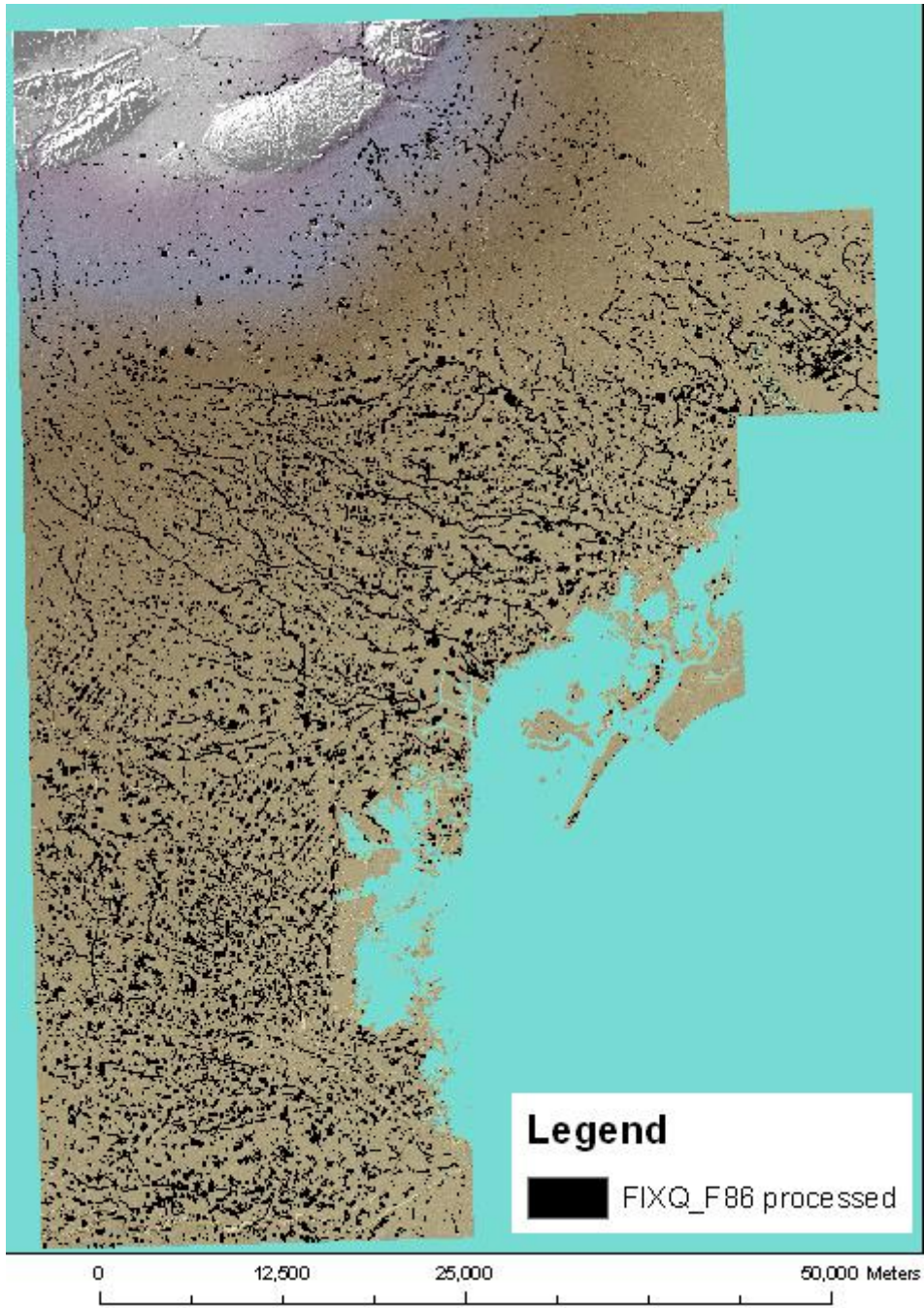


Figure 6-4 FIXK_P76

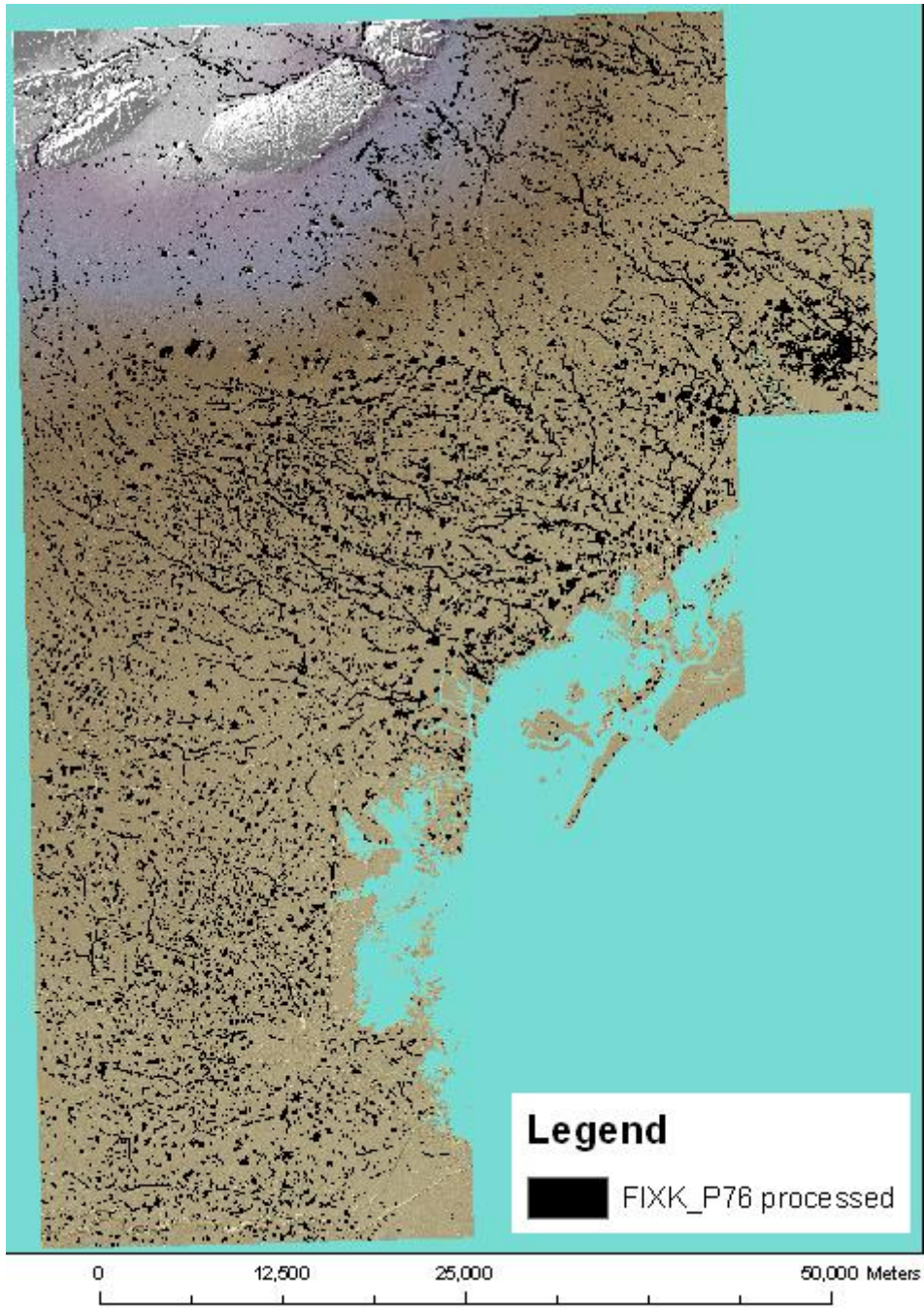


Figure 6-5 FIXC_P74

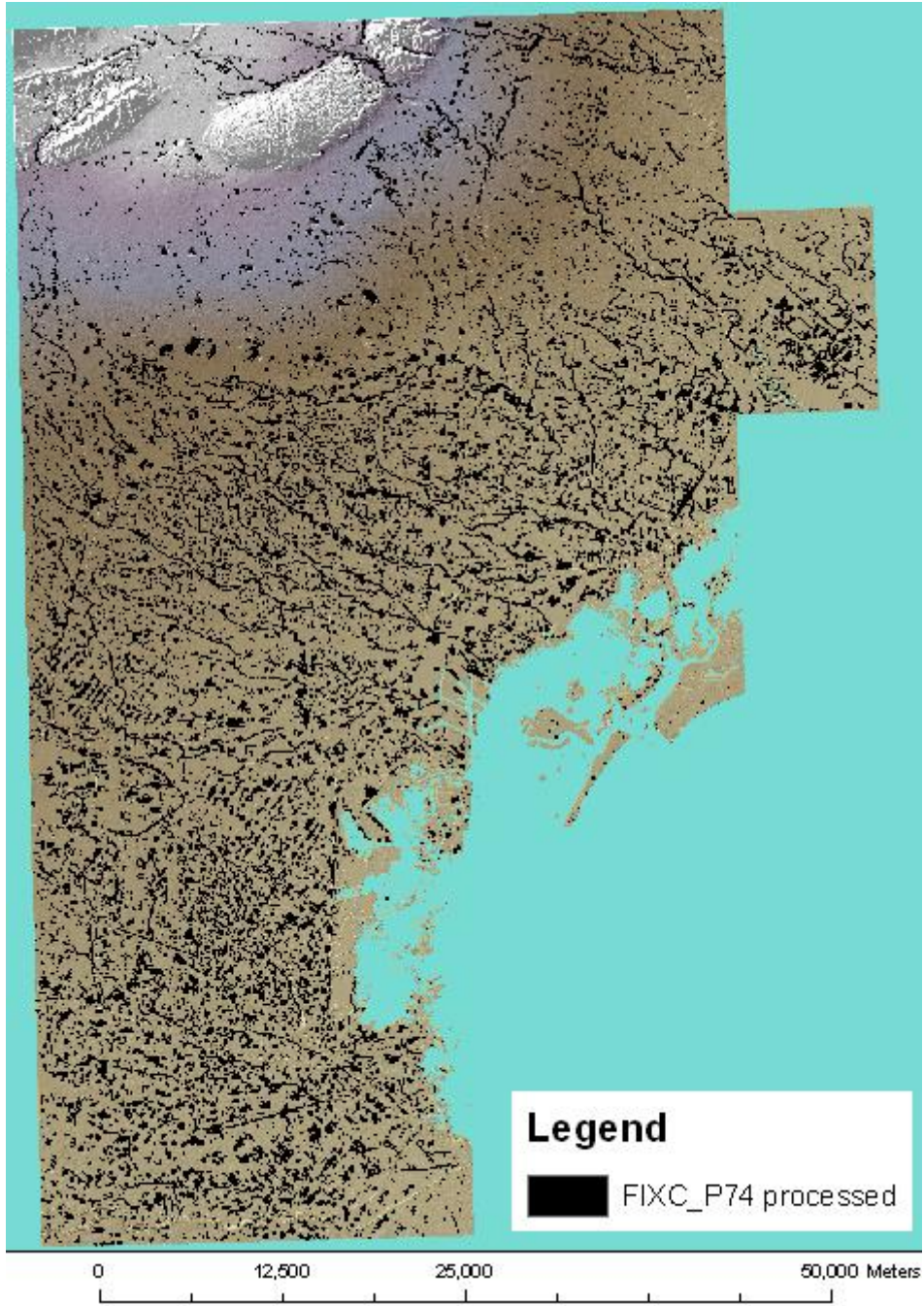


Figure 6-6 FIXC_F83

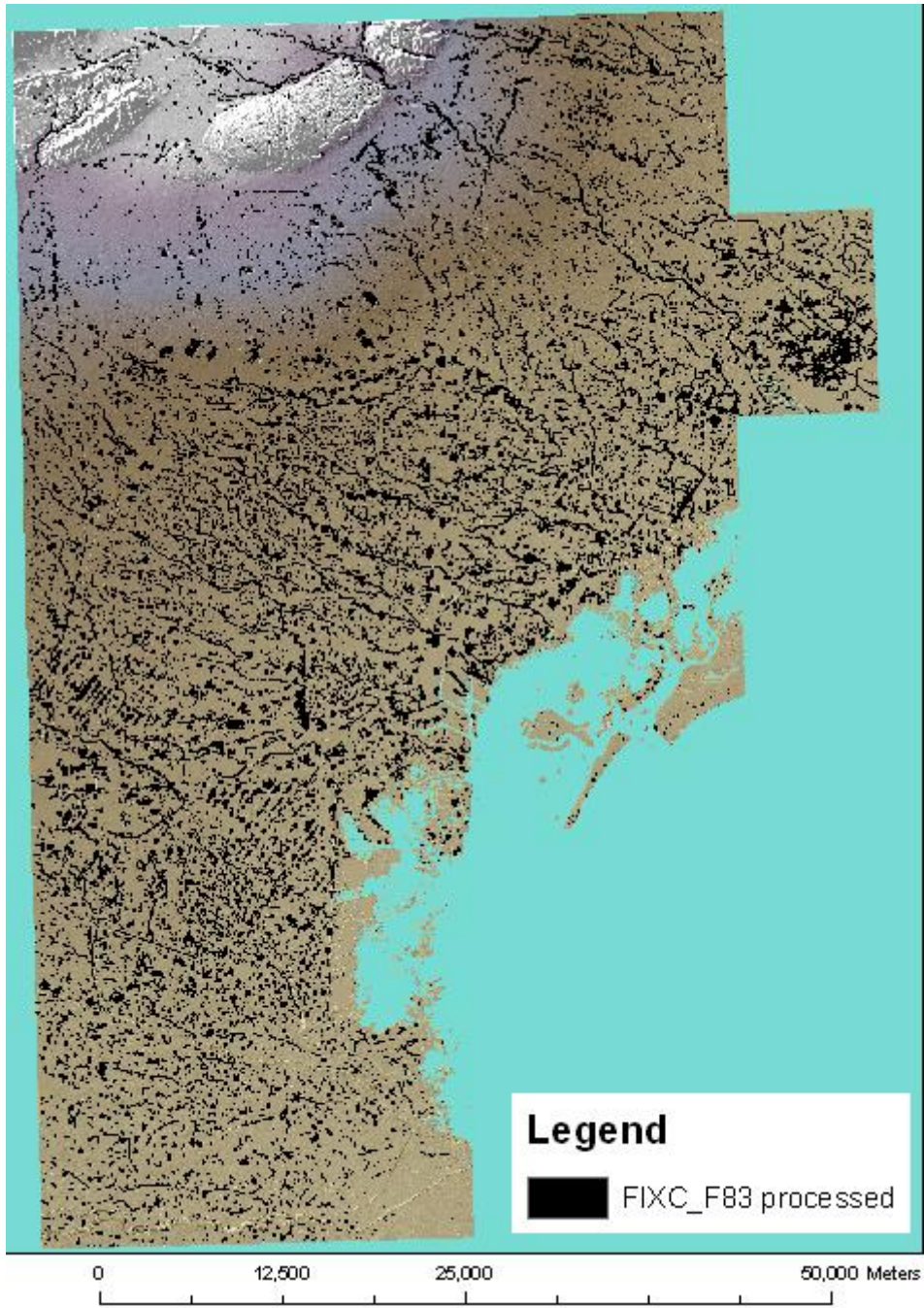


Figure 6-7 FIXQ_P74

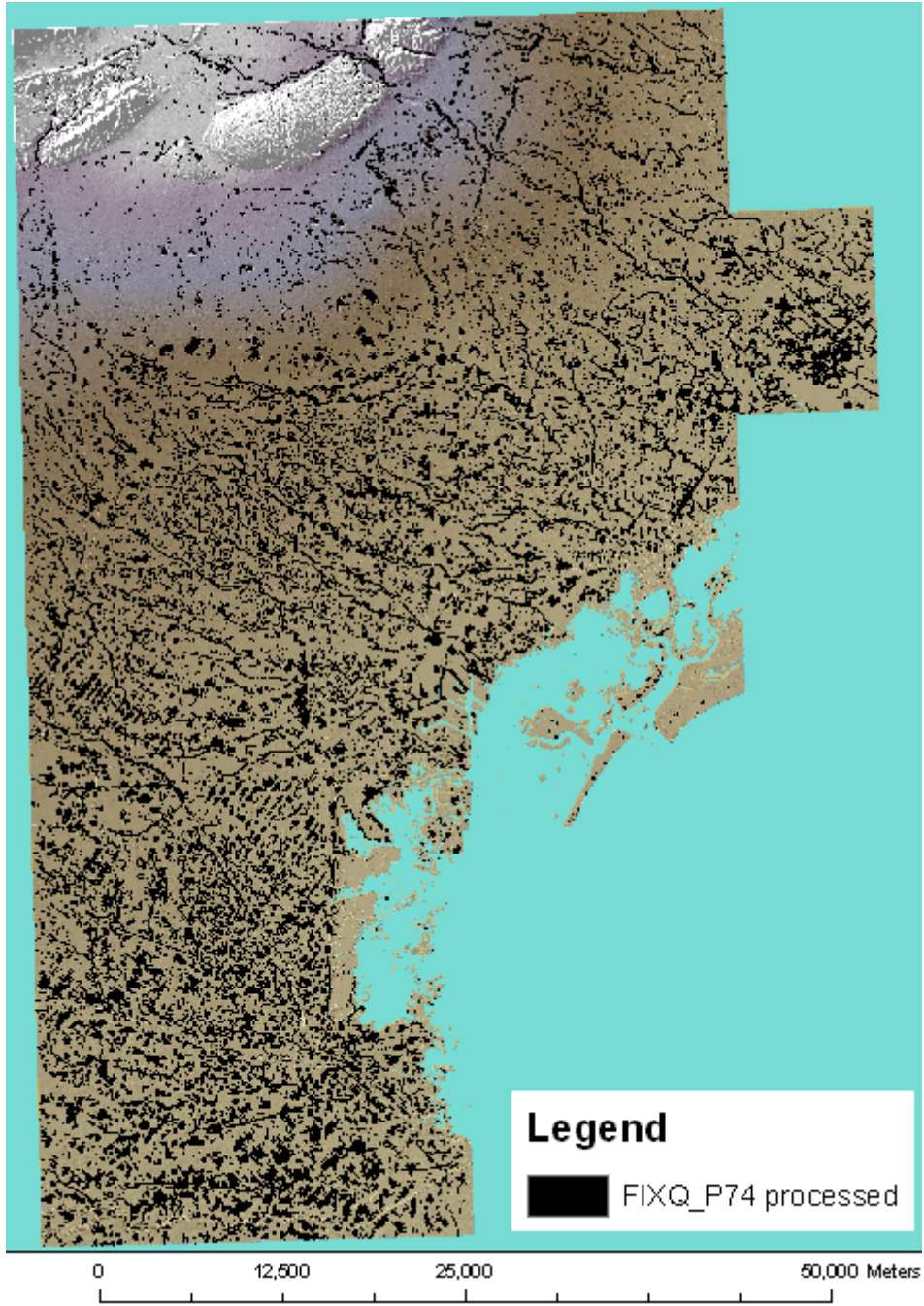


Figure 6-8 FIXK_F96

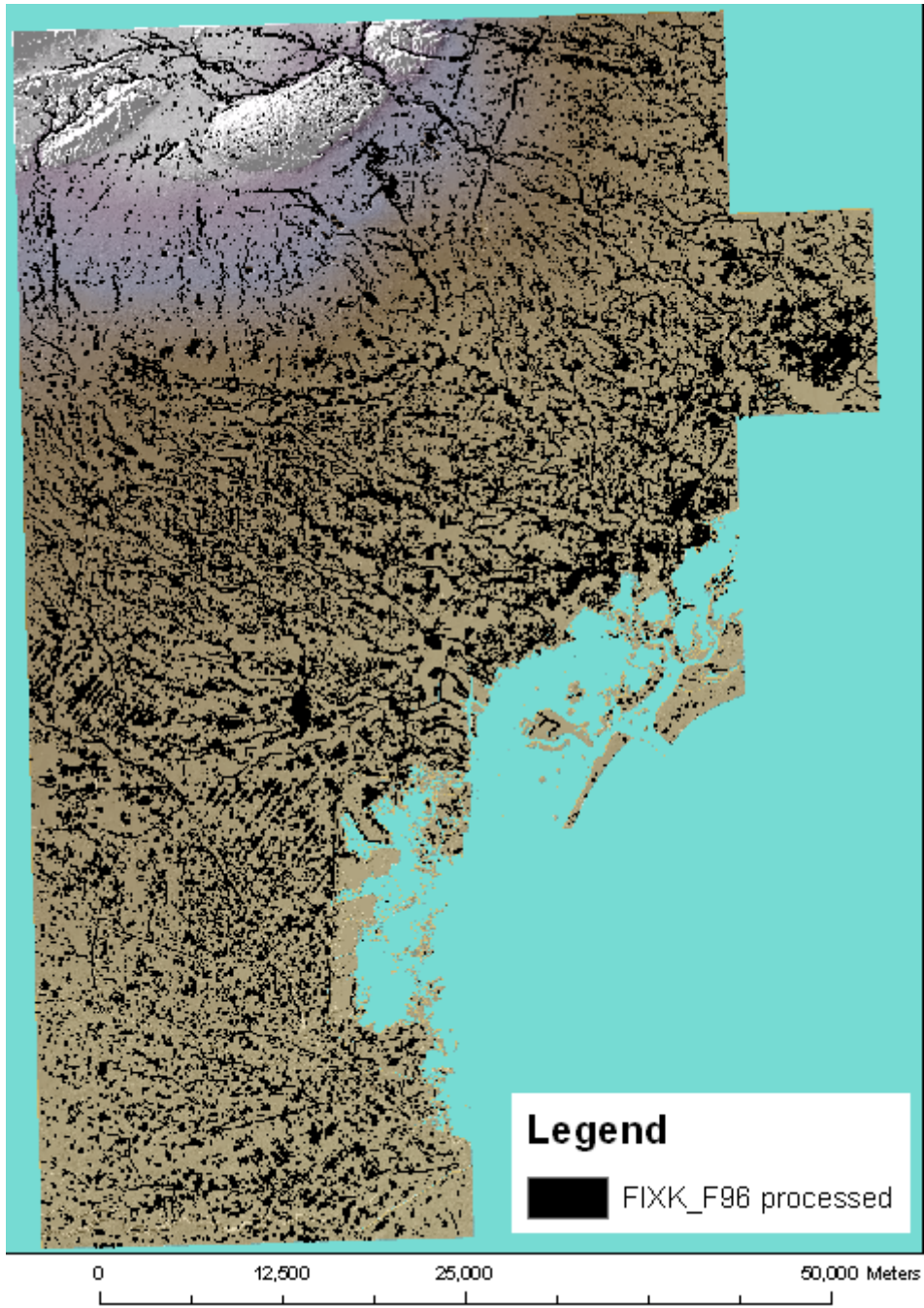
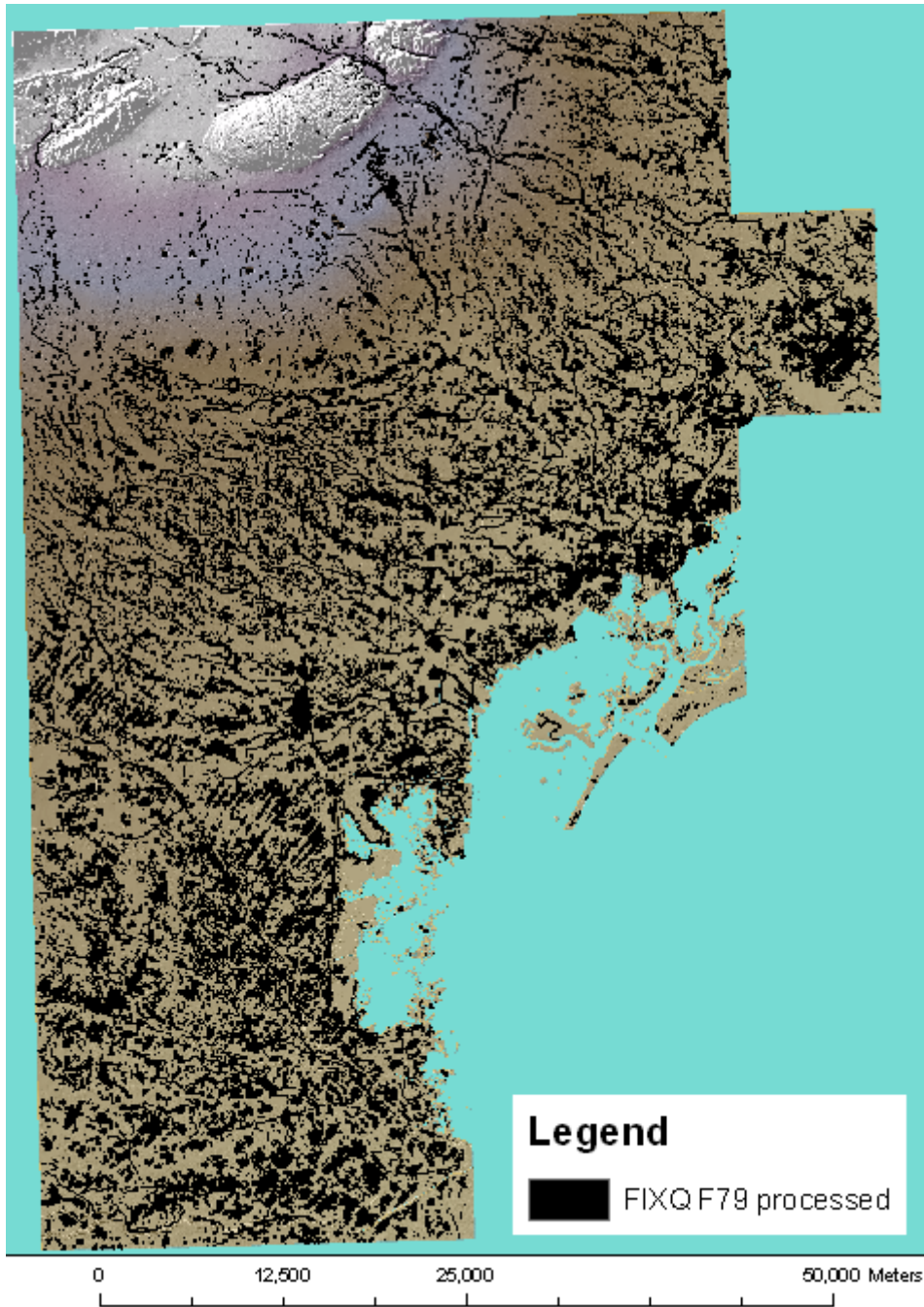


Figure 6-9 FIXQ_F79

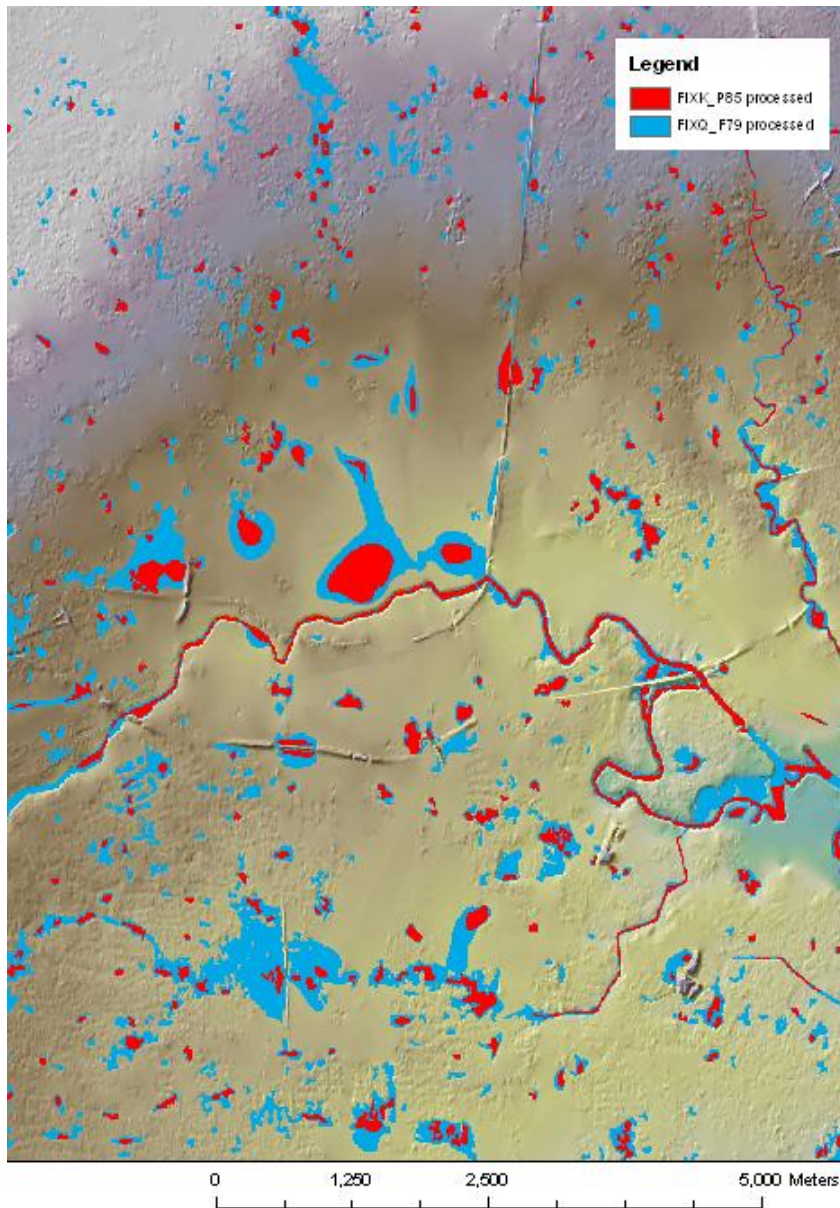


The initial series of maps display the results for all nine events from the smallest extent FIXK_P85, through to the largest event extent, FIXQ_F79.

6.2 Rank by extent

In the following map FIXQ_F79 is compared against FIXK_P85 in the area of Treviso. These have the largest and smallest extents respectively for the area, although, as will be discussed in Section 6.3, extents in one area are not necessarily reflective of the event's comparative severity across the entire model region.

Figure 6-10 FIXK_P85 vs. FIXQ_F79, Treviso



6.3 Hydrological variations

It is, however, not possible to define a ranking order of events from largest to smallest based solely on extent at any given location, due to the variable nature of the events. Rainfall intensity and volume shows significant spatial variation between the events, resulting in the discrepancy in extent ranking shown above.

Below, we demonstrate a selection of statistics derived from the supplied rainfall hyetographs for each data point and for each event to demonstrate the variability of the events:

- The average hourly rainfall throughout the event
- The maximum rainfall in any one hour of the event
- The total volume of rainfall for the entire event

For example, a short event may feature a relatively intense rainfall, resulting in a high average hourly rainfall but a lower quantity of rainfall in total, as in the case of FIXK_P85.

Equally, a long event may feature a relatively low maximum rainfall but steady rainfall throughout the duration of the event may produce a high total, as in the case of FIXQ_F79.

The following diagrams show how the rainfall for each event varies in intensity geographically and how the events vary in nature.

Figure 6-11 Comparing average hourly rainfall between events

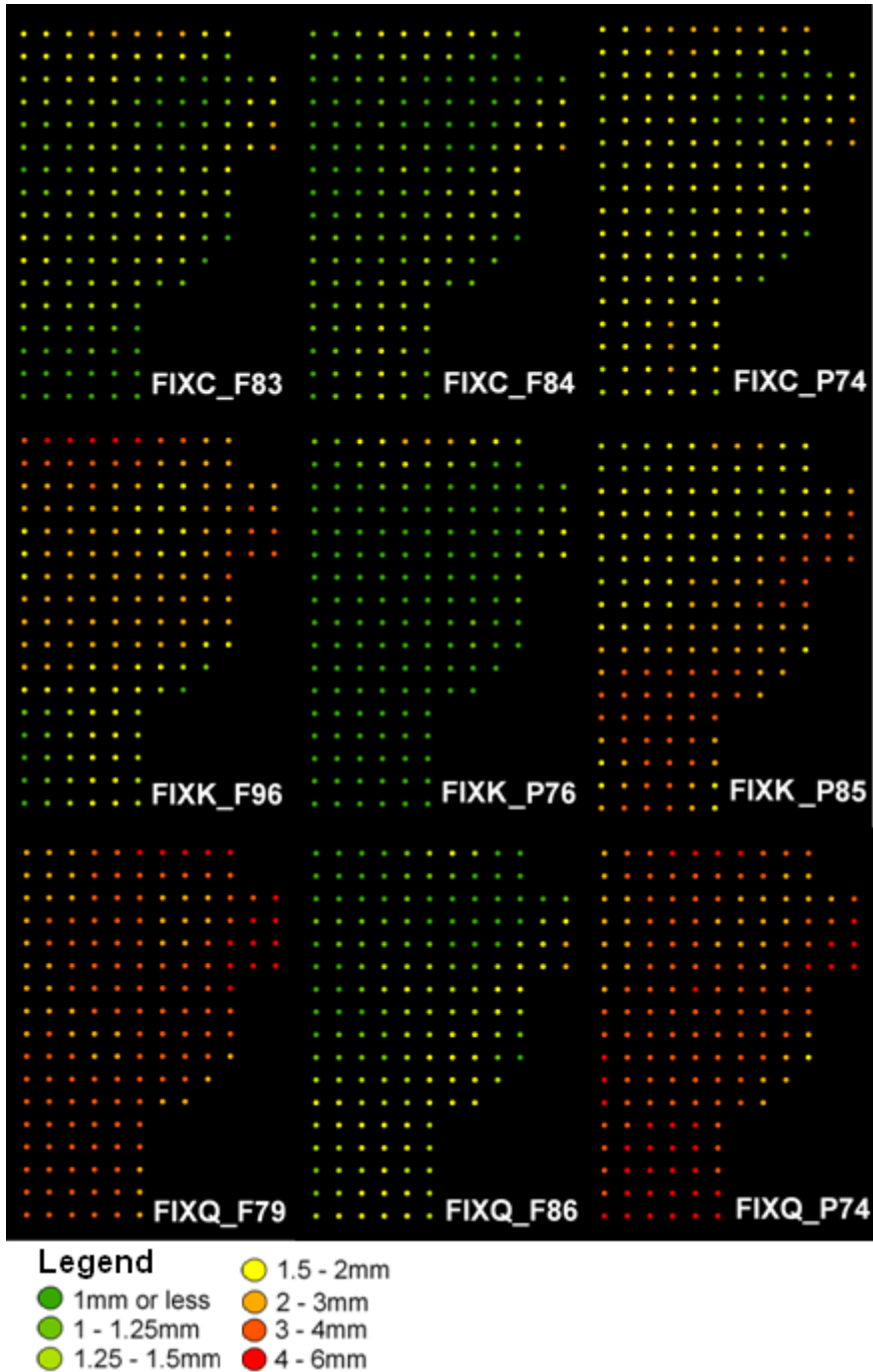


Figure 6-12 Comparing maximum hourly rainfall between events

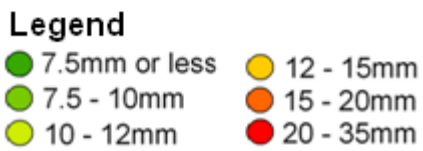
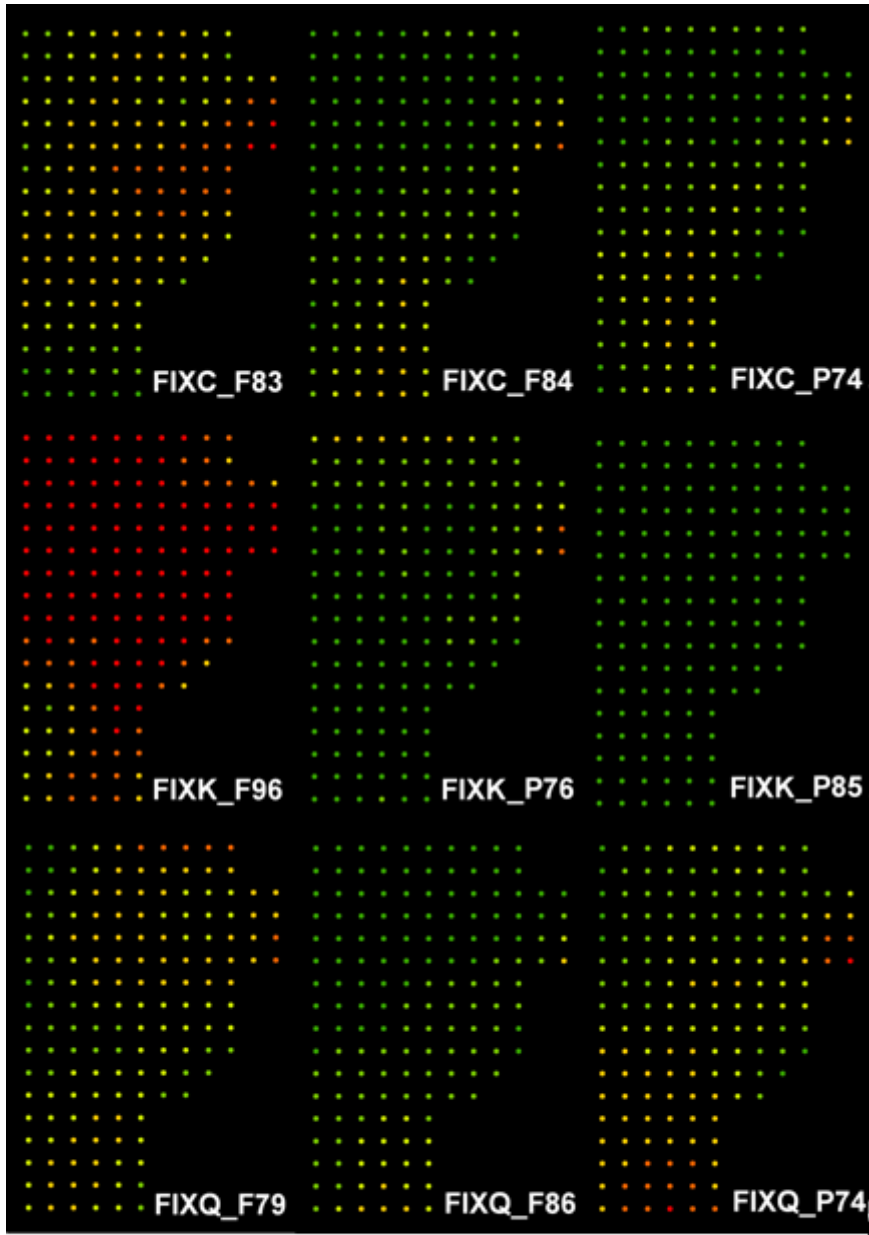


Figure 6-13 Comparing total event rainfall between events



6.4 Rank by area

Perhaps more usefully, the events may be ranked by the area of extent across the whole model area or just the intersection with urban and suburban areas as defined by the soil data, as opposed to which appears to have the widest extent at any one location.

Table 6-1 Ranking events by total area and by sub/urban intersection area

Event ranked by total area	Total area (m ²)	Rank	Event ranked by urban/suburban area	Urban/ suburban area (m ²)
FIXQ_F79	397,710,475	1	FIXK_F96	25,475,775

FIXK_F96	280,177,400	2	FIXQ_P74	19,131,289
FIXQ_P74	208,923,125	3	FIXQ_F79	16,126,167
FIXC_F83	148,536,425	4	FIXC_F83	16,126,167
FIXC_P74	146,985,025	5	FIXC_P74	14,579,120
FIXC_F84	109,636,475	6	FIXQ_F86	11,642,537
FIXQ_F86	103,670,125	7	FIXC_F84	11,537,087
FIXK_P76	101,958,350	8	FIXK_P76	10,945,913
FIXK_P85	76,679,275	9	FIXK_P85	9,063,789

6.4.1 Comparing Phase 2 scenario with Phase 1 historic event

It is not easy to determine the most appropriate place where Event 3, the September 2007 event, fits within the rank of the nine events modelled in Phase 2.

From a general overview, and shown by the maps comparing Event 3 with FIXQ_F79 in some areas Event 3 shows a greater extent, yet in others it is smaller. In the east (left) of the maps displaying the comparison of a Phase 2 extent, FIXQ_F79, with Event 3 it can be seen that Event 3 results in a greater extent, whilst in the west FIXQ_F79 is bigger. Again, this is most likely due to the variations in rainfall intensity discussed in Section 6.3.

Figure 6-14 FIXQ_F79 overlay Event 3

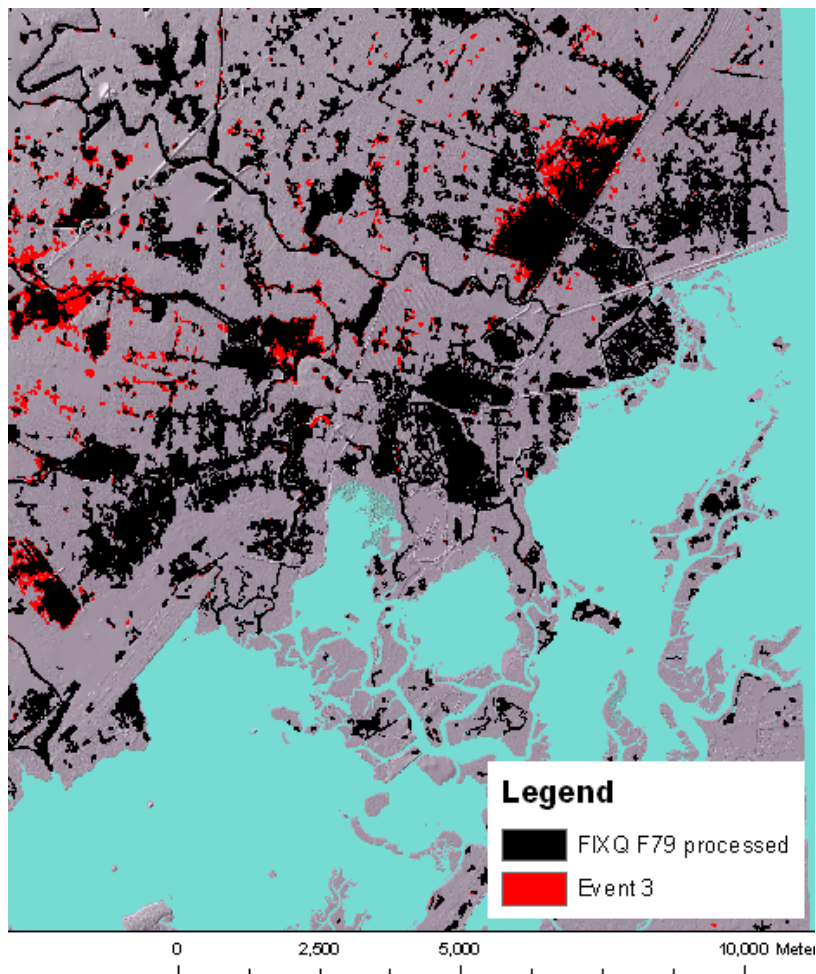
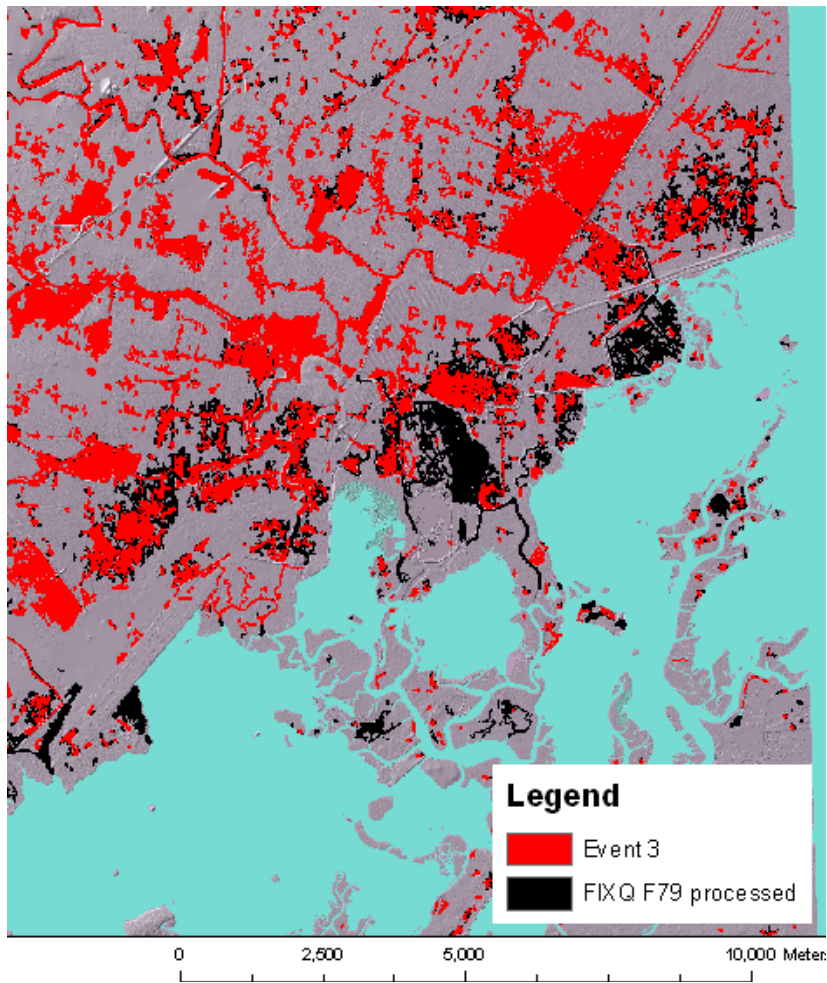


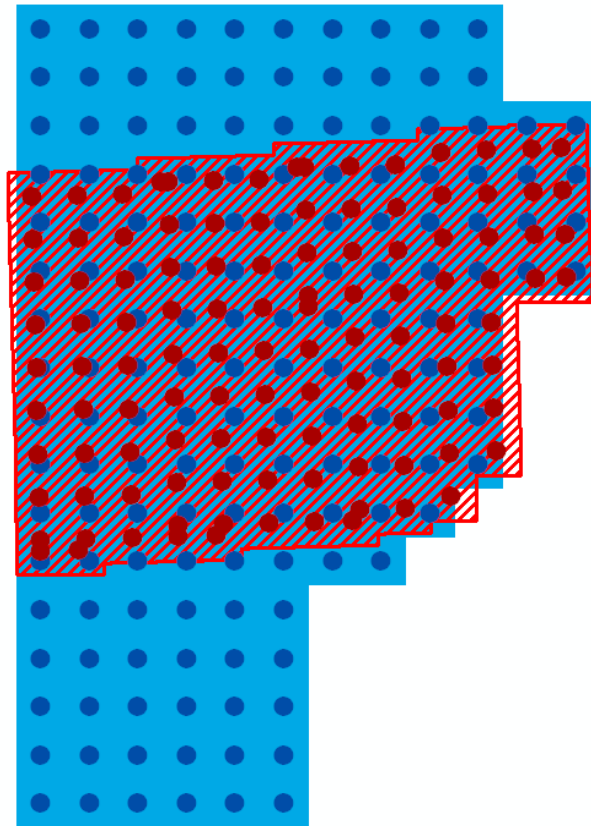
Figure 6-15 Event 3 overlay FIXQ_F79



Difficulties arise in drawing comparisons between the historic event and these scenarios for two reasons:

- The data points on which the model tiles were based are not spaced evenly for the historic events and therefore do not correspond exactly to those used for the scenarios
- The historic events were modelled for a smaller region than the scenarios, meaning that comparing directly by area of final extents includes the scenario models beyond the extent of the historic models

Figure 6-16 Showing discrepancy between Phase 1 (red) and Phase 2 (blue) modelling areas and data point locations



Nevertheless, comparing the extent areas only for that comparable area where both the climate scenario and the historic rainfalls were modelled, the comparison is as follows:

Table 6-2 Ranking events by extent area within coincident model region		
Rank	Event	Extent area (m ²)
1	FIXQ_F79	244,407,608
2	FIXK_F96	198,553,416
3	Event 03	151,663,955
4	FIXQ_P74	121,873,389
5	FIXC_F83	106,672,006
6	FIXC_P74	91,375,738
7	FIXK_P76	70,937,124
8	FIXC_F84	66,844,719
9	FIXQ_F86	64,266,679
10	FIXK_P85	48,908,410

6.5 Rank by volume

Given that each cell of the depth grids represents an area of 25m², it is possible to determine the total volume of flood water for each event by multiplying the depth of each cell by 25. This gives the following ranking:

Rank	Event	Volume (m ³)
1	FIXQ_F79	251,752,866
2	FIXK_F96	167,995,623
3	FIXQ_P74	118,062,543
4	FIXC_F83	83,539,302
5	FIXC_P74	81,544,100
6	FIXC_F84	58,316,033
7	FIXK_P76	56,428,831
8	FIXQ_F86	55,112,439
9	FIXK_P85	39,890,610

It must be borne in mind that these volumes, as with the area calculations above, are based solely on the processed depth grids and therefore exclude all depths lower than 0.3m.

6.6 Rank by score

If a score is added alongside the rankings for extent area, urban extent area, and floodwater volume, nine being the highest and one the lowest (that is, the opposite of the rankings) then a final "master" ranking may be obtained by adding these three scores together.

Rank	Score	Event
=1	25	FIXK_F96
=1	25	FIXQ_P79
2	22	FIXQ_P74
3	18	FIXC_F83
4	15	FIXC_P74
5	11	FIXC_F84
6	9	FIXQ_F86
7	7	FIXK_P76
8	3	FIXK_P85

7. Conclusion

FIXK_F96 and FIXQ_P79 are the joint highest-scoring events. Given that FIXK_F96 bears the largest extent intersection with urban areas, perhaps a characteristic that may be deemed more important than simply extent area across the whole model region due to its impacts on business and property, it seems fair to suggest that this may be termed the most severe event. Following the same reasoning, it would appear that FIXK_P85 may be termed the smallest event.

The score ranking reiterates that while it is clear to see that there is a considerable difference between the largest and the smallest, the difference between similarly ranked events is in general relatively small. It is certainly difficult to determine any general trend between future and present events in these terms.

References

Bradbrook (2006). JFLOW: A multiscale two-dimensional dynamic flood model. *Water and Environment Journal* 20, pp. 79-86.

Bradbrook, K., Lane, S.N., Waller, S., Bates, P.D. (2004) "Two dimensional diffusion wave modelling of flood inundation using a simplified channel representation", *International Journal of River Basin Management*, 2 (3), 1-13

CORINE Land Cover CLC2000

Cronshey, R. et al. (1986) "Technical Release 55: Urban Hydrology for Small Watersheds", *NRCS Conservation Engineering Division Technical Releases*, United States Department of Agriculture

The European Soil Database distribution Version 2.0, European Commission and the European Soil Bureau Network, CD-Rom, EUR 19945 EN, 2004

Hunter, N.M. et al. (2008) "Benchmarking 2D hydraulic models for urban flood simulations", *Proceedings of the Institution of Civil Engineers - Water Management*, vol.161

Lamb, R., Crossley, A., Waller, S. (2009) "A fast 2D floodplain inundation model", *Proceedings of the Institution of Civil Engineers - Water Management*, vol.162

A. Appendix A: CORINE land use classes

Code	Land use	JBA classification	
111	Continuous urban fabric	Urban	
121	Discontinuous urban fabric		
123	Industrial or commercial units		
112	Road and rail networks	Suburban	
122	Port areas		
124	Airports		
131	Mineral extraction sites		
132	Dump sites		
133	Construction sites		
141	Green urban areas		
142	Sports and leisure facilities		
211	Non-irrigated arable land		Rural
221	Vineyards		
222	Fruit tree and berry plantations		
231	Pastures		
242	Complex cultivation patterns		
243	Principally agriculture, with natural vegetation		
311	Broad-leaved forest		
312	Coniferous forest		
313	Mixed forest		
321	Natural grasslands		
322	Moors and heathland		
324	Transitional woodland shrubs		
331	Beaches, dune and sand plains		
411	Inland marshes		
421	Peat bogs		
422	Salines		
511	Watercourses		
512	Coastal lagoons		
521	Estuaries		
-99	Unknown		



Offices at

Atherstone
Doncaster
Edinburgh
Haywards Heath
Limerick
Newcastle upon Tyne
Newport
Northallerton
Northampton
Saltaire
Skipton
Tadcaster
Wallingford
Warrington

Registered Office
South Barn
Broughton Hall
SKIPTON
North Yorkshire
BD23 3AE

t:+44(0)1756 799919
e:info@jbaconsulting.co.uk

Jeremy Benn Associates Ltd
Registered in England 3246693



Visit our website
www.jbaconsulting.co.uk